The University Of Sheffield.

A Multi-Scale Agent Based Model of Colon Carcinogenesis

By:

Tim Ingham-Dempster

A thesis submitted in partial fulfilment of the requirements for the degree of Doctor of Philosophy

The University of Sheffield
Faculty of Medicine, Dentistry & Health
Department of Oncology and Metabolism

Submission Date

21/09/2018

A Multi-Scale Agent Based Model of Colon Carcinogenesis

Tim Ingham-Dempster

Supervisors: Dr Bernard Corfe, Dr Dawn Walker

Molecular Gastroenterology Research Group

Department of Oncology and Metabolism

Registration number: 140147601

Contents

Figures

Abstract

Colorectal cancer (CRC) is a major cause of cancer mortality and there remain aspects of its formation which are not understood. The colon contains an epithelium punctuated by flask shaped invaginations called the crypts of Lieberkühn. These crypts are monoclonal in nature while adenomas are thought to be polyclonal, suggesting that multiple crypts are involved in carcinogenesis. It has been reported that fields of mutated tissue surround adenomas but the causes and growth of these fields are not well understood. There are two competing hypotheses regarding growth, the first being that mutated cells from one crypt invade neighbouring crypts, and the second that mutated crypts replicate themselves more often than wild-type crypts.

To investigate these processes two agent based models were developed. The first model represents cells as agents and is similar to previous models in the field, but is novel in including the geometry of the crypt mouth. This is necessary to model multiple interacting crypts. This model is the first in the literature to be used to represent multiple crypts and is used to investigate invasion of neighbour crypts by mutated cells. The second model represents whole crypts as agents, which allows the entire colon to be simulated for multiple decades of biological time, as far as we are aware this is the first such model.

The cell scale model predicts that crypt invasion does not occur, but that mutated cells can invade the flat mucosa above neighbouring crypts. Analysis of in-vivo data is consistent with this prediction. The crypt as agent model predicts fields of ~41,000 crypts, in agreement with data in the literature, this corresponds to a field ~23mm in diameter. This project models pre-cancerous fields for the first time over a variety of scales, making specific novel predictions which are in agreement with in-vivo data where such data exist.

Two agent based models were created to study the development of precancerous fields, one a model with cells as agents to study cell scale phenomena and the other with crypts as agents to allow processes to be studied on larger spatial and temporal scales. These models could potentially be used to refine clinic practice by predicting the required frequency of post-intervention monitoring of patients or the necessity of further intervention.

Publications arising

Papers – published

INGHAM-DEMPSTER, T., CORFE, B. & WALKER, D. 2018. A cellular based model of the colon crypt suggests novel effects for Apc phenotype in colorectal carcinogenesis. *Journal of Computational Science,* 24**,** 125-131.

INGHAM-DEMPSTER, T., WALKER, D. C. & CORFE, B. M. 2017. An agent-based model of anoikis in the colon crypt displays novel emergent behaviour consistent with biological observations. Royal Society Open Science: The Royal Society Publishing.

Papers – awaiting submission

INGHAM-DEMPSTER, T., CORFE, B. & WALKER, D. Cell Shape Assumptions Affect Behaviour in Multicellular Models: Learnings from the Crypt.

INGHAM-DEMPSTER, T., WALKER, D. C., ROSSER, R., & CORFE, B. M. Multiple Scale Multi-crypt Modelling of APC- versus wild-type competition in the Human Colon Suggests Novel Processes of Field Cancerisation.

Conference presentations:

A Cellular Based Model of the Colon Crypt Suggests Multiple Roles for APC Mutation in Colorectal Carcinogenesis. Virtual Physiological Human Conference, 2016

Multi-scale Modelling of Carcinogenic Field Spread in the Human Colon. BMVA technical meeting: Computer Vision and Modelling in Cancer, 2017

Chapter 1: Introduction

The human large intestine contains a monolayer epithelium punctuated by glands known as the crypts of Lieberkhun. The crypts are the functional unit of the colonic epithelium and as such the perturbation of their turnover is implicated in formation of colorectal cancer (CRC) (Humphries and Wright, 2008) so understanding them is crucial to understanding the pathophysiology of disease. For example, it was not known how a mutation could survive in such a rapidly refreshing tissue until the process of monoclonal conversion was discovered. Processes which remain to be elucidated include the mechanism that allows crypts to regulate their cellularity, which would need to be disrupted for an adenoma to form and the interactions between crypts which are also implicated in adenoma formation (Merritt et al., 1997, Novelli et al., 1996) and have not been well characterised.

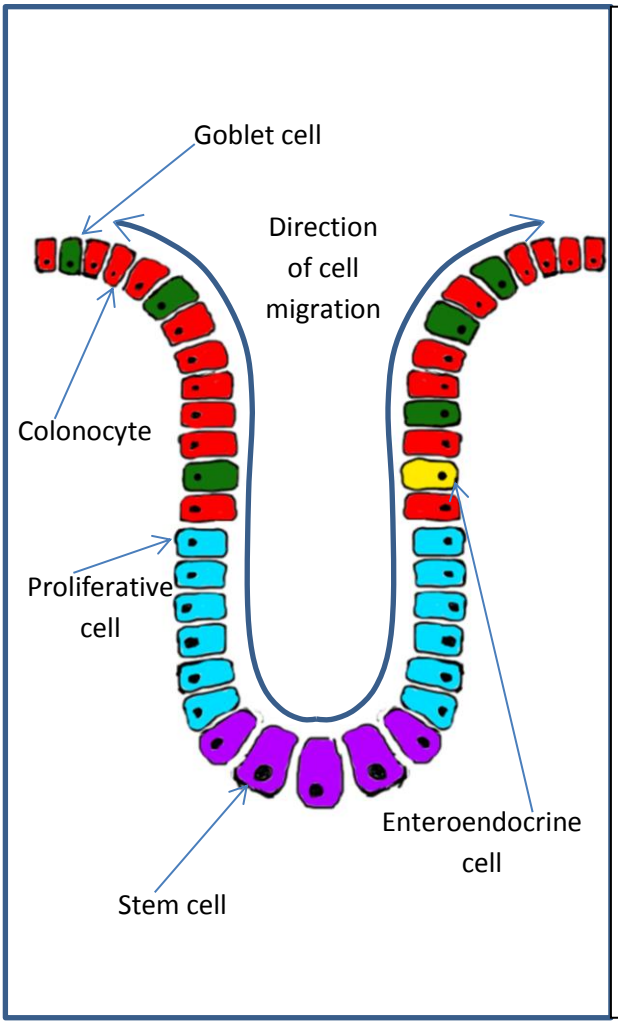

Figure 1.1: a colonic crypt. Crypts contain proliferating stem cells (purple) at the base (Barker et al., 2007) and functioning differentiated cells at the top. They also contain proliferating cells (blue) between these two areas which may or may not be able to act as stem cells (Van Landeghem et al., 2012). Other cells are water absorbing colonocytes (red), mucus secreting goblet cells (green), and hormone secreting enteroendocrine cells (yellow). Figure reused under Creative Commons Attribution License (Ingham-Dempster et al., 2017).

A human colonic crypt contains approximately 2500 cells (Cheng et al., 1984). Fully differentiated cells are water absorbing colonocytes which account for roughly 75% of differentiated cells (Cheng et al., 1984), mucus secreting goblet cells which account for roughly 24% of differentiated cells (Cheng et al., 1984) and hormone secreting enteroendocrine cells which account for less than 1% of differentiated cells (Cheng and Leblond, 1974). Cells migrate from the bottom of the crypt to the top. This movement has been shown to occur even after proliferation stops (Kaur and Potten, 1986) and to be

partially organised by EphB signalling (Batlle et al., 2002, Holmberg et al., 2006), EphB being a signalling molecule with counteracting gradients of ligands and receptors present in the crypt. Apoptotic rates are highest at the end of this migration at the top of the crypt (Potten, 1998). It is not currently known how the number of cells within the crypt is regulated.

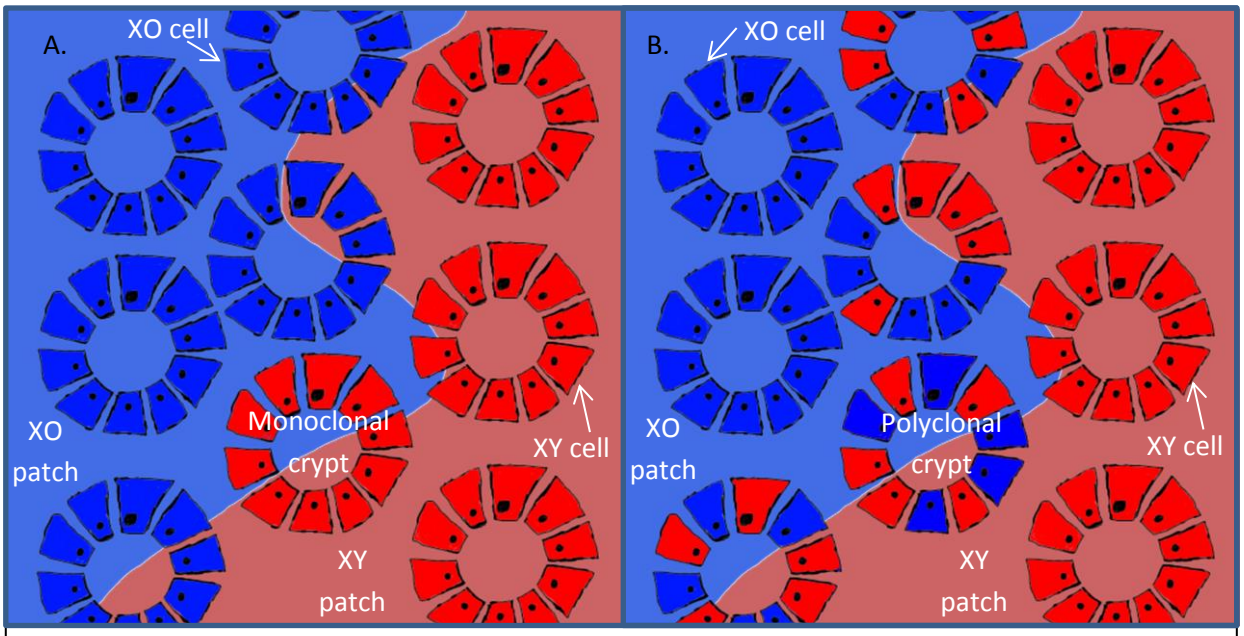

Figure 1.2: crpyts are monoclonal in nature. A. When sections of intestinal epithelium near patch boundaries are studied it is seen that all crypts on patch boundaries are derived entirely from one patch, patches being areas of tissue where all cells are either XO or XY due to patterns of cell division in early development. This has been studied in chimeric mice (Merritt et al., 1997) and an XO/XY mosaic human (Novelli et al., 1996). The situation in B where crypts contain cells from both sides of the patch boundary was never observed in either model. This supports the hypothesis that crypts are always monoclonal.

Crypts are known to be monoclonal in nature **(Fig 1.2)** (Merritt et al., 1997, Novelli et al., 1996, Novelli et al., 2003), this means that all cells within a crypt are descendants of a single original cell. The mechanism behind this phenomenon has been elucidated and involves the upward motion of cells from the crypt base to the crypt top and the location of the stem cells at the base of the crypt (Baker et al., 2014). As stem cells divide at the bottom of the crypt they force other cells out of the stem cell niche, these cells are then swept up the crypt and die at the crypt mouth or on the flat mucosa. As there are few stable cell positions at the crypt base there is a high probability that all of these positions will become occupied by descendants of a single cell at which point only the descendants of that cell can populate the crypt. The probability of this situation occurring over a span of time tends towards 1 as the span of time increases.

There are currently two hypotheses concerning the mechanism responsible for determining cell fate within the crypt (van der Wath et al., 2013). The pedigree model says that a stem

cell will divide into two stem cells, a stem cell and a transit amplifying cell, or two transit amplifying cells, at random. If a transit amplifying cell is produced it will then move up the crypt while undergoing a fixed number of divisions before differentiating into a functional colonocyte. The niche hypothesis on the other hand states that whether a cell is a stem cell, transit amplifying cell, or functional cell is determined by signalling cues from its environment, most notably from a concentration gradient of the Wnt molecule which exists within the crypt (Potten and Loeffler, 1990).

Several studies have attempted to shed light on this process, with both mouse (Snippert et al., 2010) and human (Baker et al., 2014) studies suggesting a stochastic process of neutral drift dynamics consistent with the niche hypothesis. A recent study (Carroll et al., 2017) was able to examine the process in more detail using crypt organoids and found that proximity of the resulting cells after division was a good predictor of eventual cell fate. Differential basal tethering appeared to play a key role in determining proximity after division and hence eventual cell fate.

Ephrin B is known to have a role in regulating cell positioning and sorting within the crypt (Holmberg et al., 2006) and dysregulation of this system has been shown to lead to disruption of the distinct compartments within the crypt (Genander et al., 2009). Changes to the EphB pathway may be related to CRC formation but it is not currently known if this is the case and if so in what capacity.

The Adenomatus Polyposis Coli (APC) gene is found to have loss of function mutations in the majority of CRCs and is thought to be one of the key drivers of CRC formation (Wasan et al., 1998). Loss of APC function is known to cause stem cells to cycle more quickly by reducing the time of their quiescent phases (Sansom et al., 2004), it is also thought to promote anoikis resisitance (Strater et al., 1995) and reduce cell stiffness (Sansom et al., 2004). As APC loss is so strongly implicated in CRC formation understanding the effects of these changes at the tissue level is highly important.

Crypts have been shown to be monoclonal in nature **(Fig 1.2)** but adenomas are thought to be polyclonal in the early stages (Merritt et al., 1997, Novelli et al., 1996, Novelli et al., 2003), suggesting that interaction between crypts plays a role in adenoma formation. The dynamics of this process are not well understood and it is not clear how this could be studied biologically as it is a sporadic event which cannot be predicted in order to sample tissue during the event.

It is known that fields of abnormal tissue surround adenomas (Humphries and Wright, 2008), creating fields of many thousands of crypts of abnormal tissue. How these fields form and spread is not known but is potentially relevant in preventing the formation and recurrence of CRCs. There are currently two main hypotheses on the nature of field spread, the first being the top-down hypothesis (Shih et al., 2001) which posits that mutated cells from a neighbouring crypt will invade a wild-type crypt and then through selective advantage take over the new crypt in a process related to the monoclonal conversion mechanism which caused $APC^{-/-}$ cells to dominate the mutated crypt.

The competing, bottom-up (Preston et al., 2003), hypothesis focuses on the process of crypt fission, whereby a crypt splits into two offspring crypts (Langlands et al., 2016). This is thought to be the main mechanism by which crypts replicate. This hypothesis states that

because APC loss is known to increase the rate of fission of mutated crypts the population of mutated crypts will have a competitive advantage compared to wild-type crypts and will grow the field through crypt division. This would not, however, explain adenoma polyclonality.

Many of these phenomena are hard to study by their nature, fields develop over multiple decades of time and cover tens of thousands of crypts (Humphries and Wright, 2008), meaning that in-vivo study through biopsies can only reveal a few snapshots of a developing field. APC loss is not a predictable event therefore studying crypts in the early stages of APC loss and field spread is impossible as there is no way to know where and when such events will occur. As such, methods and tools to study field growth in-vivo are non-existent and would be prohibitively difficult to develop and use.

One approach which has been successful in elucidating these hard to study processes is computer simulation. A digital model of the biological entity to study is created and designed to conform as closely as possible to the known behaviour of the biological entity. This model is then used to simulate conditions which are hard to examine in-vivo, for example a mutation event could be programmed into the model or the model could simulate long periods of biological time in a more tractable timeframe.

It is possible to study living crypts in-vivo (Ritsma et al., 2014) but the technique is complicated, expensive and time consumning.

Another approach which has been used to study crypts is the growing of organoids from cultured epithelial cells (Grabinger et al., 2014). This approach involves the culturing of ex-vivo cells in a matrigel environment to produce spherical organoids which develop crypt like structures. As these structures can be studied throughout their life and can be created on demand under differing conditions they could be invaluable for calibrating and validating models. In addition, organoids cultured from different regions (proximal, transverse, distal, rectum) of the colon and grown under conditions simulating those regions could be used to further calibrate the model as it is to be expected that crypts from different regions may have different properties and behaviours.

1.1: Computational Models

Computational simulation models allow us to generate simulated results from systems which obey any programmed hypothesis. Each hypothesis can be modelled and the results compared to experimental data to suggest which hypothesis is more likely to be accurate. Other advantages of computer modelling are the ability to simulate the results of experiments that could not be performed in-vivo or in-vitro either because of ethical concerns or practical issues such as events which are hard to predict and hence observe, or phenomena which occur over long timescales. These are the key contributions of computer modelling both in general and to this field specifically.

A timeline of key computational models relevant to CRC models appears in **Fig 1.3**.

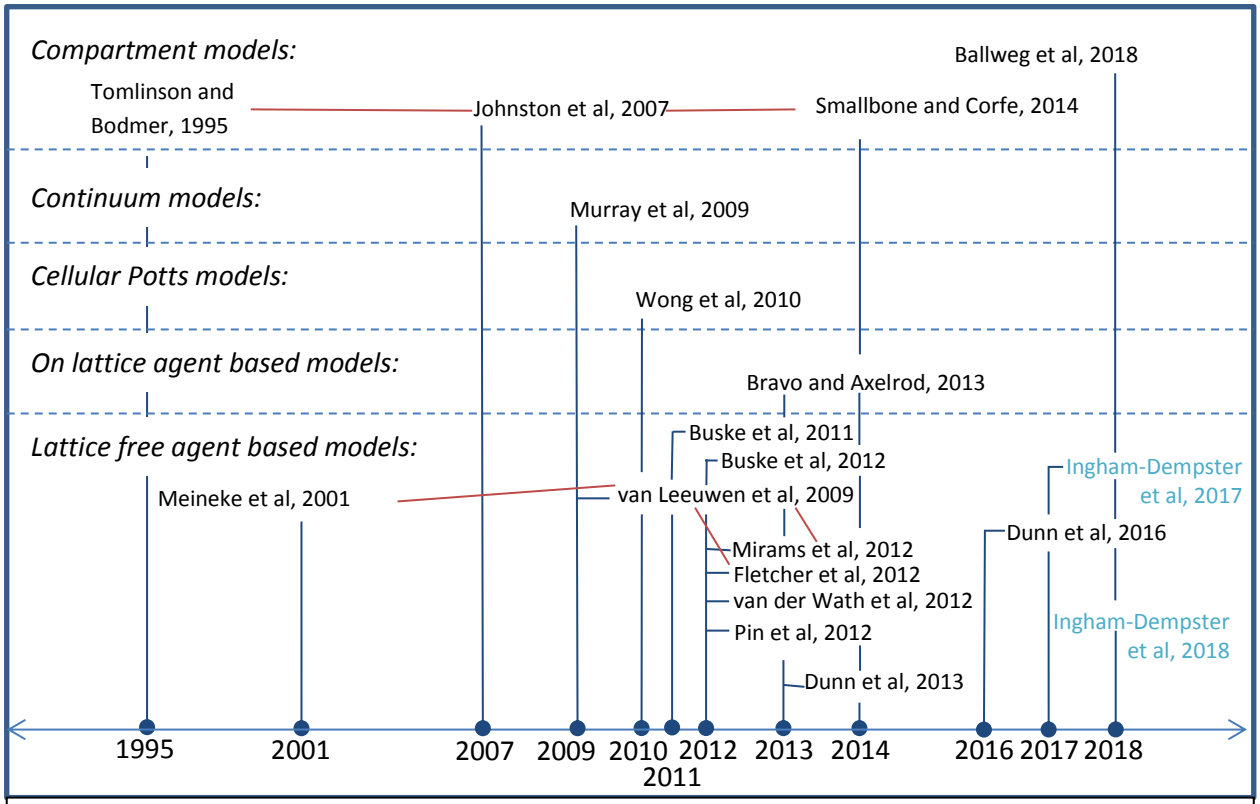

Figure 1.3: timeline of the key computational models. Papers connected by red lines indicate that the papers in question used the same base model with later papers extending and improving it. As can be seen the number of papers increases as we approach the present. This is to be expected from a relatively young field dependent on still maturing technology, and as more varied aspects of the biology are studied.

There are many different ways of representing a given biological system as a computational model, with each approach having different strengths and weaknesses. A number of these approaches have been applied to modelling colonic crypts:

1.1.1: Compartment Models

Compartment models divide the crypt into a number of populations, for example stem, transit amplifying, and differentiated cells. The size of those populations changes due to the transition of cells between the compartments. These transitions are governed by ordinary differential equations (ODEs) modelling known transition rates.

An early compartmental model looked at general tumour growth (Tomlinson and Bodmer, 1995). It resembled the crypt system but was designed to be suitable to study any tumour. It has three compartments, N_0 – stem cells, N_1 – proliferating cells and N_2 differentiated cells along with ordinary differential equations representing cells moving from one compartment to another. The main findings of this paper were from in-silico experiments studying the failure of apoptosis. They found that cells in N_0 failing to undergo apoptosis always results in exponential cell growth in a tumour like fashion. A counter intuitive finding was that cells in N_1 failing to undergo apoptosis may result in exponential growth or simply in expansion to a new equilibrium state.

This model (Tomlinson and Bodmer, 1995) was extended to account for asynchronous cell division (Johnston et al., 2007). They found that a crypt exhibiting the dynamics modelled was inherently unstable and could not be made to create a crypt in equilibrium. A system of feedback was required to simulate a crypt that did not expand exponentially or become extinct. They proposed two models of feedback. The first guaranteed crypts in equilibrium and so was not useful in modelling tumour-like exponential growth. The second allows for exponential growth via a series of ever increasing equilibrium points. This is described as the saturating feedback model. This feedback rule is speculative and not based on any known biology.

A later paper (Smallbone and Corfe, 2014) added an enteroendocrine compartment to the usual stem, proliferative and differentiated compartments of (Johnston et al., 2007). As well as being a different type of cell they consider EEC (entero-endocrine cells, a hormone-secreting cell within the crypt epithelium) cells to have an apoptosis inhibiting effect. This provides a feedback mechanism to regulate the overall crypt population, replacing the phenomenological saturating feedback from (Johnston et al., 2007). This model was shown to fit experimental data better than models without such feedback, suggesting an important role for EEC cells in regulating the crypt.

There are two major drawbacks to all compartment models. The first is that they cannot account for spatial phenomena. Since it is known that the crypt is spatially organised with stem cells at the bottom and differentiated cells at the top (Humphries and Wright, 2008) there are likely to be important effects that cannot be modelled this way.

The second major drawback is that any phenomena involving individual cells cannot be examined. One example of both of these drawbacks would be monoclonal conversion which was studied in an agent based model (Mirams et al., 2012) but could not be simulated by a compartment model.

One of the main advantages of such models is that they are very computationally efficient. This means that they can be used in situations where large numbers of runs are required.

1.1.2: Continuum Models

Continuum models are similar to compartment models in that they use equations to model populations of cells. They differ in that they account for the spatial positioning of the cell population. They model the population as a field of continuous properties somewhat similar to the modelling of heat or electric fields in engineering. This is generally done with a series of partial differential equations.

A model exists (Murray et al., 2010) that treats crypts as a line of cells with stem, proliferating and differentiated areas. It puts several of these crypts together. One way to think of an individual crypt in this model is that a cross-section of a crypt has been stretched into a flat line. In other words it is a one dimensional model. It was used to study levels of nuclear beta-catenin, i.e. the amount of the beta-catenin protein which had migrated to the nucleus of a cell, levels of which are a trigger for cell division. This model predicted nuclear beta-catenin distributions consistent with those of (van Leeuwen et al., 2009) which is to be expected as they use the same sub-cellular model. In silico experiments were performed which showed that increased proliferation alone is not sufficient to cause invasion from one crypt to another, with reduced apoptosis also being required.

Continuum models suffer from not being able to account for individual cells which could play an important role in cell signalling. They also generally involve complicated systems of equations which can be hard to modify to account for new data or to model new scenarios.

1.1.3: Individual cell models

There are a number of approaches which model individual cells interacting rather than cell populations. These include Cellular Potts Models, and Agent Based Models.

1.1.3.1: Cellular Potts Models

Cellular Potts models have been used to model systems from the sub-cellular to the multi-cellular level. These models use a stochastic method to minimise some target function rather than applying physical rules. For example, given a collection of cells at some point in time the goal of a simulation would be to calculate the configuration (i.e. the positions of the cells) at the next point in time. While a conventional simulation would do this by applying rules for forces and movement to the existing cell positions a Cellular Potts model would not, rather it would generate a number of candidate configurations by randomly perturbing the existing position of each cell. Each of these candidate configurations would then have the energy of that particular configuration measured and the configuration with the lowest energy would be chosen as the correct configuration (Graner and Glazier, 1992).

Cellular Potts models have been used to study intestinal crypts (Wong et al., 2010). They examined the mechanism by which Ephrin mediated differential adhesion causes cell sorting and migration. Ephrin receptor density was modelled as a monotonic gradient from strong at the top of the crypt to weak at the bottom. Eprhin ligand density was modelled as an opposing gradient which was weakest at the top and strongest at the bottom. This produced a function of Ephrin signalling which was strongest in the middle as the top lacked ligands and the bottom lacked receptors. Since Ephrin signalling causes repulsion, adhesion is strongest at the top and bottom where signalling is weakest. This causes cells to sort and cluster in a manner consistent with observed biology. Dysregulation of this system causes the intermixing of cell types observed in vivo by (Batlle et al., 2002). This is also the only simulation with a stable crypt naturally produced by the pedigree model of cell role. The pedigree model says that whether a cell acts as a stem, transit amplifying, or functional cell is determined at the point of cell division and is a function of the number of divisions a (non-stem) cell has undergone (Winton and Ponder, 1990). These crypts become unstable and rapidly become extinct in the case of dysregulation of adhesion. This is a known issue with the pedigree model. The results are a very good match for data gathered in vivo.

One problem with the Cellular Potts method is the computational cost. It requires multiple iterations per time step which makes it inherently slow. Another concern is the validity of reducing biological functions to an energy minimisation process.

2.1.3.2: Agent based

Agent based models model cells as individual agents that act according to predefined rules such as the cell cycle. By simulating these cells in an appropriate micro environment the dynamics of the crypt appear as emergent behaviour and can be studied, in particular it is possible to study interactions between different cells within a compartment, for example competition between wild-type and mutated cells or interactions between proliferative and differentiated cells. These types of interactions cannot be simulated with the model types discussed previously.

2.1.3.2.1: On lattice agent based models

On lattice models arrange the cells in a grid. Migration occurs by moving a cell from one grid square to another. They are sometimes erroneously referred to as cellular automata, the difference being that a cellular automaton has rules governing the state of fixed cells whereas on-lattice models have cells which are not fixed and can move between positions on the lattice.

One key lattice based model (Bravo and Axelrod, 2013) used an unwrapped cylinder mapped onto a 2d grid. Unusually migration is modelled from the top in that when cells die near the top of the crypt all cells in that column are pulled up one row rather than cells being pushed up from division events at the crypt bottom. This is based on findings by (Kaur and Potten, 1986) that cells continue to migrate even after proliferation has stopped. (Dunn et al., 2013) showed that this migration is probably due to relaxation of compressed cells but even if this had been known when the (Bravo and Axelrod, 2013) model was created it would be impossible to include this mechanism into a lattice based model.

The model replaces the Wnt gradient with a simplified gradient determining the probability that a cell will divide. It also includes a counter gradient giving the probability that a cell will die. There is a delayed response mechanism for division which prevents crypts from becoming extinct by stem cell loss. An added bonus of the delayed action is that division more closely matches the distribution of nuclear beta-catenin concentration suggested by (van Leeuwen et al., 2009)). These are all drastic simplifications but the purpose of this model was to be efficient enough to allow a search over a large parameter space.

The model was calibrated against biopsy data to produce accurate average numbers and variability of the simulated cell types. The results of various in silico experiments were then validated qualitatively by observing that they displayed many of the behaviours observed in crypts in vivo. These behaviours were the over-correction and then return to steady state observed in vivo after cytotoxic insult, and monoclonal conversion. The model reproduced both of these behaviours. They also claim to have modelled adenoma formation by mutants at different locations in the crypt but since this is still not properly understood in vivo it is questionable how useful this is for validation.

The calibrated model was then used to test a large number of potential protocols for the administration of chemotherapeutic drugs. These in silico experiments were used to suggest optimal timings and dosages for removal of mutant cell populations while minimising damage

to the normal mucosa. These are experiments that could not be performed in-vivo in humans for ethical reasons. Performing them on animal models would be difficult due to the large parameter space that would need to be searched.

One major downside of lattice based models is that they cannot simulate mechanical forces. This is because the cells are forced to move in coarse grained discrete jumps. This means that many behaviours such as passive migration in the absence of proliferation (Dunn et al., 2013) cannot be simulated and hence cannot be investigated.

2.1.3.2.2: Lattice free agent based models

Lattice free models allow the cells to move freely through space without being confined to a discrete grid or lattice. This allows mechanical effects and a wider range of cellular interactions to be simulated.

The model produced in (Meineke et al., 2001) is pivotal in the development of crypt models. For the first time cells were modelled as free agents moving on a surface rather than in a fixed grid. It also introduced the approach adopted by almost all lattice free models of the crypt since. The key points of this approach are modelling cell centres as points connected by springs and using a Delauny triangulation to determine cell-cell connections. Biological knowledge based on in vivo experiments has advanced significantly since this model was created which reveals limitation in some of its assumptions. Based on the best thinking of the time it assumes that a cell has a fixed proliferative status based on its generation whereas this idea has largely been left behind due to experiments such as (Van Landeghem et al., 2012) as well as theoretical work including (van der Wath et al., 2013). The model also assumes that stem cells are permanently attached to the crypt base which is called into question by the monoclonality of crypts (Novelli et al., 2003) since fixed stem cells would never be swept out of the crypt and so no one cell would be the progenitor of the entire crypt.

This model was extended by incorporating a sub-cellular level model (van Leeuwen et al., 2009). This was an ODE model which was already in existence (van Leeuwen et al., 2007). Stochasticity was added in the form of variable G1 times for the cells. Using this model they demonstrated that a cell's known interactions with Wnt combined with a spatial Wnt gradient accounted for the levels of nuclear beta-catenin observed in cells at various positions in the crypt. This is an important and non-trivial result as the levels observed in vivo are non-linear and do not correlate simply to the level of Wnt. They also performed in silico experiments comparing crypts under the pedigree conceptual model and those under the niche model. The niche model hypothesises that whether a cell behaves as a stem, transit amplifying, or differentiated cell is determined by signalling cues from its environment, and hence its position in the crypt (Potten and Loeffler, 1990). They found that the niche model produced more realistic crypts. These two findings counter two of the major arguments against the niche model.

This model was then further extended (Fletcher et al., 2012), with the simulation being changed to a 3d mesh rather than an unwrapped cylinder which produced more realistic niche geometry. Comparing this to the same simulation using cylindrical geometry they found that the realistic geometry took less time to achieve mononclonal conversion. This is because there are less stem cells competing with one another as the stem cell niche is smaller when using the more accurate fully 3d geometry. They also compared both models

to a compartment model and found that the compartmental model has a longer time until monoclonal conversion occurs. Both these results suggest that spatial considerations are important in crypt dynamics. The main purpose of this paper was to study the difference between the niche and pedigree models. To do this they had to make the pedigree stem cells have an active downward migration which is not based on any biological evidence. Even with these changes the pedigree crypts eventually became extinct on timescales short enough that it should be observed in-vivo whereas the niche model crypts were naturally stable.

Monoclonal conversion was investigated in a model (Mirams et al., 2012) which built on an earlier model (van Leeuwen et al., 2009). A series of in-silico experiments were performed which showed that crypts will always become monoclonal over time. The only cell behaviour required to cause this is proliferation below a certain height in the crypt and shedding at the top.

It was also shown that monoclonal conversion is a continuous phenomenon. Once a crypt is completely occupied by the progeny of a single cell one of those descendant cells will eventually come to dominate the crypt with its own progeny. This concept of continuous re-conversion is known as niche succession (Leedham, 2014).

Simulations examining the role of the starting position of the cell that eventually dominates the crypt show that it is unlikely to arise above the +2 position in the crypt (Fig 1.4). This model uses a cylindrical geometry and the +2 position is within the region where the model geometry differs greatly from the biological geometry, as such it would be interesting to see similar experiments done on a model with 3d crypt geometry.

The model showed that cells with a higher adhesion to the basement membrane had a higher chance of dominating the crypt. This is because the basement force slows them down so they spend longer in the crypt and can proliferate more. They are also more able to push cells with lower adhesion levels out of the crypt. This paper then described in silico experiments on the effect of differing proliferation heights on monoclonal conversion. It was found that a mutant cell which can continue proliferating higher into the crypt than the competing cells was more likely to dominate the crypt than cells with a lower proliferating ceiling. This effect reduces in strength after the proliferation ceiling reaches 50% of the crypt height. The interaction of proliferation ceiling and adhesion was investigated and it was found that adhesion advantages were unaffected by proliferation ceiling but that the advantages of an increased proliferation ceiling were reduced by an increase in adhesion. Finally it was shown that the progeny of a cell that has been swept out of the crypt can still come to dominate the crypt even if they do not already do so by the time the cell is swept out (Mirams et al., 2012).

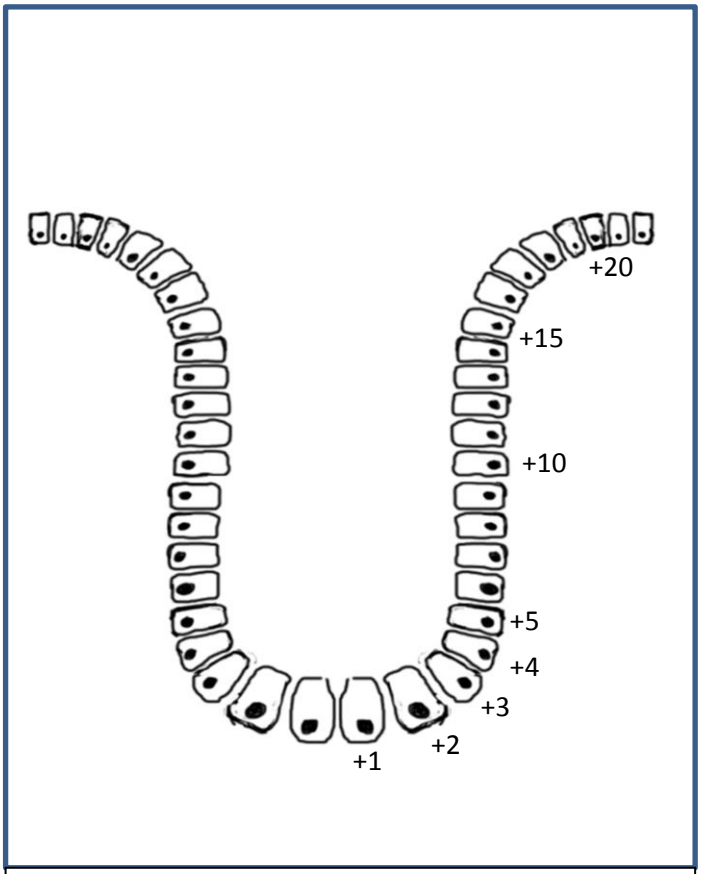

Figure 1.4: the position index system. Cells are indexed by how many cells they are from the crypt base.

A model by (Pin et al., 2012) accounts for the different cell lineages within the small intestinal crypt. Small intestinal crypts differ from those in the large intestine in that they contain a cell type, the Paneth cell, which large intestinal crypts do not. They are otherwise similar and so this model is relevant when studying CRC. It uses a model based on Wnt and Notch signalling to control differentiation and fate decisions. The resulting crypt has the correct distributions of cell types for a mouse small intestine. While this is described as a lattice free model that is only partially correct. It actually constrains the cells to a helical structure and instead of modelling forces when a cell divides, space for the new cell is created by moving every cell above the dividing one up one turn. This prevents its use in studying the mechanical phenomena present in the crypt. A good example of this is that Paneth cells move down without any active migration force as a consequence of the model design. The paper claims that this is how non-proliferating cells behave in vivo however in-vivo data (Batlle et al., 2002) suggest that these predictions may not be accurate. This model also does not simulate the effects of the different cell types. As an example (May and Kaestner, 2010) show that enteroendocrine cells have an effect on local rates of proliferation, and (Gulubova and Vlaykova, 2008) and (Yu et al., 2011) show that some EEC cells express molecules involved in apoptotic signalling. (Smallbone and Corfe, 2014) produced a compartmental model which showed these phenomena could provide a feedback

mechanism to regulate the crypt. It would be interesting to see how these ideas would affect crypt dynamics and a model such as (Pin et al., 2012) is the only one produced so far that models the different cell lineages in sufficient detail to investigate this.

A model was developed to compare the niche and pedigree conceptual models (van der Wath et al., 2013). Unusually this model uses an overlapping circles method rather than a Delauny triangulation. This means that any cells within a certain radius of each other are considered to be overlapping whereas other models use a meshing technique to find interacting cells. It was found that the niche model fitted observed data better and produced more ordered crypts. However (Holmberg et al., 2006) and (Batlle et al., 2002) show that in-vivo crypts are not naturally well ordered and require an EphB mediated sorting mechanism to maintain order so we appear to have one result favouring the niche concept and the other the pedigree concept. It is probable that the overly simplified version of the niche conceptual model used here is responsible for this discrepancy in the niche simulation model as (van Leeuwen et al., 2009) showed that nuclear beta-catenin is not directly proportional to extra cellular Wnt levels as assumed in this model. They also found that the pedigree model requires stem cells to be anchored to the crypt base to prevent them being flushed out of the crypt which would result in crypt extinction. This precludes the possibility of niche succession and monoclonal conversion of the crypt. They suggest mechanisms by which the pedigree concept could be altered to allow these phenomena by making it more niche-like.

The model of (Dunn et al., 2013), explained a phenomenon that could have cast doubt on the validity of most existing models. All the lattice free models described here assume that the migration of cells up the crypt is due to pressure from mitosis of cells at the bottom. (Kaur and Potten, 1986) showed that migration continues to occur even after all mitosis has been stopped. (Dunn et al., 2013) performed an in silico recreation of the (Kaur and Potten, 1986) experiment using three different models, all of which assumed passive migration due to mitotic pressure. They obtained results in good agreement with those of (Kaur and Potten, 1986) and conclude that the continued migration was due to the relaxation of cells that had been under compression. By using three separate models and obtaining very similar results they minimised the chance that the post-mitotic migration was due to a model artefact. They did not address the sorting effect due to EphB signalling reported in (Holmberg et al., 2006) and (Batlle et al., 2002).

1.2: Summary

Simulation models have achieved a great deal. From elucidating a mechanism by which passive migration can occur after proliferation (Dunn et al., 2013) to discovering emergent processes relating to mutation fixation (van Leeuwen et al., 2006) and studying in depth the implications of those same processes (Mirams et al., 2012). There is however still much that is not fully understood:

- It is not known how crypts regulate their cellularity. As the accretion of excess cells is a key behaviour of all cancers, including CRCs this is an important aspect of crypt homeostasis which is currently underrepresented in the literature.

- Another aspect that has not been modelled is how neoplastic crypts interact with healthy crypts. To do this a model would need to be created that simulates multiple crypts. Whilst (Murray et al., 2010) modelled multiple crypts they did so in a one

dimensional continuum model which was limited to a very specific subset of crypt behaviour. A model of multiple crypts as agents would allow tissue dynamics to be studied both for healthy tissue and for tissue with one or more neoplastic crypts. This model would have to model crypts at a cellular level to determine factors such as overall forces acting on the crypt and to signal fission events. Such a model would have to include crypt feedback regulation to simulate crypt growth. As this is such an untapped area there are surely novel and valuable insights to be gained by studying it.

- No large scale models of the colon have been attempted, since mutated fields are known to develop over multiple decades of time and cover tens of thousands of crypts studying the dynamics of mutated crypts over these scales should produce novel insights.

1.3: Aims and Objectives

Section 1.2 makes it clear that there are gaps in the literature related to the colonic crypt, the processes within it, and the dysregulations which give rise to CRC. This project aims to investigate the following under-studied biological questions related to the spread of pre-cancerous fields:

- What are the relative contributions of crypt fission and crypt invasion in field spread?
- What are the consequences of multiple fields interacting?
- What effect does an APC mutation in a crypt have on the neighbouring wild-type crypts?

To achieve this aim, models will be built on multiple scales. One scale will model the crypt as an environment containing cells with each cell represented as an individual agent. Another scale will model a larger section of tissue with each crypt being represented as a single agent. This multi-scale model will provide a tool to explore hypotheses related to the questions above.

The following objectives will be met to achieve this:

1. Create a model of a single crypt with cells as agents
2. Calibrate and validate this model
3. Use this to model the process of mutation fixation via niche succession
4. Model up to 100 crypts interacting with each other at this scale and test the assumption that the computational cost of thousands of crypts will be prohibitive
5. Abstract behavioural rules for crypts as agents from the cell as agent model
6. Develop a model at the tissue scale with crypts as agents
7. Model field cancerisation at this level

1.4: References

BAKER, A.-M., CERESER, B., MELTON, S., FLETCHER, A. G., RODRIGUEZ-JUSTO, M., TADROUS, P. J., HUMPHRIES, A., ELIA, G., MCDONALD, S. A. C., WRIGHT, N. A., SIMONS, B. D., JANSEN, M. & GRAHAM, T. A. 2014. Quantification of Crypt and Stem Cell Evolution in the Normal and Neoplastic Human Colon. *Cell Reports,* 8**,** 940-947.

BARKER, N., VAN ES, J. H., KUIPERS, J., KUJALA, P., VAN DEN BORN, M., COZIJNSEN, M., HAEGEBARTH, A., KORVING, J., BEGTHEL, H., PETERS, P. J. & CLEVERS, H. 2007. Identification of stem cells in small intestine and colon by marker gene Lgr5. *Nature,* 449**,** 1003-U1.

BATLLE, E., HENDERSON, J. T., BEGHTEL, H., VAN DEN BORN, M. M. W., SANCHO, E., HULS, G., MEELDIJK, J., ROBERTSON, J., VAN DE WETERING, M., PAWSON, T. & CLEVERS, H. 2002. beta-catenin and TCF mediate cell positioning in the intestinal epithelium by controlling the expression of EphB/EphrinB. *Cell,* 111**,** 251-263.

BRAVO, R. & AXELROD, D. E. 2013. A calibrated agent-based computer model of stochastic cell dynamics in normal human colon crypts useful for in silico experiments. *Theoretical Biology and Medical Modelling,* 10**,** 24.

CARROLL, T. D., LANGLANDS, A. J., OSBORNE, J. M., NEWTON, I. P., APPLETON, P. L. & NATHKE, I. 2017. Interkinetic nuclear migration and basal tethering facilitates post-mitotic daughter separation in intestinal organoids. *Journal of Cell Science,* 130**,** 3862-3877.

CHENG, H., BJERKNES, M. & AMAR, J. 1984. METHODS FOR THE DETERMINATION OF EPITHELIAL-CELL KINETIC-PARAMETERS OF HUMAN COLONIC EPITHELIUM ISOLATED FROM SURGICAL AND BIOPSY SPECIMENS. *Gastroenterology,* 86**,** 78-85.

CHENG, H. & LEBLOND, C. P. 1974. ORIGIN, DIFFERENTIATION AND RENEWAL OF 4 MAIN EPITHELIAL-CELL TYPES IN MOUSE SMALL INTESTINE .5. UNITARIAN THEORY OF ORIGIN OF 4 EPITHELIAL-CELL TYPES. *American Journal of Anatomy,* 141**,** 537-&.

DUNN, S.-J., NAETHKE, I. S. & OSBORNE, J. M. 2013. Computational Models Reveal a Passive Mechanism for Cell Migration in the Crypt. *Plos One,* 8.

FLETCHER, A. G., BREWARD, C. J. W. & CHAPMAN, S. J. 2012. Mathematical modeling of monoclonal conversion in the colonic crypt. *Journal of Theoretical Biology,* 300**,** 118-133.

GENANDER, M., HALFORD, M. M., XU, N.-J., ERIKSSON, M., YU, Z., QIU, Z., MARTLING, A., GREICIUS, G., THAKAR, S., CATCHPOLE, T., CHUMLEY, M. J., ZDUNEK, S., WANG, C., HOLM, T., GOFF, S. P., PETTERSSON, S., PESTELL, R. G., HENKEMEYER, M. & FRISEN, J. 2009. Dissociation of EphB2 Signaling Pathways Mediating Progenitor Cell Proliferation and Tumor Suppression. *Cell,* 139**,** 679-692.

GRABINGER, T., LUKS, L., KOSTADINOVA, F., ZIMBERLIN, C., MEDEMA, J. P., LEIST, M. & BRUNNER, T. 2014. Ex vivo culture of intestinal crypt organoids as a model system for assessing cell death induction in intestinal epithelial cells and enteropathy. *Cell Death & Disease,* 5.

GRANER, F. & GLAZIER, J. A. 1992. SIMULATION OF BIOLOGICAL CELL SORTING USING A 2-DIMENSIONAL EXTENDED POTTS-MODEL. *Physical Review Letters,* 69**,** 2013-2016.

GULUBOVA, M. & VLAYKOVA, T. 2008. Chromogranin A-, serotonin-, synaptophysin- and vascular endothelial growth factor-positive endocrine cells and the prognosis of colorectal cancer: An immunohistochemical and ultrastructural study. *Journal of Gastroenterology and Hepatology,* 23**,** 1574-1585.

HOLMBERG, J., GENANDER, M., HALFORD, M. M., ANNEREN, C., SONDELL, M., CHUMLEY, M. J., SILVANY, R. E., HENKEMEYER, M. & FRISEN, J. 2006. EphB receptors coordinate migrationand proliferation in the intestinal stem cell niche. *Cell,* 125**,** 1151-1163.

HUMPHRIES, A. & WRIGHT, N. A. 2008. Colonic crypt organization and tumorigenesis. *Nature Reviews Cancer,* 8**,** 415-424.

INGHAM-DEMPSTER, T., WALKER, D. C. & CORFE, B. M. 2017. An agent-based model of anoikis in the colon crypt displays novel emergent behaviour consistent with biological observations. Royal Society Open Science: The Royal Society Publishing.

JOHNSTON, M. D., EDWARDS, C. M., BODMER, W. F., MAINI, P. K. & CHAPMAN, S. J. 2007. Mathematical modeling of cell population dynamics in the colonic crypt and in colorectal cancer. *Proceedings of the National Academy of Sciences of the United States of America,* 104**,** 4008-4013.

KAUR, P. & POTTEN, C. S. 1986. CELL-MIGRATION VELOCITIES IN THE CRYPTS OF THE SMALL-INTESTINE AFTER CYTOTOXIC INSULT ARE NOT DEPENDENT ON MITOTIC-ACTIVITY. *Cell and Tissue Kinetics,* 19**,** 601-610.

LANGLANDS, A. J., ALMET, A. A., APPLETON, P. L., NEWTON, I. P., OSBORNE, J. M. & NATHKE, I. S. 2016. Paneth Cell-Rich Regions Separated by a Cluster of Lgr5+Cells Initiate Crypt Fission in the Intestinal Stem Cell Niche. *Plos Biology,* 14.

LEEDHAM, S. J. 2014. Measuring stem cell dynamics in the human colon - where there's a wiggle, there's a way. *The Journal of pathology,* 234**,** 292-5.

MAY, C. L. & KAESTNER, K. H. 2010. Gut endocrine cell development. *Molecular and Cellular Endocrinology,* 323**,** 70-75.

MEINEKE, F. A., POTTEN, C. S. & LOEFFLER, M. 2001. Cell migration and organization in the intestinal crypt using a lattice-free model. *Cell Proliferation,* 34**,** 253-266.

MERRITT, A. J., GOULD, K. A. & DOVE, W. F. 1997. Polyclonal structure of intestinal adenomas in Apc-(Min)/+ mice with concomitant loss of Apc(+) from all tumor lineages. *Proceedings of the National Academy of Sciences of the United States of America,* 94**,** 13927-13931.

MIRAMS, G. R., FLETCHER, A. G., MAINI, P. K. & BYRNE, H. M. 2012. A theoretical investigation of the effect of proliferation and adhesion on monoclonal conversion in the colonic crypt. *Journal of Theoretical Biology,* 312**,** 143-156.

MURRAY, P. J., KANG, J.-W., MIRAMS, G. R., SHIN, S.-Y., BYRNE, H. M., MAINI, P. K. & CHO, K.-H. 2010. Modelling Spatially Regulated beta-Catenin Dynamics and Invasion in Intestinal Crypts. *Biophysical Journal,* 99**,** 716-725.

NOVELLI, M., COSSU, A., OUKRIF, D., QUAGLIA, A., LAKHANI, S., POULSOM, R., SASIENI, P., CARTA, P., CONTINI, M., PASCA, A., PALMIERI, G., BODMER, W., TANDA, F. & WRIGHT, N. 2003. X-inactivation patch size in human female tissue confounds the assessment of tumor clonality. *Proceedings of the National Academy of Sciences of the United States of America,* 100**,** 3311-3314.

NOVELLI, M. R., WILLIAMSON, J. A., TOMLINSON, I. P. M., ELIA, G., HODGSON, S. V., TALBOT, I. C., BODMER, W. F. & WRIGHT, N. A. 1996. Polyclonal origin of colonic adenomas in an XO/XY patient with FAP. *Science,* 272**,** 1187-1190.

PIN, C., WATSON, A. J. M. & CARDING, S. R. 2012. Modelling the Spatio-Temporal Cell Dynamics Reveals Novel Insights on Cell Differentiation and Proliferation in the Small Intestinal Crypt. *Plos One,* 7.

POTTEN, C. S. 1998. Stem cells in gastrointestinal epithelium: numbers, characteristics and death. *Philosophical Transactions of the Royal Society B-Biological Sciences,* 353**,** 821-830.

POTTEN, C. S. & LOEFFLER, M. 1990. STEM-CELLS - ATTRIBUTES, CYCLES, SPIRALS, PITFALLS AND UNCERTAINTIES - LESSONS FOR AND FROM THE CRYPT. *Development,* 110**,** 1001-1020.

PRESTON, S. L., WONG, W. M., CHAN, A. O. O., POULSOM, R., JEFFERY, R., GOODLAD, R. A., MANDIR, N., ELIA, G., NOVELLI, M., BODMER, W. F., TOMLINSON, I. P. & WRIGHT, N. A. 2003. Bottom-up histogenesis of colorectal adenomas: Origin in the monocryptal adenoma and initial expansion by crypt fission. *Cancer Research,* 63**,** 3819-3825.

RITSMA, L., ELLENBROEK, S. I. J., ZOMER, A., SNIPPERT, H. J., DE SAUVAGE, F. J., SIMONS, B. D., CLEVERS, H. & VAN RHEENEN, J. 2014. Intestinal crypt homeostasis revealed at single-stem-cell level by in vivo live imaging. *Nature,* 507**,** 362-+.

SANSOM, O. J., REED, K. R., HAYES, A. J., IRELAND, H., BRINKMANN, H., NEWTON, I. P., BATLLE, E., SIMON-ASSMANN, P., CLEVERS, H., NATHKE, I. S., CLARKE, A. R. & WINTON, D. J. 2004. Loss of Apc in vivo immediately perturbs Wnt signaling, differentiation, and migration. *Genes & Development,* 18**,** 1385-1390.

SHIH, I.-M., WANG, T.-L., TRAVERSO, G., ROMANS, K., HAMILTON, S. R., BEN-SASSON, S., KINZLER, K. W. & VOGELSTEIN, B. 2001. Top-down morphogenesis of colorectal tumors. *Proceedings of the National Academy of Sciences of the United States of America,* 98**,** 2640-2645.

SMALLBONE, K. & CORFE, B. M. 2014. A mathematical model of the colon crypt capturing compositional dynamic interactions between cell types. *International Journal of Experimental Pathology,* 95**,** 1-7.

SNIPPERT, H. J., VAN DER FLIER, L. G., SATO, T., VAN ES, J. H., VAN DEN BORN, M., KROON-VEENBOER, C., BARKER, N., KLEIN, A. M., VAN RHEENEN, J., SIMONS, B. D. & CLEVERS, H. 2010. Intestinal Crypt Homeostasis Results from Neutral Competition between Symmetrically Dividing Lgr5 Stem Cells. *Cell,* 143**,** 134-144.

STRATER, J., KORETZ, K., GUNTHERT, A. R. & MOLLER, P. 1995. In-Situ Detection of Enterocytic Apoptosis in Normal Colonic Mucosa and in Familial Adenomatous Polyposis. *Gut,* 37**,** 819-825.

TOMLINSON, I. P. M. & BODMER, W. F. 1995. FAILURE OF PROGRAMMED CELL-DEATH AND DIFFERENTIATION AS CAUSES OF TUMORS - SOME SIMPLE MATHEMATICAL-MODELS. *Proceedings of the National Academy of Sciences of the United States of America,* 92**,** 11130-11134.

VAN DER WATH, R. C., GARDINER, B. S., BURGESS, A. W. & SMITH, D. W. 2013. Cell Organisation in the Colonic Crypt: A Theoretical Comparison of the Pedigree and Niche Concepts. *Plos One,* 8.

VAN LANDEGHEM, L., SANTORO, M. A., KREBS, A. E., MAH, A. T., DEHMER, J. J., GRACZ, A. D., SCULL, B. P., MCNAUGHTON, K., MAGNESS, S. T. & LUND, P. K. 2012. Activation of two distinct Sox9-EGFP-expressing intestinal stem cell populations during crypt regeneration after irradiation. *American Journal of Physiology-Gastrointestinal and Liver Physiology,* 302**,** G1111-G1132.

VAN LEEUWEN, I. M. M., BYRNE, H. M., JENSEN, O. E. & KING, J. R. 2006. Crypt dynamics and colorectal cancer: advances in mathematical modelling. *Cell Proliferation,* 39**,** 157-181.

VAN LEEUWEN, I. M. M., BYRNE, H. M., JENSEN, O. E. & KING, J. R. 2007. Elucidating the interactions between the adhesive and transcriptional functions of beta-catenin in normal and cancerous cells. *Journal of theoretical biology,* 247**,** 77-102.

VAN LEEUWEN, I. M. M., MIRAMS, G. R., WALTER, A., FLETCHER, A., MURRAY, P., OSBORNE, J., VARMA, S., YOUNG, S. J., COOPER, J., DOYLE, B., PITT-FRANCIS, J., MOMTAHAN, L., PATHMANATHAN, P., WHITELEY, J. P., CHAPMAN, S. J., GAVAGHAN, D. J., JENSEN, O. E., KING, J. R., MAINI, P. K., WATERS, S. L. & BYRNE, H. M. 2009. An integrative computational model for intestinal tissue renewal. *Cell Proliferation,* 42**,** 617-636.

WASAN, H. S., PARK, H. S., LIU, K. C., MANDIR, N. K., WINNETT, A., SASIENI, P., BODMER, W. F., GOODLAD, R. A. & WRIGHT, N. A. 1998. APC in the regulation of intestinal crypt fission. *Journal of Pathology,* 185**,** 246-255.

WINTON, D. J. & PONDER, B. A. J. 1990. STEM-CELL ORGANIZATION IN MOUSE SMALL-INTESTINE. *Proceedings of the Royal Society B-Biological Sciences,* 241**,** 13-18.

WONG, S. Y., CHIAM, K. H., LIM, C. T. & MATSUDAIRA, P. 2010. Computational model of cell positioning: directed and collective migration in the intestinal crypt epithelium. *Journal of the Royal Society Interface,* 7**,** S351-S363.

YU, D. C. W., BURY, J. P., TIERNAN, J., WABY, J. S., STATON, C. A. & CORFE, B. M. 2011. Short-chain fatty acid level and field cancerization show opposing associations with enteroendocrine cell number and neuropilin expression in patients with colorectal adenoma. *Molecular Cancer,* 10.

Chapter 2: An Agent Based Model of Anoikis in the Colon Crypt Displays Novel Emergent Behaviour Consistent with Biological Observations

This chapter is in the form of a paper which was published in the journal Royal Society Open Science in 2017. This paper describes the cell level model which was developed for the project, the main novel features of this model were a representation of the crypt mouth and rules simulating a mechanism for cell death through anoikis. The model is shown to recapitulate predictions from previous models for the commonly observed phenomena of passive migration and niche succession.

The objective of this study was to investigate the effect of dysregulation of cell production rates on homeostasis within the crypt. The model predicted a feedback mechanism which would upregulate anoikis rates in response to higher cell division rates. This mechanism appears to be novel in the literature.

The model was developed by myself and I conducted the simulations and data analysis, I also wrote the paper and produced the diagrams. My supervisors gave guidance on the design of the study and acted as editors for the paper.

Since the publication of this paper it has been pointed out that several improvements could be made to table 2, in particular since the lengths are in arbitrary units one of the parameters should be scaled to unity, that the attachment strength parameter should have units specified, and that the length of the stem cell quiescent time should be justified. To preserve the paper as it was published the modified entries are reproduced here:

Crypt radius	1.0
Crypt height	11.8 crypt radii
Anoikis threshold	0.2 crypt radii
Differentiation boundary	3.6 crypt radii
Proliferation boundary	0.6 crypt radii
Attachment strength	0.01-0.0001
G_0 time	270h

The attachment strength parameter corresponds to the parameter α in (Meineke et al., 2001, Mirams et al., 2012) and, as in those studies, is unitless.

The value of G_0 time was based on the observation that only one in ten cells in the crypt niche is in cycle at once (Baker et al., 2014). Whilst it is likely that in-vivo there is a population of stem cells which are permanently in G_0 and a smaller population that is in constant cycle, it was a better fit for the model to produce the same average number of division events over a given period of time by having every cell alternate between cycling and quiescent behaviour, with the quiescent phase being nine times the length of the cycle time of 30 hours, which was also taken from the literature (Potten et al., 1992).

BAKER, A.-M., CERESER, B., MELTON, S., FLETCHER, A. G., RODRIGUEZ-JUSTO, M., TADROUS, P. J., HUMPHRIES, A., ELIA, G., MCDONALD, S. A. C., WRIGHT, N. A., SIMONS, B. D., JANSEN, M. & GRAHAM, T. A. 2014. Quantification of Crypt and Stem Cell Evolution in the Normal and Neoplastic Human Colon. *Cell Reports,* 8**,** 940-947.

MEINEKE, F. A., POTTEN, C. S. & LOEFFLER, M. 2001. Cell migration and organization in the intestinal crypt using a lattice-free model. *Cell Proliferation,* 34**,** 253-266.

MIRAMS, G. R., FLETCHER, A. G., MAINI, P. K. & BYRNE, H. M. 2012. A theoretical investigation of the effect of proliferation and adhesion on monoclonal conversion in the colonic crypt. *Journal of Theoretical Biology,* 312**,** 143-156.

POTTEN, C. S., KELLETT, M., ROBERTS, S. A., REW, D. A. & WILSON, G. D. 1992. Measurement of

Downloaded from http://rsos.royalsocietypublishing.org/ on June 2, 2018

ROYAL SOCIETY OPEN SCIENCE

rsos.royalsocietypublishing.org

Research

Cite this article: Ingham-Dempster T, Walker DC, Corfe BM. 2017 An agent-based model of anoikis in the colon crypt displays novel emergent behaviour consistent with biological observations. *R. Soc. open sci.* **4**: 160858. http://dx.doi.org/10.1098/rsos.160858

Received: 26 October 2016
Accepted: 14 March 2017

Subject Category:
Cellular and molecular biology

Subject Areas:
synthetic biology/theoretical biology

Keywords:
agent-based model, colonic crypt, anoikis, homeostasis

Author for correspondence:
Bernard M. Corfe
e-mail: b.m.corfe@sheffield.ac.uk

†These authors contributed equally to this study.

Electronic supplementary material is available online at https://dx.doi.org/10.6084/m9.figshare.c.3729919.

THE ROYAL SOCIETY PUBLISHING

An agent-based model of anoikis in the colon crypt displays novel emergent behaviour consistent with biological observations

Tim Ingham-Dempster[1,2], Dawn C. Walker[1,3,†] and Bernard M. Corfe[1,2,†]

[1]Insigneo Institute for in silico medicine, Pam Liversedge Building, University of Sheffield, Sir Frederick Mappin Building, Mappin Street, Sheffield S1 3JD, UK
[2]Department of Oncology and Metabolism, The Medical School, University of Sheffield, Beech Hill Road, Sheffield S10 2RX, UK
[3]Department of Computer Science, University of Sheffield, 211 Portobello, Sheffield S1 4DP, UK

BMC, 0000-0003-0449-2228

Colorectal cancer (CRC) is a major cause of cancer mortality. Colon crypts are multi-cellular flask-shaped invaginations of the colonic epithelium, with stem cells at their base which support the continual turnover of the epithelium with loss of cells by anoikis from the flat mucosa. Mutations in these stem cells can become embedded in the crypts, a process that is strongly implicated in CRC initiation. We describe a computational model which includes novel features, including an accurate representation of the geometry of the crypt mouth. Model simulations yield previously unseen emergent phenomena, such as localization of cell death to a small region of the crypt mouth which corresponds with that observed *in vivo*. A mechanism emerges in the model for regulation of crypt cellularity in response to changes in either cell proliferation rates or membrane adhesion strengths. We show that cell shape assumptions influence this behaviour, with cylinders recapitulating biology better than spheres. Potential applications of the model include determination of roles of mutations in neoplasia and exploring factors for altered crypt morphodynamics.

1. Introduction

The human large intestine consists of a monolayer epithelium covering a flat mucosal surface punctuated by glands known as the crypts of Lieberkühn (figure 1*a*). These crypts are the

© 2017 The Authors. Published by the Royal Society under the terms of the Creative Commons Attribution License http://creativecommons.org/licenses/by/4.0/, which permits unrestricted use, provided the original author and source are credited.

Downloaded from http://rsos.royalsocietypublishing.org/ on June 2, 2018

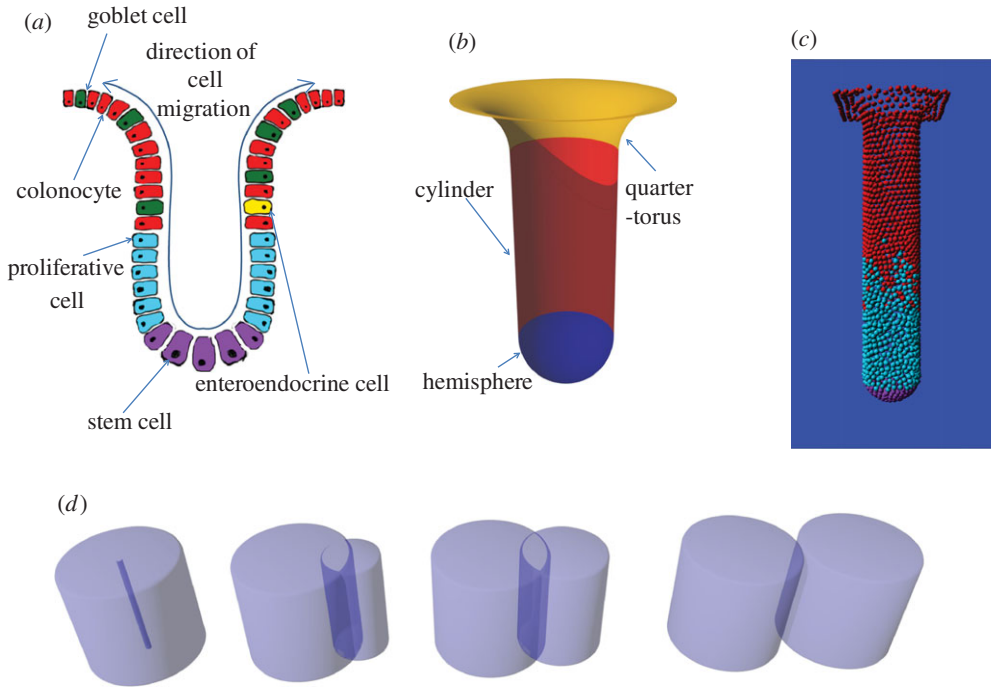

Figure 1. (*a*) Crypts act as cell factories. Stem cells divide at the bottom to provide cells for the proliferating compartment. Cells in the proliferating compartment divide rapidly to provide the various cell types for the constantly refreshing colonic epithelium. (*b*) Visualization of the model crypt membrane. The geometry is modelled as three mathematical shapes, a hemisphere, a cylinder and a quarter torus. (*c*) An image taken from the model during a simulation. (*d*) The process of cell division within the model where a second cell is created, initially with zero radius. As the parent cell shrinks back to its normal volume from the enlarged volume it has at the end of G phase, the new cell expands to the same size and finally detaches. This process takes place through the dividing cell's M phase.

functional unit of the colonic epithelium, supporting the rapid turnover of cells in the organ through constant division and differentiation of stem cells located at their base. As such, the perturbation of their turnover and abnormal accumulation of cells is implicated in the formation of colorectal cancer (CRC) [1]. The identification and modelling of underlying processes is therefore crucial to understanding the pathophysiology of disease.

A human colonic crypt contains approximately 2500 cells, or colonocytes [2]. There is a stem cell compartment at the base of the crypt which is estimated to comprise around 10 cells [3]. Cells exiting the stem cell compartment (variously called transit amplifying cells or proliferating cells) account for around 25% of cells in the crypt [4]. Fully differentiated cells include water-absorbing colonocytes which account for roughly 75% of differentiated cells, mucus secreting goblet cells which account for roughly 24% of differentiated cells and hormone secreting enteroendocrine cells which differentiate directly from stem cells rather than from transit amplifying cells and account for less than 1% of differentiated cells [2,5]. There are two main hypotheses concerning the processes governing whether a cell exhibits stem, proliferating, or differentiated behaviour: the *niche* hypothesis suggests that location within the crypt determines cell type, whereas according to the *pedigree* hypothesis cell type is a function of the number of divisions a cell has undergone [6]. Cells migrate from the bottom of the crypt to the top. This movement has been shown to occur even after proliferation stops [7] and to be partially organized by EphB signalling [8,9]. Apoptotic rates are highest at the top of the crypt [10]. A key mechanism of apoptosis within the normal homeostatic epithelium is anoikis [11], whereby loss of contact with the extracellular matrix induces apoptosis. This is known to occur in colonic crypts and its dysregulation is thought to play a role in CRC progression [12] and crypt homeostasis [13].

1.1. Computational modelling

A range of computational models have been applied to crypt dynamics, which vary in terms of their basic assumptions, underlying methodologies and degree of spatial resolution. Compartment models consider the composite behaviour of different populations of cells within the crypt. An early

Downloaded from http://rsos.royalsocietypublishing.org/ on June 2, 2018

compartmental model simulated general tumour growth but was directly applicable to the crypt system [14]. It comprised three compartments, stem cells, proliferating cells and differentiated cells, and implemented rules governing the growth and interactions between these populations in the form of ordinary differential equations (ODEs). Individual cells were not modelled, but rather the total number of cells in each compartment. This model focused on the role of changes to apoptosis and differentiation in tumour formation. It predicted that changes in these processes would lead to increasing plateaus of cellularity before exponential cell growth would occur. The crypt has also been modelled as a continuum [15] using partial differential equations to represent the spatial distribution of the different cell compartments. In this context, cells are still modelled as populations rather than discrete entities. This model was used to investigate the possibility of a neoplastic crypt invading a neighbouring healthy crypt. The model predicted that this type of invasion is a possible mechanism for expansion of the neoplastic tissue.

The first models to consider cells as individual entities were lattice based models—an approach still in use due to its computational efficiency [4]. Here the crypt is modelled as a lattice, or grid, where each lattice point or node can be occupied by a cell. The limitation here is that cells can only move between lattice sites in discrete jumps, meaning intercellular interactions and forces cannot be explicitly considered. The Bravo & Axelrod model [4] focused on calibrating emergent cell turnover rates against known biological parameters and was used to assess various chemotherapeutic protocols from a theoretical viewpoint. Early agent-based models (ABMs) for the first time represented cells as free agents moving on a surface rather than in a fixed grid [16]. These models built on lattice free models of generic epithelial monolayers [17]. Each cell acts as an independent agent with no globally overarching control. This approach is appealing for biological modelling as it captures the nature of biological cells as individual autonomous entities that can respond to signalling cues, and also allows the modeller to capture the important concept of intercellular heterogeneity [18].

Buske *et al.* [19] developed a sophisticated model of the crypt which made a number of predictions about the behaviour of cell populations in the crypt. In particular it showed that cell populations can be regenerated within a crypt even after population extinction. Although this model incorporated the concept of anoikis, the crypt mouth was not included with cells being automatically killed at a certain height from the crypt base.

In most existing models cell death is not explicitly related to a biological mechanism, but there are attempts to capture phenomenologically the known behaviour that cells predominantly die at the top of the crypt. For instance, a deterministic cell death rule is activated as soon as a cell reaches the top of the crypt [16], or cells die stochastically with a probability that increases towards the crypt top [4].

Dunn *et al.* [20] used an agent-based model to examine the role of the basement membrane in crypt formation and also included the concept of anoikis. The model predicted that while anoikis did occur at the crypt mouth, it was also seen throughout the crypt and was most prominent at the crypt base. As such, there was no significant cell migration in the simulated crypt and a rule dictating cell death at the crypt mouth was introduced to give rise to the correct migration behaviour. This could be explained by a putative signalling-related regulatory mechanism at the crypt mouth; however, there is currently no biological evidence for or against such a mechanism.

For a further overview of crypt modelling see Fletcher *et al.* [21].

We sought to develop an ABM in order to explore factors governing cellular homeostasis in the colon crypt, including an explicit representation of the anoikis mechanism. In particular, we hoped to establish whether the anoikis mechanism is sufficient to localize cell death to the crypt mouth and to regulate crypt cellularity without an external control mechanism. Unlike most previous models, we also include a realistic crypt geometry incorporating a section of flat mucosa above the crypt mouth.

2. Methods

This model is described using the Overview, Design concepts and Description (ODD) framework [22].

2.1. Purpose

The purpose of the model is to investigate the process of anoikis within the colonic crypt. This will be achieved by developing a lattice free model of the crypt similar to previous models [16,23,24]. This model will then be extended to include features which are hypothesized to be important factors in the anoikis process such as the geometry of the crypt top and the attachment force between cells and the basement membrane.

Downloaded from http://rsos.royalsocietypublishing.org/ on June 2, 2018

Table 1. Per-cell variables, including usage and source where relevant.

variable	use	source
position	cell position	emergent property, initially random
radius	cell radius	calculated from crypt radius and data from the literature [10]
current cycle time	How long has the cell been in the current cycle stage?	emergent property
cycle stage	the current stage of the cell in the model cell cycle	emergent property
growth stage time	length of growth cycle stage for this cell	drawn from a normal distribution with mean of 30 h and s.d. of 2.62 h [10]

Table 2. Simulation parameters, including usage and source where relevant.

property	use	source	default value
timestep	number of seconds per timestep	value determined to achieve stable simulation	30 s
G0-phase time	length of time a stem cell spends in quiescence before cell cycle re-entry	value determined from average cycle time (30 h) and number of stem cells biologically expected to be in cycle simultaneously (1 in 10), both taken from the literature [10]	270 h
M-phase time	length of time it takes a cell to divide	calculated from mean cycle time and proportion of cycling cells in M-phase in published literature from biological study [25]	20 min
crypt radius	radius of the vertical portion of the crypt	arbitrary property that all other sizes are calculated relative to	500[a]
crypt height	the total height of the crypt	calculated from cell radius and data in the literature [10]	5918[a]
anoikis threshold	minimum separation required to trigger anoikis	arbitrary value (sensitivity analysis showed no effect on simulation results, see electronic supplementary material)	100[a]
differentiation boundary	position relative to crypt height at which cells stop proliferating	set manually to match qualitative data from the literature [4]	1776[a]
proliferation boundary	position relative to crypt height of switch between stem and proliferating cells	set manually to match qualitative data from the literature [10]	296[a]
attachment strength	the strength of the cell binding to the basement membrane	range determined by parameter tuning (see Results section)	0.01–0.0001[b]

[a]Distances in the model are expressed in arbitrary units as all scales are calculated relative to crypt radius.
[b]Unitless parameter.

2.2. Entities, state variables and scales

Entities in the model represent the cells of the colorectal crypt. Agent state variables are listed in table 1 and global state variables are listed in table 2.

2.3. Process overview and scheduling

The model updates in a series of discrete timesteps, each representing 30 seconds of biological time. At each timestep a series of separate rules are applied (figure 2*a*).

Downloaded from http://rsos.royalsocietypublishing.org/ on June 2, 2018

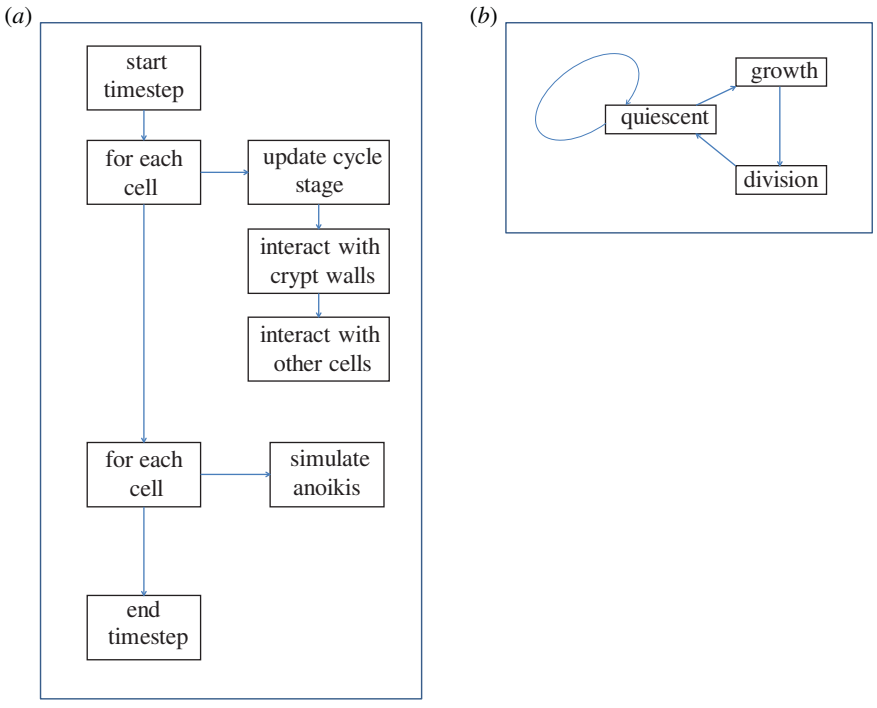

Figure 2. (*a*) Flow chart showing a broad overview of the update process at each timestep of the model. (*b*) Flow chart showing the model cell cycle.

Box 1. Overlap resolution rule.
For every other cell
  If cell overlaps other cell
    Calculate restoration force based on equation (2.1).
    Apply restoration force to both cells

2.4. Design concepts

2.4.1. Basic principles

The model is an agent-based model. Each cell is represented by a software agent which behaves autonomously with no overarching control mechanism, each agent displaying a number of biologically based behaviours.

2.4.2. Movement

Movement and division of cell agents results in collisions. Detected overlaps are corrected by applying forces based on the concept of cell centres connected by stiff springs (box 1). These forces are modelled by equation (2.1):

$$\mathbf{F} = (r(i) + r(j) - |\mathbf{x}(t,i) - \mathbf{x}(t,j)|) \times \frac{\mathbf{x}(t,i) - \mathbf{x}(t,j)}{|\mathbf{x}(t,i) - \mathbf{x}(t,j)|} \times a, \tag{2.1}$$

where $\mathbf{x}(t,i)$ is the position of cell i at iteration t, $r(i)$ is the radius of cell i, cell i and cell j are the overlapping cells, and a is a constant representing the spring stiffness. This has been shown to be a valid method to represent cell–cell interactions in tissue simulations [26] and has been used in colorectal crypt simulations since the earliest agent-based models [16]. This equation is solved using Euler integration. The equation is applied in the plane tangential to the basement membrane at the point where the cells contact. This causes the cells to behave as cylinders rather than the more commonly modelled spheres, as a cylinder better represents the shape of cells seen in *in vivo* crypt sections [27].

Downloaded from http://rsos.royalsocietypublishing.org/ on June 2, 2018

Box 2. Membrane attachment rule.
Find closest point to cell on membrane
Move cell towards membrane point

Box 3. Quiescent phase rule.
If cell is quiescent
  If cell has been quiescent longer than G0 time
    Cell enters G1

Box 4. Growth phase rule.
If cell is growing
  If cell has been growing longer than G1 time
    Create child cell
    Cell enters M phase
  Else
    Cell gets bigger

Box 5. M phase rule.
If cell is in M phase
  If cell has been mitotic longer than M time
    Child cell splits off
    Cell enters G0
Else
    Child cell gets bigger
    Cell gets smaller

2.4.3. Crypt geometry

The crypt shape is modelled as three conjoined mathematical surfaces, a hemisphere, an open cylinder and a quarter-torus (figure 1*b*), to which the cells are attached by a damped spring force rule based on the collision resolving force rule. This rule represents a spring, with rest length 0, between the cell centre and the closest point on the basement membrane (box 2).

2.4.4. Cell cycle

The cell is modelled as a finite state machine undergoing transitions between a pre-defined number of states which represent the phases of the cell cycle (figure 2*b*). A cell has one of three types determined by its location within the crypt (figure 1*c*, table 2): differentiated (red), proliferating (blue) or stem (purple). Not all cells are in cycle at all times. Differentiated cells never enter the cell cycle. Proliferating cells re-enter the cell cycle immediately after division. Stem cells enter a quiescent phase after division before re-entering the cell cycle. This corresponds to the niche hypothesis of crypt organization [6]. Cell division at the end of the cycle is modelled by growing a new cell from zero size inside the dividing cell (box 3, figure 1*d*), an approach which prevents artefacts arising from the sudden force associated with the instantaneous appearance of two full sized cells. This ensures that by the end of the mitosis phase the new cell is located adjacent to the original cell on a random bearing and that it is fully integrated with the surrounding cells in terms of contact forces. The random bearing of the new cell is not necessarily in the plane of the basement membrane but the membrane attachment force will rapidly move it into this plane. See boxes 4, 5 and 6 for pseudocode describing the rules governing the cycle stages.

Downloaded from http://rsos.royalsocietypublishing.org/ on June 2, 2018

Box 6. Simulation boundary rule.
If cell is beyond simulation boundary
  Move cell towards simulation boundary

Box 7. Anoikis rule.
Find closest point to cell on membrane
If distance from cell to membrane is greater than anoikis threshold
  Kill cell

2.4.5. Simulation boundary

Cells which pass beyond the simulation boundary have a spring-based restoring force applied to them which causes the boundary to act as a mirror of the model crypt, producing the same result as if the crypt had neighbouring crypts on all sides as seen in the biology (i.e. reflective boundary conditions are imposed). See box 6 for more details.

2.4.6. Anoikis

Our model includes the process of anoikis whereby if a cell moves more than a certain threshold distance, defined in table 2, from the basement membrane, it is considered to have lost contact and cell death is triggered (box 7).

2.5. Stochasticity

Stochasticity is introduced into the model by varying the cell cycle time per cell. Every time a cell divides, the two daughter cells are designated values of cell cycle times that are sampled from a normal distribution with mean and standard deviation extrapolated from *in vivo* data [10].

2.6. Output

The overall cellularity of the crypt was tracked throughout the simulation. The rates of anoikis and division events were recorded. The position of each anoikis event relative to crypt height was also recorded.

2.7. Access to code

The code generated and used in virtual experiments is available at the Dryad Digital Repository: http://datadryad.org/review?doi=doi:10.5061/dryad.800pj [28].

2.8. Initialization

The model is initialized as a single empty crypt. This crypt is uniformly filled with cells spaced at two cell radii apart. Cells are not placed closer than this to avoid generating large forces due to over-packing. The initial type of each cell depends on its location in the crypt according to the niche hypothesis. The time of the first division event for each cell is initialized independently to a value drawn from a uniform random distribution. This results in a realistic distribution of cell cycle phase throughout the crypt.

2.9. Virtual experiments

A number of virtual experiments were carried out to investigate homeostatic processes within the model crypt. Each simulation was run for approximately 1 year of simulated biological time and was repeated ten times with results being analysed as mean and standard deviation of these repeats to account for stochasticity.

Downloaded from http://rsos.royalsocietypublishing.org/ on June 2, 2018

3. Results

3.1. Anoikis localizes to the crypt mouth as an emergent behaviour

The mean cell cycle time was set to 30 h. Other parameters are as recorded in table 2. For each simulation, the position of anoikis events within the crypt was recorded and distributed into a series of 100 bins, each one representing 1% of crypt height. The mean and standard deviation of the total number of events in each bin was calculated over the ten runs.

Our model includes migration and membrane attachment rules, but does not formally direct anoikis events, rather they occur emergently as a response to local conditions within the crypt. This simulation series aimed to establish the predicted location of anoikis in the model crypt and used ten repeat simulations to account for stochasticity.

Figure 3*a* shows that anoikis is localized to the top 5% of the crypt. As can be seen by the small error bars there is very little variation across different simulation runs. Figure 3*b*(ii) visualizes the anoikis events localizing to the upper region of the crypt on a heat map on a geometrical representation of the crypt. Comparison with the crypt visualization in figure 3*b*(i) shows that events are confined to the curved area at the mouth of the crypt. This experiment was re-run with different cell cycle times and attachment forces all of which produced identical localization of anoikis. These results are provided in the electronic supplementary material. Mean lifetime of a differentiated cell was 3.4 days, which is biologically realistic [25]. The cells in the crypt displayed migratory behaviour, moving steadily from the crypt base to the crypt mouth with a mean migration velocity of 0.73 cell radii per hour, which also reflects biological results [25].

3.2. Anoikis rate is a potential determinant of cellular homeostasis at the crypt level in response to alteration in proliferation

Model simulations were undertaken to assess the impact on crypt cellularity of altered lengths of cell cycle. The model was run ten times with mean cell cycle times of 20, 25, 30, 35 and 40 h for each set of simulations. The total cell number, number of birth events and number of anoikis events were recorded every 200 timesteps. The mean and standard deviation of each set of data produced across the ten replicates were calculated and results are presented in figure 4. With a biologically relevant range of cell cycle times of 20, 25, 30, 35 and 40 h, the crypt reaches equilibrium in all cases (figure 4*a*).

Birth rates (defined here as number of cell division events in a two hour time period) increase as cycle time reduces, as might be expected (figure 4*b*). This shows a snapshot of birth rates taken at a single time point across all ten runs. The chosen time point was equivalent to approximately six months of biological time since the start of the simulation to ensure that equilibrium had been reached. The increase in birth rate as cycle time reduces emerges partly as a result of the rules governing cell division. However, the rules alone would only account for a linear increase. The greater than linear increase is a non-intuitive result and is discussed further below.

Figure 4*c* shows that anoikis rates (events per two hours) quantitatively match birth rates, which causes the model to reach equilibrium and is a non-enforced emergent phenomenon. This is again a snapshot taken at the six month point across all runs. Matching of birth rates is an emergent phenomenon and not encoded in the rule-set of the model.

3.3. Membrane attachment force influences cellularity of the crypt

During the earliest stages of carcinogenesis, mutation of APC is hypothesized to lead to elevated attachment between the cell and the basement membrane; this occurs through derangement of the β-catenin role [29]. We sought to investigate the consequence of altered attachment force on crypt cellularity. The model was run ten times with a mean cycle time of 30 h. As absolute attachment force values are not available, we chose to select parameter values across a three-log range of 0.01, 0.001, 0.005 and 0.0001, with 0.001 being the default value in our model. Figure 5*a* shows that increasing the attachment force increases the equilibrium cellularity level. In order to investigate the basis of this effect, we assessed the impact of change in attachment force parameter upon birth rate and anoikis. Figure 5*b* shows that increasing the attachment force parameter does not increase the birth rate. Figure 5*c* shows that, again, anoikis rates adapt to match birth rates for the range of attachment forces modelled. This is also an emergent phenomenon that cannot be attributed to any single underlying rule.

Downloaded from http://rsos.royalsocietypublishing.org/ on June 2, 2018

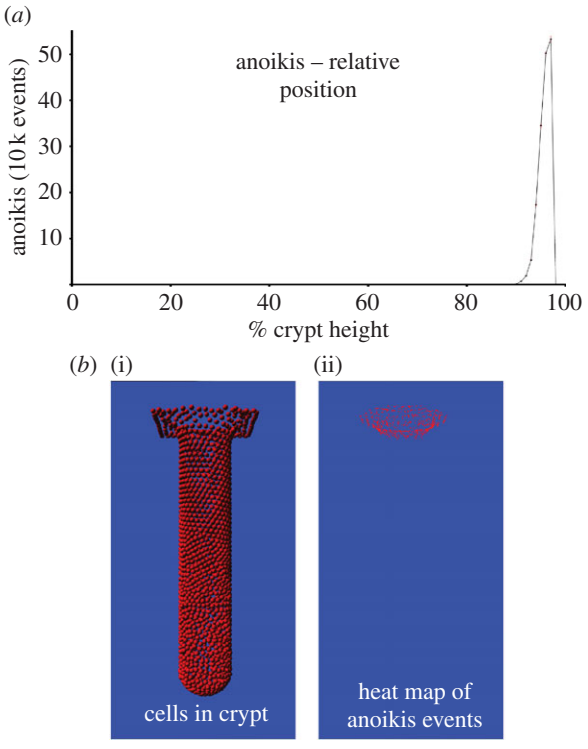

Figure 3. (*a*) Graph of anoikis locations in the model crypt. (*b*(i)) Image of cells within the model crypt for comparison to (*b*(ii)), ashowing heat map of anoikis locations during a simulation. These results are from ten repeat simulations with a cycle time of 30 h and attachment parameter of 0.001.

4. Discussion

We have built an ABM to explore interrelationships between cell cycle rate, attachment force, crypt morphology and homeostasis. We show that anoikis emerges in the regions of the crypt where it is primarily observed *in vivo* [30]. In addition to this, the localization of anoikis to the crypt top causes the model to exhibit the emergent migration of cells documented *in vivo* [7], without the presence of any apoptotic signal at the crypt top. It is possible that such signalling exists *in vivo*, alongside the apoptosis mechanism modelled here, and the relative impact of the two mechanisms is an open question. There are no data in the literature seeking to clarify the balance of active signalling and passive attachment force in modelling anoikis. The predicted localization of anoikis may be due to the negative curvature at the top of the crypt which causes the lateral forces the cells exert on each other to be directed away from the membrane, in turn pushing the cells off the membrane in this, and only this, region of the crypt. This varies from the predictions of previous models in which anoikis did not correctly localize to the crypt top [20]. The difference is accounted for by the more accurate cell geometry used in this study. When the model presented here is run with spherical, rather than cylindrical, cells, anoikis no longer localizes to the crypt top (see electronic supplementary material).

The second series of simulations suggested that anoikis regulates crypt cellularity. In the simulation, cellularity always reached equilibrium, even without an imposed, signalling-based apoptotic mechanism (although, as mentioned above, such a mechanism is not ruled out *in vivo*). The simulation shows that the model contains an emergent regulatory mechanism whereby increased proliferation drives a compensatory elevation of anoikis. This occurs because higher cellularity causes greater compression of the cells, which in turn causes higher forces, pushing the cells off the membrane more rapidly. This feedback mechanism raises interesting questions for biological study, as it suggests that hyperproliferation alone would not be a sufficient cause of neoplasia, and that other alterations (mutations or pleiotropies) permitting progressive acquisition of excess cells would need to be invoked. This is in agreement with biological studies which have suggested that anoikis could act as a homeostatic mechanism and frequently occurs for non-apoptotic cells [13].

It may seem that the balancing of anoikis and birth rate is an expected outcome since the geometry cannot expand to incorporate new cells. However, while it is true that the geometry is fixed, the cells

Downloaded from http://rsos.royalsocietypublishing.org/ on June 2, 2018

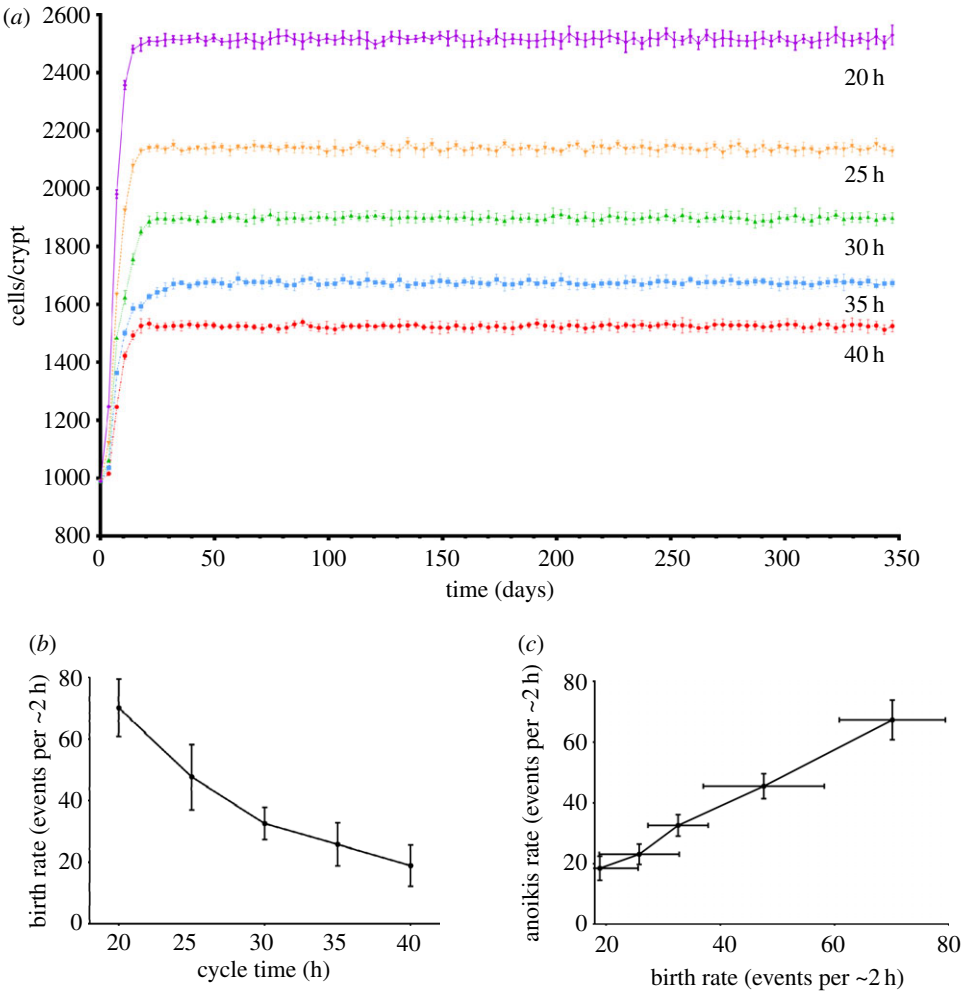

Figure 4. (*a*) Graph of number of cells in crypt over time for different cell cycle times. (*b*) Graph of birth rate against cycle time. (*c*) Graph of birth rate against anoikis rate for this set of simulations.

are able to compress such that if no coupling emerged between anoikis and birth rate then the cells may eventually compress to zero size. This would be biologically unrealistic but could be interpreted as a trigger for biological phenomena that the model in its current form cannot explicitly represent, for example crypt fission or the formation of an adenoma. This model does not reach such a state due to the tracking of anoikis to birth rate, which is not an explicit rule of the model but is emergent. This coupling is a consequence of the linking of cellularity to anoikis rates through compression forces. It is not a foregone conclusion that such a coupling will arise in the model as over most of the crypt the forces generated from cellular compression are either orthogonal to or opposing the forces required for anoikis; it is only in the crypt mouth that these forces align and if this was not the case there would be no coupling between birth rate and anoikis rate.

Our simulations also show that birth rates (where birth rate is the total number of divisions per two hour period, and hence is dependent on the size of the cell population) increase when cell cycle times are reduced. This is a result expected to arise from the rules implemented in the model. However, the amount of increase observed is exponential (figure 4*b*), in contrast to a linear increase that would naively be expected. This emergent behaviour can be accounted for as follows: reducing the cycle time increases the birth rate and thus indirectly the total cellularity of the crypt. This additional cellularity is contained within the crypt by the cells becoming more compressed and hence more closely packed. This means that, in line with the assumed niche hypothesis, any fixed size portion of the crypt, including the proliferative compartment, will have more cells in it as a consequence of higher cellularity, leading to more cells being in cycle at any one time. This accounts for the additional increase in birth rates in the model. It has been observed *in vivo* that the proliferative compartment expands in proximity to a

Downloaded from http://rsos.royalsocietypublishing.org/ on June 2, 2018

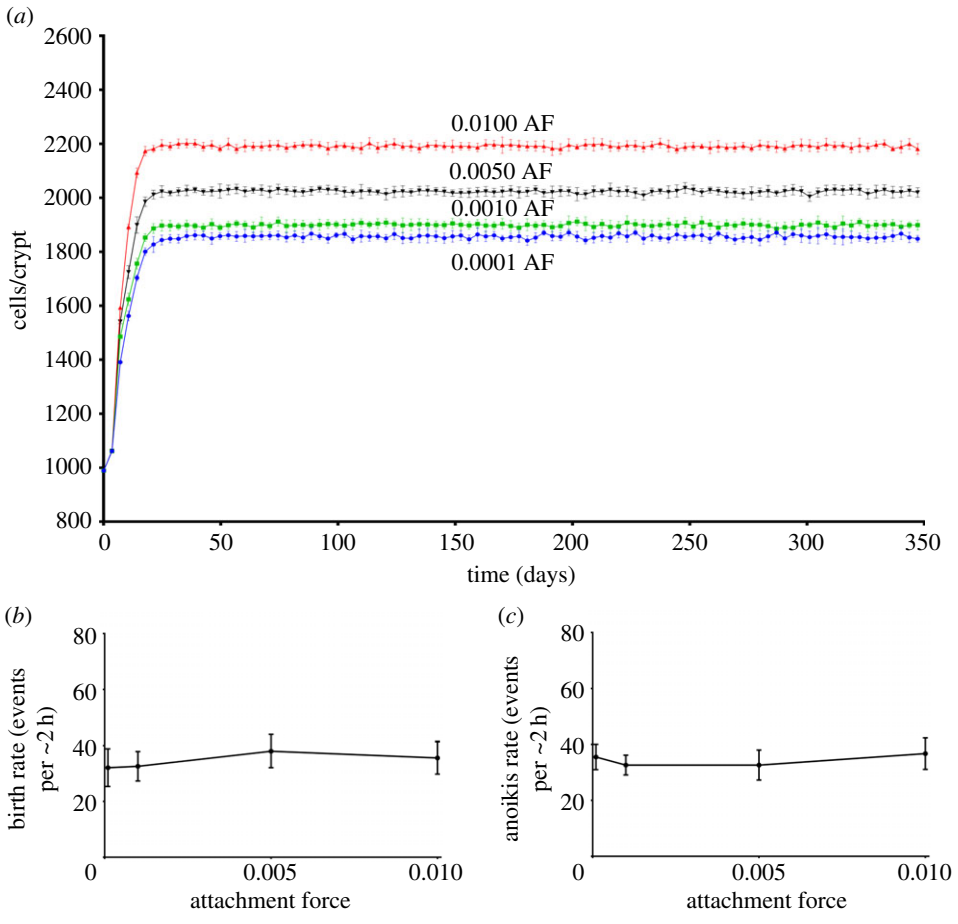

Figure 5. (*a*) Graph of number of cells in crypt over time for different membrane attachment values (AF). (*b*) Graph of birth rate against attachment value. (*c*) Graph of anoikis rate against attachment value.

lesion [31]. This may be due to increased pressure being exerted on the healthy crypt from neoplastic neighbours due to their higher rates of proliferation and lower rates of anoikis. This increased pressure might compress the healthy crypt and so force more cells into the proliferating compartment (again, assuming the niche hypothesis). The model could be used to investigate this phenomenon further in the future. An interesting feature of the cycle time simulations was that increased cell turnover led to increased crypt cellularity even though death rates rose to match increased birth rates. This is because the increased death rates were a result of greater compression forces in the crypt. As such, higher cellularity is required to achieve this greater compression and cause death rates to catch up to birth rates. Attachment strength affects cellularity in a similar manner: greater compression is required to overcome the greater attachment strength and induce anoikis.

We explored the consequences of varying the parameter representing the strength of attachment between colonocytes and the underlying basement membrane. As attachment is modelled using the same damped spring model as cell–cell overlap resolution, attachment strength is represented by a spring stiffness parameter which cannot directly translate to specific values of attachment force. It does, however, allow the model to make qualitative predictions of the behaviour resulting from stronger and weaker attachments. By regulating how strongly the cells are attached to the basement membrane, the parameter therefore influences how much they resist anoikis. Increased adhesion is a potential feature of cells with APC loss [29]. This parameter is dependent *in vivo* on a number of factors (e.g. β-catenin localizing to adherens junctions [29]) but actual forces have not been measured quantitatively. A stronger attachment requires a greater force to achieve the same rate of anoikis, resulting in higher cellularity in the model. The forces acting on the cells are driven by the level of cell compression, which is in turn driven by cellularity. This means that a higher cellularity is required in order for anoikis rate to match a given birth rate.

Downloaded from http://rsos.royalsocietypublishing.org/ on June 2, 2018

By explicitly resolving interactions between cells and cells, and cells and the basement membrane, this model offers a distinct advantage to compartmental and continuum models for understanding the mechanical processes within the crypt, and furthermore extends the application of previous ABMs by extending the rules governing cell death to better reflect the underlying biology. The model might be used to discriminate between different hypotheses for mutation embedding. By incorporating a region of flat mucosa the model extends the spatial extent of the biological region represented. Future developments will include upscaling the model to simulate multiple interacting crypts, and extending the cell model to reflect the effects of known pre-cancerous mutations.

5. Conclusion

A new computational model of the colonic crypt has been developed. Unlike previous crypt models, the geometry of the crypt top has been included, as well as the explicit mechanism of attachment related cell death, or anoikis. In agreement with published biological observations, our results predict the localization of anoikis events exclusively to the top of the crypt. These results also suggest that anoikis plays an important role in regulating crypt cellularity against changes in proliferation and membrane attachment. This suggests a potentially chemo-preventive function for this previously unknown mechanism, which may be a worthwhile focus for future *in vivo* study.

Data accessibility. Code generated and used in this paper is available at the Dryad Digital Repository: http://datadryad.org/review?doi=doi:10.5061/dryad.800pj [28].

Authors' contributions. T.I.-D.: contributed to the design of the study, developed the model, performed the study, contributed to the analysis of the data, contributed to the writing of this article. D.C.W.: contributed to the design of the study, contributed to the analysis of the data, contributed to the writing of this article. B.M.C.: contributed to the design of the study, contributed to the analysis of the data, contributed to the writing of this article. All three authors give final approval for publication.

Competing interests. We declare we have no competing interests.

Funding. T.I.-D. was funded by The University of Sheffield Faculties of Medicine and Engineering.

Acknowledgements. We would like to thank the University of Sheffield Medical School and the INSIGNEO Institute for in-silico medicine for supporting this project.

References

1. Humphries A, Wright NA. 2008 Colonic crypt organization and tumorigenesis. *Nat. Rev. Cancer* **8**, 415–424. (doi:10.1038/nrc2392)
2. Cheng H, Bjerknes M, Amar J. 1984 Methods for the determination of epithelial-cell kinetic parameters of human colonic epithelium isolated from surgical and biopsy specimens. *Gastroenterology* **86**, 78–85.
3. Baker A-M *et al.* 2014 Quantification of crypt and stem cell evolution in the normal and neoplastic human colon. *Cell Rep.* **8**, 940–947. (doi:10.1016/j.celrep.2014.07.019)
4. Bravo R, Axelrod DE. 2013 A calibrated agent-based computer model of stochastic cell dynamics in normal human colon crypts useful for in silico experiments. *Theor. Biol. Med. Model.* **10**, 66. (doi:10.1186/1742-4682-10-66)
5. Cheng H, Leblond CP. 1974 Origin, differentiation and renewal of 4 main epithelial-cell types in mouse small intestine. *Am. J. Anat.* **141**, 537–561.
6. van der Wath RC, Gardiner BS, Burgess AW, Smith DW. 2013 Cell organisation in the colonic crypt: a theoretical comparison of the pedigree and niche concepts. *PLoS ONE* **8**, e73204. (doi:10.1371/journal.pone.0073204)
7. Kaur P, Potten CS. 1986 Cell-migration velocities in the crypts of the small-intestine after cytotoxic insult are not dependent on mitotic-activity. *Cell Tissue Kinet.* **19**, 601–610.
8. Batlle E *et al.* 2002 β-Catenin and TCF mediate cell positioning in the intestinal epithelium by controlling the expression of EphB/EphrinB. *Cell* **111**, 251–263. (doi:10.1016/S0092-8674(02)01015-2)
9. Holmberg J, Genander M, Halford MM, Anneren C, Sondell M, Chumley MJ, Silvany RE, Henkemeyer M, Frisén J. 2006 EphB receptors coordinate migration and proliferation in the intestinal stem cell niche. *Cell* **125**, 1151–1163. (doi:10.1016/j.cell.2006.04.030)
10. Potten CS. 1998 Stem cells in gastrointestinal epithelium: numbers, characteristics and death. *Phil. Trans. R. Soc. Lond. B* **353**, 821–830. (doi:10.1098/rstb.1998.0246)
11. Frisch SM, Francis H. 1994 Disruption of epithelial cell-matrix interactions induces apoptosis. *J. Cell Biol.* **124**, 619–626. (doi:10.1083/jcb.124.4.619)
12. Windham TC, Parikh NU, Siwak DR, Summy JM, McConkey DJ, Kraker AJ, Gallick GE. 2002 Src activation regulates anoikis in human colon tumor cell lines. *Oncogene* **21**, 7797–7807. (doi:10.1038/sj.onc.1205989)
13. Eisenhoffer GT, Loftus PD, Yoshigi M, Otsuna H, Chien C-B, Morcos PA, Rosenblatt J. 2012 Crowding induces live cell extrusion to maintain homeostatic cell numbers in epithelia. *Nature* **484**, 546–549. (doi:10.1038/nature10999)
14. Tomlinson IPM, Bodmer WF. 1995 Failure of programmed cell-death and differentiation as causes of tumors—some simple mathematical-models. *Proc. Natl Acad. Sci. USA* **92**, 11 130–11 134. (doi:10.1073/pnas.92.24.11130)
15. Murray PJ, Kang J-W, Mirams GR, Shin S-Y, Byrne HM, Maini PK, Cho K-H. 2010 Modelling spatially regulated beta-catenin dynamics and invasion in intestinal crypts. *Biophys. J.* **99**, 716–725. (doi:10.1016/j.bpj.2010.05.016)
16. Meineke FA, Potten CS, Loeffler M. 2001 Cell migration and organization in the intestinal crypt using a lattice-free model. *Cell Prolif.* **34**, 253–266. (doi:10.1046/j.0960-7722.2001.00216.x)
17. Galle J, Loeffler M, Drasdo D. 2005 Modeling the effect of deregulated proliferation and apoptosis on the growth dynamics of epithelial cell populations in vitro. *Biophys. J.* **88**, 62–75. (doi:10.1529/biophysj.104.041459)
18. Walker DC, Southgate J. 2009 The virtual cell—a candidate co-ordinator for 'middle-out' modelling of biological systems. *Brief. Bioinform.* **10**, 450–461. (doi:10.1093/bib/bbp010)
19. Buske P, Galle J, Barker N, Aust G, Clevers H, Loeffler M. 2011 A comprehensive model of the spatio-temporal stem cell and tissue organisation in the intestinal crypt. *PLoS Comput. Biol.* **7**, e1001045. (doi:10.1371/journal.pcbi.1001045)
20. Dunn SJ, Appleton PL, Nelson SA, Nathke IS, Gavaghan DJ, Osborne JM. 2012 A two-dimensional model of the colonic crypt accounting for the role of

Downloaded from http://rsos.royalsocietypublishing.org/ on June 2, 2018

the basement membrane and pericryptal fibroblast sheath. *PLoS Comput. Biol.* **8**, 20. (doi:10.1371/journal.pcbi.1002515)

21. Fletcher AG, Murray PJ, Maini PK. 2015 Multiscale modelling of intestinal crypt organization and carcinogenesis. *Math. Models Methods Appl. Sci.* **25**, 2563–2585. (doi:10.1142/S0218202515400187)
22. Grimm V, Berger U, DeAngelis DL, Polhill JG, Giske J, Railsback SF. 2010 The ODD protocol: a review and first update. *Ecol. Modell.* **221**, 2760–2768. (doi:10.1016/j.ecolmodel.2010.08.019)
23. Fletcher AG, Breward CJW, Chapman SJ. 2012 Mathematical modeling of monoclonal conversion in the colonic crypt. *J. Theor. Biol.* **300**, 118–133. (doi:10.1016/j.jtbi.2012.01.021)
24. Mirams GR, Fletcher AG, Maini PK, Byrne HM. 2012 A theoretical investigation of the effect of proliferation and adhesion on monoclonal conversion in the colonic crypt. *J. Theor. Biol.* **312**, 143–156. (doi:10.1016/j.jtbi.2012.08.002)
25. Potten CS, Kellett M, Roberts SA, Rew DA, Wilson GD. 1992 Measurement of in vivo proliferation in human colorectal mucosa using bromodeoxyuridine. *Gut* **33**, 71–78. (doi:10.1136/gut.33.1.71)
26. Pathmanathan P, Cooper J, Fletcher A, Mirams G, Murray P, Osborne J, Pitt-Francis J, Walter A, Chapman SJ. 2009 A computational study of discrete mechanical tissue models. *Phys. Biol.* **6**, 036001. (doi:10.1088/1478-3975/6/3/036001)
27. Radtke F, Clevers H. 2005 Self-renewal and cancer of the gut: two sides of a coin. *Science* **307**, 1904–1909. (doi:10.1126/science.1104815)
28. Ingham-Dempster T, Walker DC, Corfe BM. 2017 Data from: An agent-based model of anoikis in the colon crypt displays novel emergent behaviour consistent with biological observations. Dryad Digital Repository. (http://dx.doi.org/10.5061/dryad.800pj)
29. van Leeuwen IMM, Byrne HM, Jensen OE, King JR. 2007 Elucidating the interactions between the adhesive and transcriptional functions of beta-catenin in normal and cancerous cells. *J. Theor. Biol.* **247**, 77–102. (doi:10.1016/j.jtbi.2007.01.019)
30. Strater J, Koretz K, Gunthert AR, Moller P. 1995 In-situ detection of enterocytic apoptosis in normal colonic mucosa and in familial adenomatous polyposis. *Gut* **37**, 819–825. (doi:10.1136/gut.37.6.819)
31. Gerdes H, Gillin JS, Zimbalist E, Urmacher C, Lipkin M, Winawer SJ. 1993 Expansion of the epithelial-cell proliferative compartment and frequency of adenomatous polyps in the colon correlate with the strength of family history of colorectal-cancer. *Cancer Res.* **53**, 279–282.

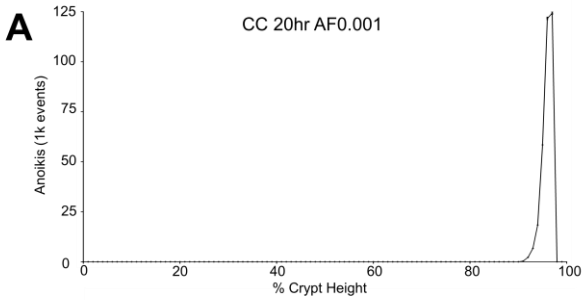

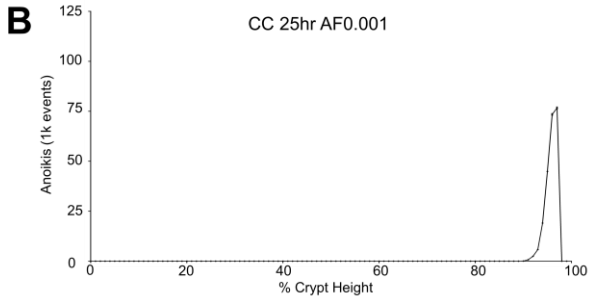

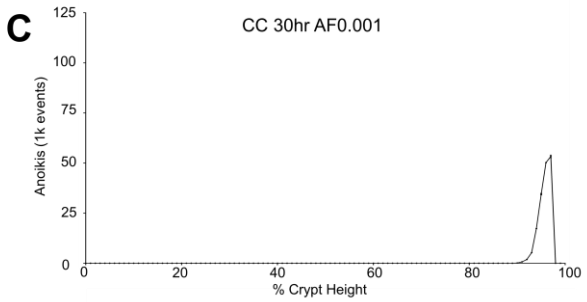

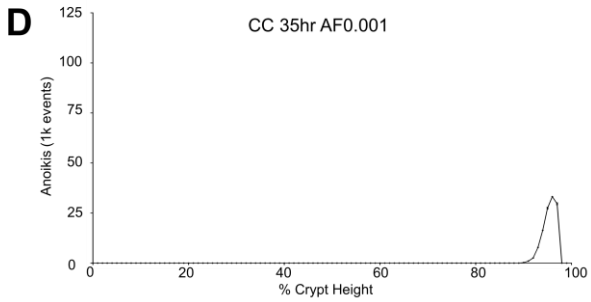

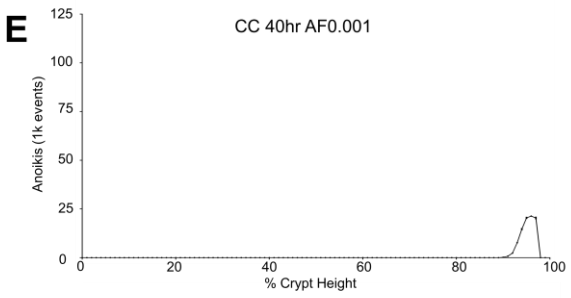

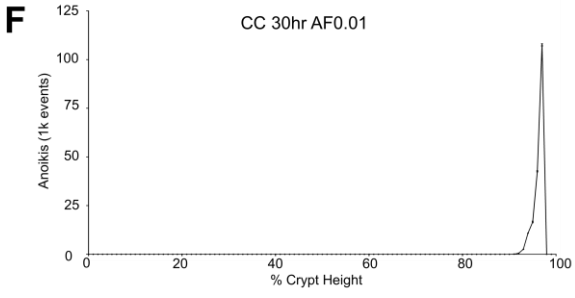

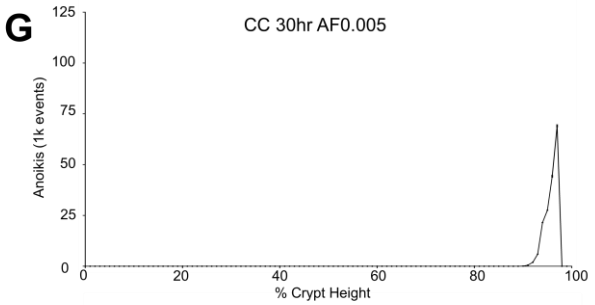

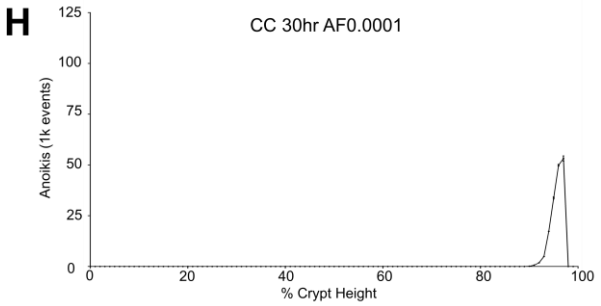

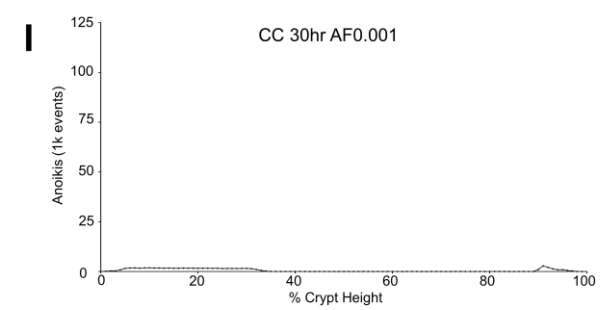

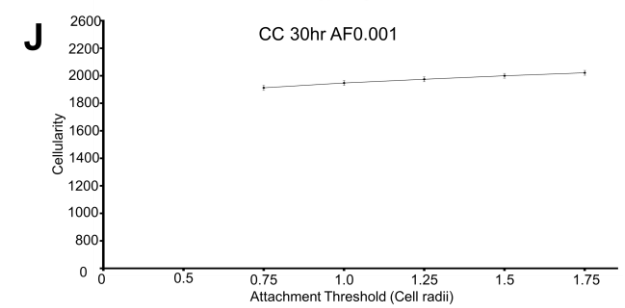

Anoikis localisation graphs for the other parameters tested in the study.

A cell cycle time 20h, attachment parameter 0.001.

B cell cycle time 25h, attachment parameter 0.001.

C cell cycle time 30h, attachment parameter 0.001.

D cell cycle time 35h, attachment parameter 0.001.

E cell cycle time 40h, attachment parameter 0.001.

F cell cycle time 30h, attachment parameter 0.01.

G cell cycle time 30h, attachment parameter 0.005.

H cell cycle time 30h, attachment parameter 0.0001.

I Spherical cell model, cell cycle time 30h, attachment parameter 0.001.

J Cellularity at a variety of attachment thresholds.

Chapter 3: Cell Shape Assumptions Affect Behaviour in Multicellular Models: Learnings from the Crypt

This chapter is a manuscript which is intended for publication, it was submitted to the journal Royal Society Open Science and underwent two rounds of peer review before being rejected. The reason for rejection was that the paper represents only an incremental increase in knowledge of the field, it is included in this thesis as it contains information vital to reproducing the results in the rest of the thesis and describes novel aspects of the cell level model that are not discussed elsewhere.

The study described in the manuscript focused on cell shape assumptions in crypt modelling. Rules representing different cell shapes were implemented and simulations were run which measured the spatial distribution of anoikis events. The predicted distributions were compared with biologically observed distributions to determine which cell shape model produced the most accurate predictions.

This study represents a step forward in the field because previous attempts to model anoikis as a mechanism within simulations have been unable to recapitulate the biologically observed distribution of anoikis events. Due to this limitation it has been impossible to perform studies such as the one in the first paper which examine aspects of crypt behaviour strongly involving interactions with the anoikis mechanism. Previous studies have either attempted to model anoikis and failed or have imposed anoikis on cells arbitrarily to fit the known biological distribution. With the findings of this manuscript it is now possible to perform such studies.

All model development and the design and execution of the simulation experiments were carried out by myself as was the analysis of the data and the writing of the manuscript. My supervisors advised on the study and acted as editors for the manuscript.

Cell Shape Assumptions Affect Behaviour in Multicellular Models: Learnings from the Crypt

Tim A Ingham-Dempster[1,2,3],
Bernard M. Corfe,[1,2], and Dawn C. Walker[*,1,3]

[1]*INSIGNEO Institute, University of Sheffield, The Pam Liversidge Building, Mappin Street, Sheffield, S1 3JD, UK*

[2]*Department of Oncology and Metabolism, The Medical School, University of Sheffield, Beech Hill Road, Sheffield, S10 2RX, UK*

[3]*Department of Computer Science, University of Sheffield, Regent Court, 211 Portobello, Sheffield, S1 4DP, UK*

[*]Corresponding author, E-mail: d.c.walker@sheffield.ac.uk

3.1: Abstract Agent based models have been applied to a number of areas of biology, yielding insights into emergent phenomena which cannot readily be investigated using empirical methods. When applied to modelling biological cell populations, these models usually assume cells are spherical in shape whereas in reality, cells in a tissue typically have more complex morphologies.

This study aimed to investigate the validity of the spherical assumption by comparing the results of simulations with cells represented as spheres, with simulations where cells were modelled as cylinders, in an otherwise identical model. Cylinders are more complex to represent but are closer to the shape observed in epithelial monolayers in-vivo, such as the colorectal crypt considered herein. The outcome measured for comparison was the location within the crypt of cell detachments from the underlying membrane (anoikis). These events are known to localise to the crypt mouth in-vivo, a phenomenon which in-silico models have previously failed to recapitulate.

The comparison showed a significant difference in behaviour according to the cell shape representation, with cylindrical representations yielding more biologically plausible results than spheres. This suggests that for the context modelled, cell shape is an important factor and an assumption of cellular sphericity is a significant limitation.

Keywords: agent based modelling, cell shape, colorectal crypt, anoikis

3.2: Introduction

In an agent based model, real-world entities, e.g. biological cells, are represented as independent virtual "software agents". This approach has allowed investigations of phenomena which would be inaccessible to experimental studies, such as clonal dynamics in the colorectal crypt (Fletcher et al., 2012). Colorectal crypts are structures which punctuate the colonic epithelium and are responsible for generating the large number of cells required constantly to refresh the gut wall. Cells divide at the base of the crypt and migrate upwards to the crypt mouth where they die through anoikis (Hall et al., 1994), induced when a cell loses contact with the basement membrane of the crypt (Frisch and Francis, 1994).

A standard assumption commonly applied in agent based models of biological tissues is that the cells are assumed to be spherical (Meineke et al., 2001). This is a simplifying assumption for the purpose of streamlining the mathematics used in calculating intercellular forces, resulting in overlap resolution. However, cells in-vivo are not spherical, often adopting complex shapes to optimise the packing structure of the tissue (Farhadifar et al., 2007).

A number of more detailed approaches to modelling cell morphology have been developed to investigate phenomena where changing cell shape is important to tissue development. These methods include the *vertex method* where the cell boundary is represented as a series of vertices able to move independently, which allows it to deform, the *sub-cellular element method* where each cell is represented by a number of smaller sub-cellular regions, and the *finite element method* where the cell is broken down into finite elements each with defined mechanical properties and movement of nodes connecting elements calculated as a result of stresses arising in the tissue (Fletcher et al., 2017). These approaches have shown that cell shape is important in tissue morphogenesis. For example, one study using the vertex method found that deforming cells can create crypt-like invaginations in spherical organoids (Misra et al., 2016). Whilst these more complex approaches do provide a much more detailed representation of cell shape than methods assuming a simple, fixed shape, they are also more computationally expensive which renders them impractical when applied to large cell populations. Furthermore, such approaches have not been applied to the study of homeostasis and as far as we are aware, there are no studies in the literature on the importance of cell shape when modelling such phenomena.

A previous model of homeostasis in the colorectal crypt considered the process of anoikis, using a spherical shape assumption, but found that it did not predict the localisation of anoikis to the crypt mouth, as seen in-vivo (Dunn et al., 2012). By contrast, our previously published work, based on a cylindrical cell shape assumption, reported the correct localisation of anoikis (Ingham-Dempster et al., 2017).

In this study we investigate the validity of the spherical cell assumption by comparing the output of a computational model of a biological system when run with the spherical cell assumption to the output when run with a more realistic cylindrical cell shape.

3.3: Methods To assess the impact of cell shape a previously developed model (Ingham-Dempster et al., 2017) was used to generate predictions with both spherical and cylindrical cell shapes used for comparison.

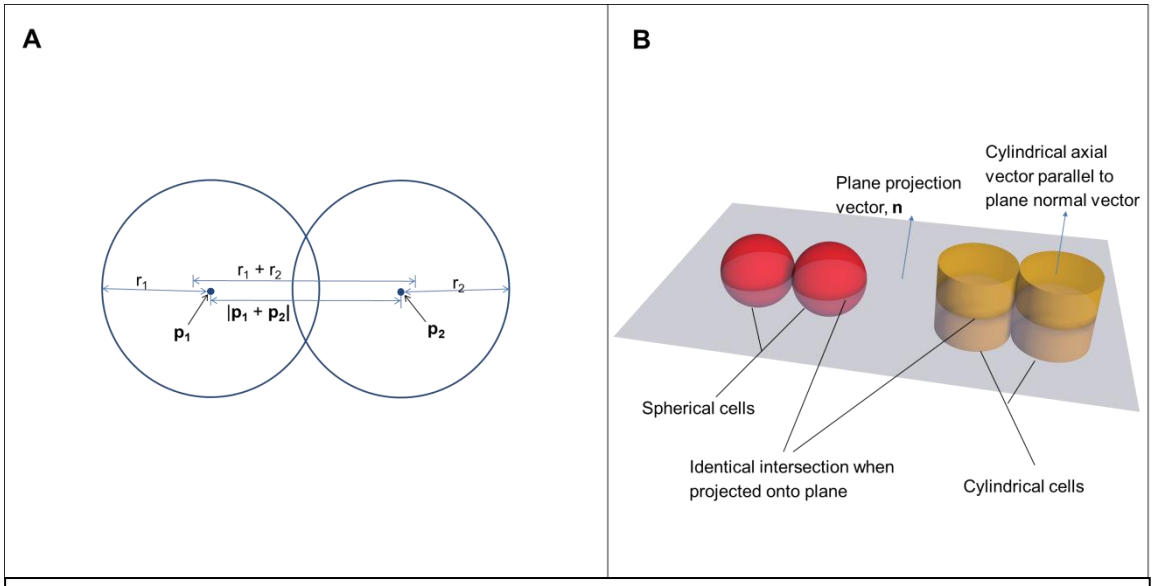

Figure 3.1: Graphical comparison of parameters for spherical and cylindrical projections. A: Two overlapping cells showing the parameters which form equations 1 and 2. **B**: Projecting a spherical force onto a plane transforms it into a circular force suitable for simulating cylindrical cells.

Spherical cells were modelled by applying a spring force between the centres of any cells with overlapping boundaries, this takes the form of a pairwise damped spring system following **Eq 1**

$$\mathbf{F} = ((r_1 + r_2 - |\mathbf{p_1} - \mathbf{p_2}|) * ((\mathbf{p_1} - \mathbf{p_2}) / |\mathbf{p_1} - \mathbf{p_2}|) * k) \text{ if } |\mathbf{p_1} - \mathbf{p_2}| < r_1 + r_2 \quad \text{(Eq1)}$$

Where k is a spring constant determining cell stiffness, $\mathbf{p_1}$ and $\mathbf{p_2}$ are the cell centre locations and r_1 and r_2 are the two cell radii (**Fig 3.1A**).

To derive this equation we consider the force created by a spring:

$$\mathbf{F} = (l - s) * \mathbf{x} * k$$

Where l is the equilibrium length of the spring, s is the actual length, x is the normalised direction of the spring, and k is the spring stiffness constant.

In our case $l = r_1 + r_2$,

$s = |\mathbf{p_1} - \mathbf{p_2}|$, and

$\mathbf{x} = (\mathbf{p_1} - \mathbf{p_2}) / |\mathbf{p_1} - \mathbf{p_2}|$ (**Fig 3.1A**)

Therefore **Eq1** results in a force proportional to the product of the compression of the spring and the spring constant and applied along the axis of the spring (i.e. along a vector joining the two cell centres).

To derive cell velocity from this force, we apply Newton's second law $\mathbf{F}=m\mathbf{a}$,

Which can be rearranged to give

$\mathbf{a} = \mathbf{F} / m$

Using Euler integration and the method of finite differences $\mathbf{v_t} = \mathbf{v_{t-1}} + \mathbf{a}dt$ (Eq2)

Where $\mathbf{v_t}$ is the current velocity and $\mathbf{v_{t-1}}$ is the velocity at the previous timestep, we also include a viscous drag force sufficient to render inertia negligible: $\mathbf{F_d} = -m\mathbf{v_{t-1}}/dt$. This gives:

$\mathbf{a} = (\mathbf{F} / m) - \mathbf{v_{t-1}}/dt$,

$\mathbf{v_t} = \mathbf{a}dt = (\mathbf{F}/m)dt$

Since the simulation updates at a fixed timestep both dt and m are finite constants and can therefore be factored into k to give:

$\mathbf{v_t} = \mathbf{F} = ((r_1 + r_2 - |\mathbf{p_1} - \mathbf{p_2}|) * ((\mathbf{p_1} - \mathbf{p_2}) / |\mathbf{p_1} - \mathbf{p_2}|) * k)$ if $|\mathbf{p_1} - \mathbf{p_2}| < r_1 + r_2$ (Eq3)

Cylindrical cells use the same force rule but this is transformed into a cylindrical force by projecting vectors $\mathbf{p_1}$ and $\mathbf{p_2}$ onto a plane that lies on the crypt membrane and has a normal equal to the normal of the closest point on the membrane to the mean of the two cell centre locations (**Fig 3.1B**). This projection transforms the spherical force in the three-dimensional space of the simulation into a circular force in the two-dimensional local coordinate system of the plane, which is the force that would be experienced by two cylinders with axes normal to the plane interacting with each other. The projection is of the form:

$$\mathbf{p'} = \mathbf{p} - \mathbf{p.n} \quad \text{(Eq4)}$$

Where **p'** is the projected position, **p** is the original position and **n** is the normal of the plane, which is calculated from the geometry of the basement membrane. Incorporating this projection into **Eq3** will therefore result in a cylindrical, rather than a spherical, force being applied to the two interacting cells.

A number of assumptions are made about the cylindrical cells. It is assumed that they are always oriented perpendicularly to the basement membrane and cell height is not considered, instead the assumption is made that the cells always contact each other where they intersect the basement membrane. This contrasts with approaches using a more detailed model of cell shape such as the subcellular element model (Marin-Riera et al., 2016) which gives a more accurate representation of cell shape but is much less computationally demanding, allowing many more cells to be simulated with a given amount of computational resource. Other simplified models of cylindrical cells exist (Nissen et al., 2017) but focus on signalling changes due to axial alignment rather than physical forces, and are still more computationally expensive than the model used in the current study.

The crypt was "seeded" by generating cells in a uniform distribution over the crypt membrane using an identical procedure for both the spherical and cylindrical cell based simulations. Each simulation was run for a period representing approximately one year of biological time with ten repeats of each simulation, leading to a total of twenty simulation runs.

The model uses the niche hypothesis whereby a cell's function is decided by its position in the crypt. There is an alternative called the pedigree hypothesis which postulates that the number of divisions a cell has undergone determines its function. A previous study looked at the differences between models using the niche and pedigree hypotheses (van der Wath et al., 2013) and based on these results we believe that the results we report here would be identical if carried out in a model using the pedigree hypothesis.

3.4: Results The position of anoikis, an emergent property of the model, was plotted for each of the ten repeat simulations for each shape assumption as follows: the location of each event was assigned to one of a hundred bins to give a frequency count of the number of events predicted at that location, and then mean and standard deviation of each bin for each simulation set were calculated and plotted. Further repeats were not deemed necessary due to the highly consistent results, with standard deviation of each bin being on average less than six percent of the bin value. The model using spherical cells showed anoikis across the crypt with localisation in the lower 40% and the upper 15% (**Fig 3.2A**) with low rates and a wide distribution. In contrast, simulations using cylindrical cells predicted anoikis localising exclusively to the top 15% of the crypt (**Fig 3.2B**), a closer representation of biological observation (Potten, 1998).

Cellularity was also compared between spherical and cylindrical assumptions (**Fig 3.4**). Simulations with spherical cells showed lower overall cellularity. Migration velocities were 0.73 cell radii per hour for cells in simulations with cylindrical cells and zero in simulations with spherical cells.

Computational time for both simulations was recorded for five repeats, it was found that simulations with cylindrical cells took 1.4+/-0.008ms per timestep (averaged over 10000 timesteps). Simulations with cylindrical cells took 0.7+/-0.005ms.

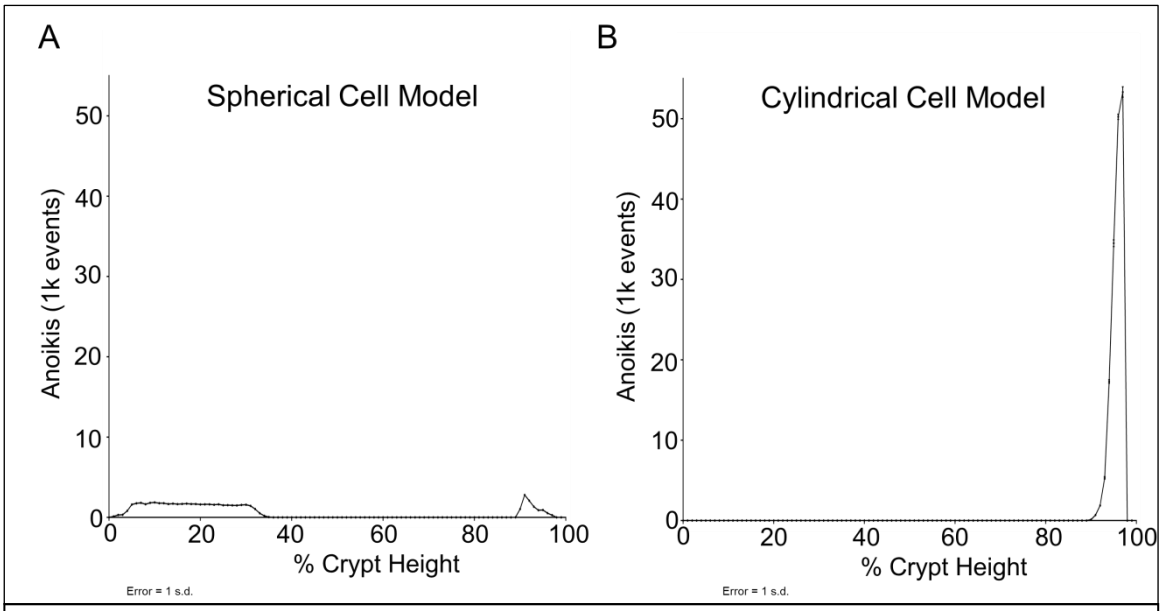

Figure 3.2: Position of anoikis is cell-shape dependent. A total of twenty simulations were run for our crypt model using either a spherical shape formalism (Panel A) or a cylindrical formalism (Panel B). In both cases the rate of anoikis (/1000 cells, y-axis) is shown against the relative height of the crypt (% of height where 1% is crypt base and 100% is crypt mouth).

3.5: Discussion The results of this study clearly show a difference in outcome according to whether cells were represented as spheres or cylinders. The results derived using a spherical cell assumption showed a high level of anoikis around the proliferative region and the crypt mouth with a low level throughout the rest of the crypt. These results agree qualitatively with those reported by Dunn et al, in the only previous computational study of anoikis in the crypt, but show a stronger localisation than previously reported (Dunn et al., 2012). The localisation in the proliferative region obtained using the spherical model arises as this area has higher cell density and hence higher compressive forces, which together can lead to loss of membrane attachment. The localisation in the crypt mouth is due to the curvature of the mouth causing a greater proportion of the compression forces being directed into the lumen and therefore moving cells further from the membrane (Fig 3.3).

The cylindrical model showed localisation of anoikis exclusively to the crypt mouth. This localisation is due to the cylindrical forces being parallel to the basement membrane at the point of contact. The entirety of the crypt apart from the mouth has zero or positive vertical curvature and positive horizontal curvature. This means that any force acting parallel to the basement membrane will act to move the cells along and into the membrane. The crypt mouth, however, has negative vertical curvature. This means that any vertical forces parallel to the basement membrane in this region will act to move the cells along and away from the latter, thus promoting anoikis. For a graphical representation of these concepts see Figure 3.3. The consequence of this mechanism is that the model cannot generate anoikis events occurring in the flat inter-crypt region of the flat mucosa of the gut, but can represent anoikis in curved regions of the flat mucosa.

The localisation seen in the cylindrical model reflects biological observations reporting that anoikis occurs primarily at the crypt mouth (Hall et al., 1994). This localisation causes migration of cells from the crypt base, which is vital for the correct functioning of the crypt and its ability to replenish the gut wall (Dunn et al., 2013). Cell migration velocities consistent with biological observations (Kaur and Potten, 1986) was observed in the cylindrical model but not in the spherical model where zero net migration was observed, suggesting that the latter may be associated with the absence of localised anoikis. The model predicted a mean cell velocity of 0.73+/-0.25 cell radii per hour compared to 0.74+/-0.02 cell radii per hour seen in the literature (Kaur and Potten, 1986). The spherical model showed a lower overall cellularity due to the increased levels of anoikis.

In terms of simulation time, tests demonstrated that there is a simulation overhead associated with running a cylindrical, rather than a spherical model, which may be related to an unavoidable cache miss introduced by the cylindrical simulation. A cache miss occurs when a value that is required for a computation is not present in the small but very fast cache memory in a computer processor and has to be retrieved from the much slower main memory. However, given that the overhead amounts to only 0.5us per cell per timestep, this overhead is not considered to be significant.

One potential future application of the technique presented in this paper is to investigate the consequences of cell shape de-regulation, where cells take on unusual shapes due to alterations of their mechanical properties, seen in colon cancer. This well-known phenomenon (Kalluri and Weinberg, 2009) has potential implications for aspects of the crypt including migration and homeostasis but these issues cannot be investigated in a model which does not account for cell shape.

This study has shown that in the case of modelling the process of anoikis in the colorectal crypt, it is not sufficient to model cells as spherical in shape, a common assumption across all previous agent based crypt models. If we extend this premise more generally: it is an unsafe assumption that biological properties of cells can be adequately captured when cell shape is assumed to be spherical. In adherent cell-systems in particular, modellers need to consider carefully whether a simplifying assumption is justifiable for the context being modelled.

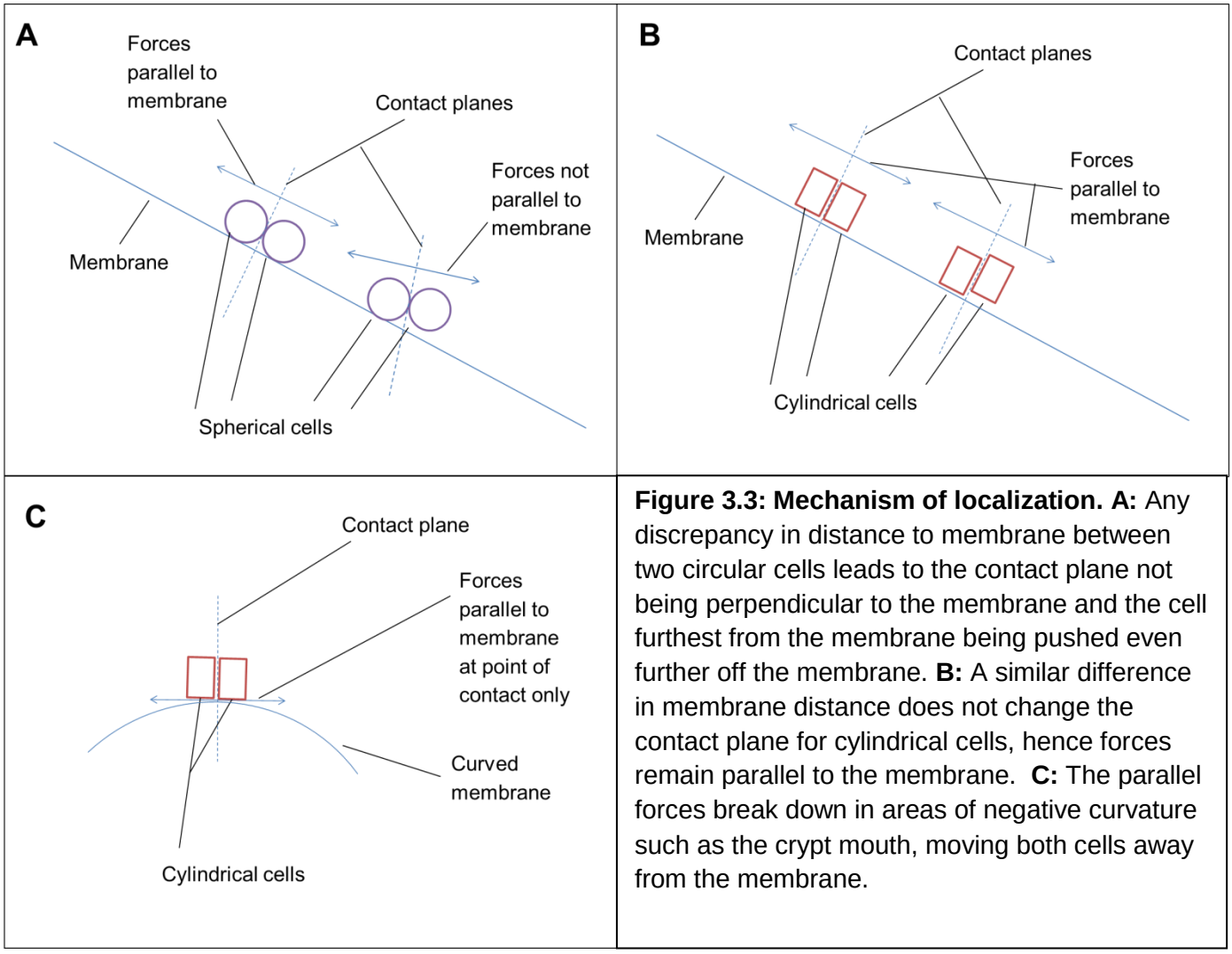

Figure 3.3: Mechanism of localization. A: Any discrepancy in distance to membrane between two circular cells leads to the contact plane not being perpendicular to the membrane and the cell furthest from the membrane being pushed even further off the membrane. **B:** A similar difference in membrane distance does not change the contact plane for cylindrical cells, hence forces remain parallel to the membrane. **C:** The parallel forces break down in areas of negative curvature such as the crypt mouth, moving both cells away from the membrane.

Ethics

No human or animal experiments were undertaken within this research, ethics approval from an LREC was therefore not required.

Data Accessibility

Code generated and used in this paper is available at the Dryad Repository. The DOI during peer review is: http://dx.doi.org/10.5061/dryad.800pj

Competing Interests

We have no competing interests.

Author Contributions

Tim Ingham Dempster: Contributed to the design of the study, developed the model, performed the study, contributed to the analysis of the data, contributed to the writing of this article.

Dawn C. Walker: Contributed to the design of the study, contributed to the analysis of the data, contributed to the writing of this article.

Bernard Corfe: Contributed to the design of the study, contributed to the analysis of the data, contributed to the writing of this article.

All three authors give final approval for publication.

Acknowledgements

We would like to thank the University of Sheffield Medical School and the INSIGNEO Institute for In-Silico Medicine for supporting this project.

Funding

Tim Ingham-Dempster was funded by The University of Sheffield Faculties of Medicine and Engineering.

3.6: References

DUNN, S.-J., NAETHKE, I. S. & OSBORNE, J. M. 2013. Computational Models Reveal a Passive Mechanism for Cell Migration in the Crypt. *Plos One,* 8.

DUNN, S. J., APPLETON, P. L., NELSON, S. A., NATHKE, I. S., GAVAGHAN, D. J. & OSBORNE, J. M. 2012. A Two-Dimensional Model of the Colonic Crypt Accounting for the Role of the Basement Membrane and Pericryptal Fibroblast Sheath. *Plos Computational Biology,* 8**,** 20.

FARHADIFAR, R., ROEPER, J.-C., ALGOUY, B., EATON, S. & JUELICHER, F. 2007. The influence of cell mechanics, cell-cell interactions, and proliferation on epithelial packing. *Current Biology,* 17**,** 2095-2104.

FLETCHER, A. G., BREWARD, C. J. W. & CHAPMAN, S. J. 2012. Mathematical modeling of monoclonal conversion in the colonic crypt. *Journal of Theoretical Biology,* 300**,** 118-133.

FLETCHER, A. G., COOPER, F. & BAKER, R. E. 2017. Mechanocellular models of epithelial morphogenesis. *Philosophical Transactions of the Royal Society B-Biological Sciences,* 372**,** 50519-50519.

FRISCH, S. M. & FRANCIS, H. 1994. Disruption of Epithelial Cell-Matrix Interactions induces Apoptosis. *Journal of Cell Biology,* 124**,** 619-626.

HALL, P. A., COATES, P. J., ANSARI, B. & HOPWOOD, D. 1994. REGULATION OF CELL NUMBER IN THE MAMMALIAN GASTROINTESTINAL-TRACT - THE IMPORTANCE OF APOPTOSIS. *Journal of Cell Science,* 107**,** 3569-3577.

INGHAM-DEMPSTER, T., WALKER, D. C. & CORFE, B. M. 2017. An agent-based model of anoikis in the colon crypt displays novel emergent behaviour consistent with biological observations. Royal Society Open Science: The Royal Society Publishing.

KALLURI, R. & WEINBERG, R. A. 2009. The basics of epithelial-mesenchymal transition. *Journal of Clinical Investigation,* 119**,** 1420-1428.

KAUR, P. & POTTEN, C. S. 1986. Cell-Migration Velocities in the Crypts of the Small-Intestine after Cytotoxic Insult are not Dependent on Mitotic-Activity. *Cell and Tissue Kinetics,* 19**,** 601-610.

MARIN-RIERA, M., BRUN-USAN, M., ZIMM, R., VALIKANGAS, T. & SALAZAR-CIUDAD, I. 2016. Computational modeling of development by epithelia, mesenchyme and their interactions: a unified model. *Bioinformatics,* 32**,** 219-225.

MEINEKE, F. A., POTTEN, C. S. & LOEFFLER, M. 2001. Cell migration and organization in the intestinal crypt using a lattice-free model. *Cell Proliferation,* 34**,** 253-266.

MISRA, M., AUDOLY, B., KEVREKIDIS, I. G. & SHVARTSMAN, S. Y. 2016. Shape Transformations of Epithelial Shells. *Biophysical Journal,* 110**,** 1670-1678.

NISSEN, S. B., PERERA, M., GONZALEZ, J. M., MORGANI, S. M., JENSEN, M. H., SNEPPEN, K., BRICKMAN, J. M. & TRUSINA, A. 2017. Four simple rules that are sufficient to generate the mammalian blastocyst. *Plos Biology,* 15.

POTTEN, C. S. 1998. Stem cells in gastrointestinal epithelium: numbers, characteristics and death. *Philosophical Transactions of the Royal Society B-Biological Sciences,* 353**,** 821-830.

VAN DER WATH, R. C., GARDINER, B. S., BURGESS, A. W. & SMITH, D. W. 2013. Cell Organisation in the Colonic Crypt: A Theoretical Comparison of the Pedigree and Niche Concepts. *Plos One,* 8.

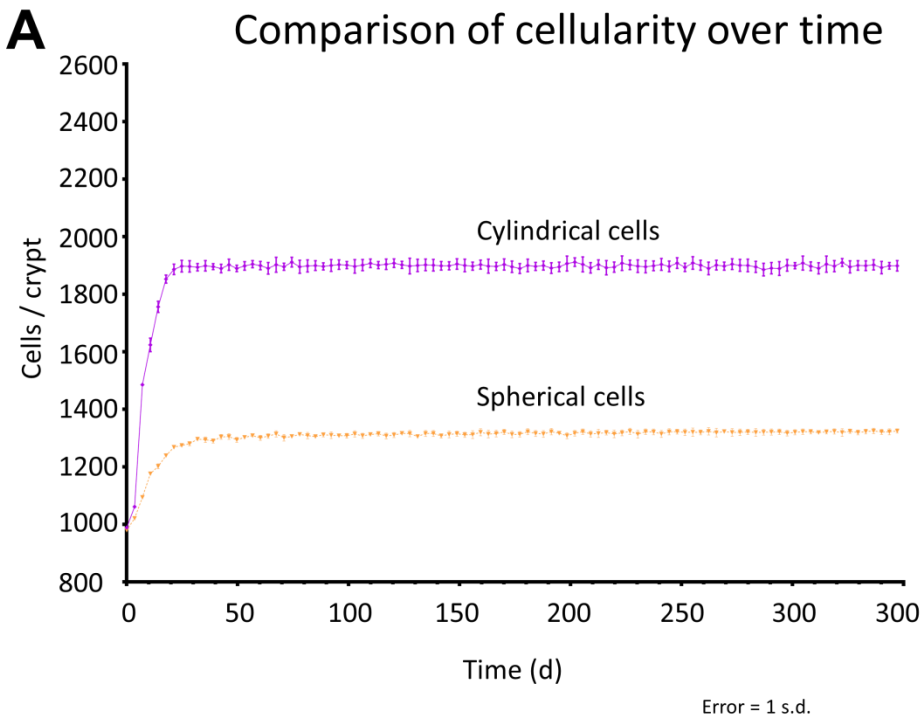

Figure 3.4: Comparison of Cellularity for Different Cell Shape Models. Cellularity plotted against time for cylindrical cell model (purple) and spherical cell model (orange).

Chapter 4: A Cellular Based Model of the Colon Crypt Suggests Novel Effects for APC Phenotype in Colorectal Carcinogenesis

This chapter is a paper which was published in the Journal of Computational Science in 2018. This paper examined the consequences of APC loss in the model crypt developed for the first paper, the main novelty being the interaction of APC loss with the crypt mouth and the anoikis mechanism. Whilst APC loss in the crypt has been modelled previously that study did not include a representation of the crypt mouth or anoikis. APC forms a destruction complex responsible for breaking down β-Catenin in the canonical Wnt pathway:

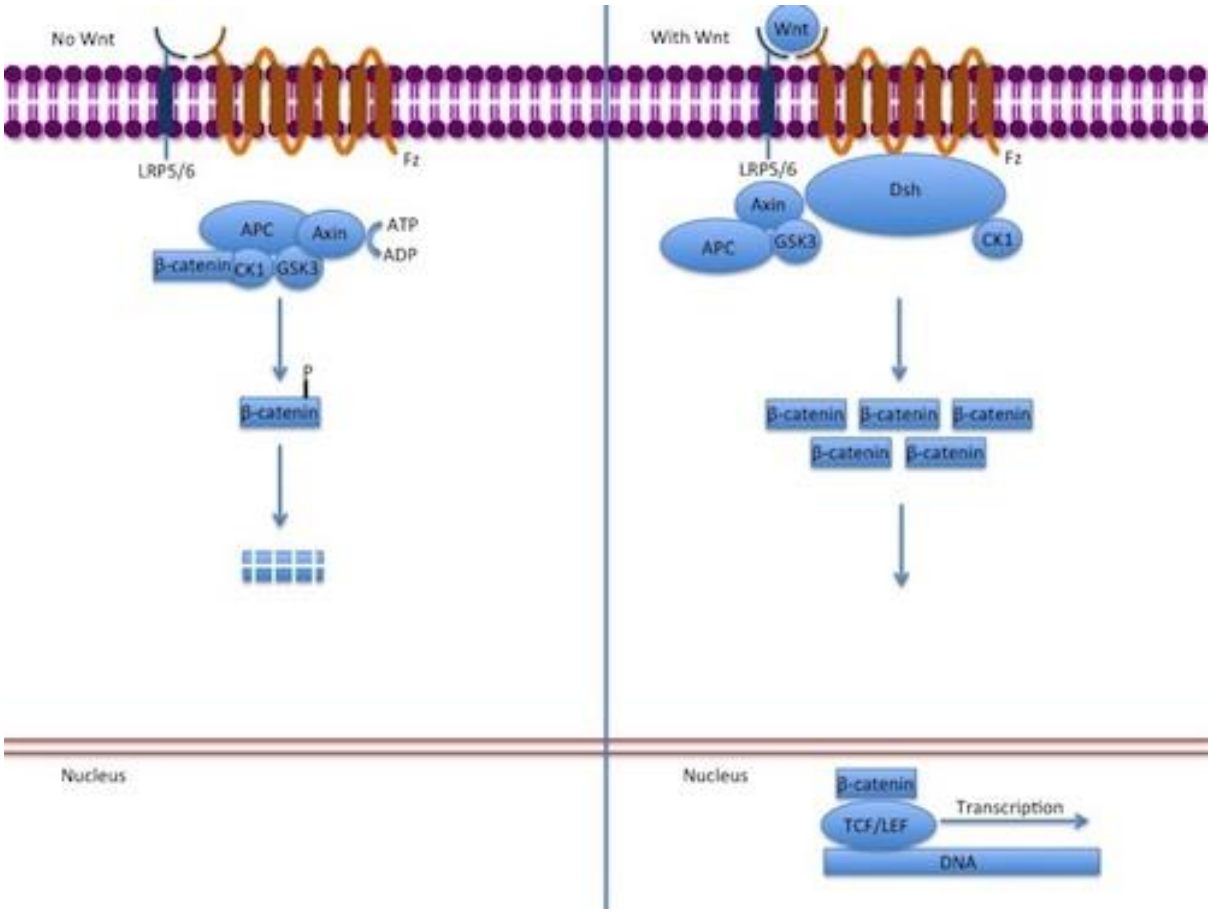

(Diagram used under CC attribution license, Gpruett2 [CC BY-SA 3.0 (https://creativecommons.org/licenses/by-sa/3.0)], from Wikimedia Commons, https://commons.wikimedia.org/wiki/File:Canonical_Wnt_pathway_(height%3D375px).jpg)

This study recapitulated the findings of the previous study into APC mutation in the crypt by predicting that reduction of quiescent time would give mutated cells an advantage in the niche succession process leading to mutation fixation in the crypt. Our study also produced novel findings by predicting that mutated cells will have a competitive advantage in the crypt mouth, this is the part of the crypt which connects with neighbouring crypts and might have important consequences for the interaction between wild-type and mutated crypts.

There is an error in the text as published, the second sentence of section 1.2 states “Biopsies and animal models can only provide snapshotsof the crypt at a single moment in time”, however there are some animal models which can observe the development of tissue

over time (Ritsma et al., 2014) but such techniques are extremely expensive and still restricted to animal models.

I carried out the modification to represent APC loss in the model and performed the simulation work, I also analysed the data and wrote the paper. My supervisors provided feedback and suggestions on the paper, the experiments and the analysis.

RITSMA, L., ELLENBROEK, S. I. J., ZOMER, A., SNIPPERT, H. J., DE SAUVAGE, F. J., SIMONS, B. D., CLEVERS, H. & VAN RHEENEN, J. 2014. Intestinal crypt homeostasis revealed at single-stem-cell level by in vivo live imaging. *Nature,* 507**,** 362-+.

Journal of Computational Science 24 (2018) 125–131

Contents lists available at ScienceDirect

Journal of Computational Science

journal homepage: www.elsevier.com/locate/jocs

A cellular based model of the colon crypt suggests novel effects for Apc phenotype in colorectal carcinogenesis

Tim Ingham-Dempster[a,b,*], Bernard Corfe[a,b], Dawn Walker[a,c]

[a] INSIGNEO Institute, University of Sheffield, England, United Kingdom
[b] Molecular Gastroenterology Research Group, Department of Oncology and Metabolism, University of Sheffield, England, United Kingdom
[c] Department of Computer Science, University of Sheffield, England, United Kingdom

ARTICLE INFO

Article history:
Received 23 December 2016
Received in revised form 7 June 2017
Accepted 19 June 2017
Available online 22 June 2017

Keywords:
Agent based modelling
Colon crypt
Apc loss

ABSTRACT

Colorectal cancer (CRC) is a major cause of cancer mortality; loss of the Apc gene is an early step in the formation of CRC.

A new computational model of the colonic crypt has been developed to simulate the effects of Apc loss. The model includes a region of flat mucosa, which has not previously been considered in the context of Apc loss.

The model suggests that Apc loss confers a survival advantage at the crypt mouth which may be a previously unknown method of mutation fixation.

© 2017 Elsevier B.V. All rights reserved.

1. Introduction

1.1. Biological background

The human large intestine consists of an epithelial monolayer forming the flat mucosal surface, punctuated by glands known as the crypts of Lieberkuhn (Fig. 1**A**). These crypts are the functional unit of the colonic epithelium, supporting the rapid turnover of cells in the organ through constant division and differentiations of stem cells located at their base: as such the perturbation of their turnover and inappropriate accumulation of cells is implicated in formation of colorectal cancer (CRC) [1]. Identifying these underlying homeostatic processes is therefore crucial in understanding the pathophysiology of colorectal disease.

A human colonic crypt contains approximately 2500 cells, or colonocytes [2]. There is a stem cell compartment at the base of the crypt which is estimated to comprise around 10 cells [3] which are purple in Fig. 1**A**. Cells exiting the stem cell compartment (variously called transit amplifying cells or proliferating cells, light blue in the figure) account for around 25% of cells in the crypt [4]. Fully differentiated cells include water-absorbing colonocytes (red) which compose roughly 75% of differentiated cells, mucus secreting goblet (green) cells which account for roughly 24% of differentiated cells and hormone secreting enteroendocrine cells (yellow) which differentiate directly from stem cells rather than from transit amplifying cells and account for less than 1% of differentiated cells [2,5].

Cell proliferation and differentiation along the crypt axis is governed by a gradient of Wnt3, being strongest at the bottom of the crypt where proliferation rates are highest [6]. This proliferation is balanced by anoikis – a form of cell death occurring when a cell loses contact with the basement membrane [7]. It is thought to occur at the top of the crypt where cells are shed into the intestinal lumen as a normal physiological process maintaining cellular homeostasis in the tissue [8]. In normal tissue a constant cycle of cell proliferation and loss results in a homeostatic condition where the entire crypt (stem cells aside) is turned over every 4–7 days in humans [9].

Abnormalities in these cell replacement processes are strongly implicated as the earliest stages in CRC development. Loss of function of the tumour-suppressor protein Apc due to mutation is a known step in early carcinogenesis [1]. The changes in cell properties due to Apc loss are characterised in-vitro but their overall effect on crypt dynamics is not well understood.

There are two main effects of Apc loss on epithelial cells. The first effect is upregulation of proliferation due to activation of the Wnt pathway. APC forms a destruction complex for β-catenin preventing it from accumulating in the nucleus where it upregulates proliferative genes. WNT3 acts by binding APC and preventing it from forming the beta-catenin destruction complex thus allowing beta-catenin to accumulate and migrate to the nucleus, loss

* Corresponding author at: The Medical School, The University of Sheffield, Beech Hill Road, Sheffield, S10 2RX, United Kingdom.
E-mail address: taingham-dempster1@sheffield.ac.uk (T. Ingham-Dempster).

https://doi.org/10.1016/j.jocs.2017.06.013
1877-7503/© 2017 Elsevier B.V. All rights reserved.

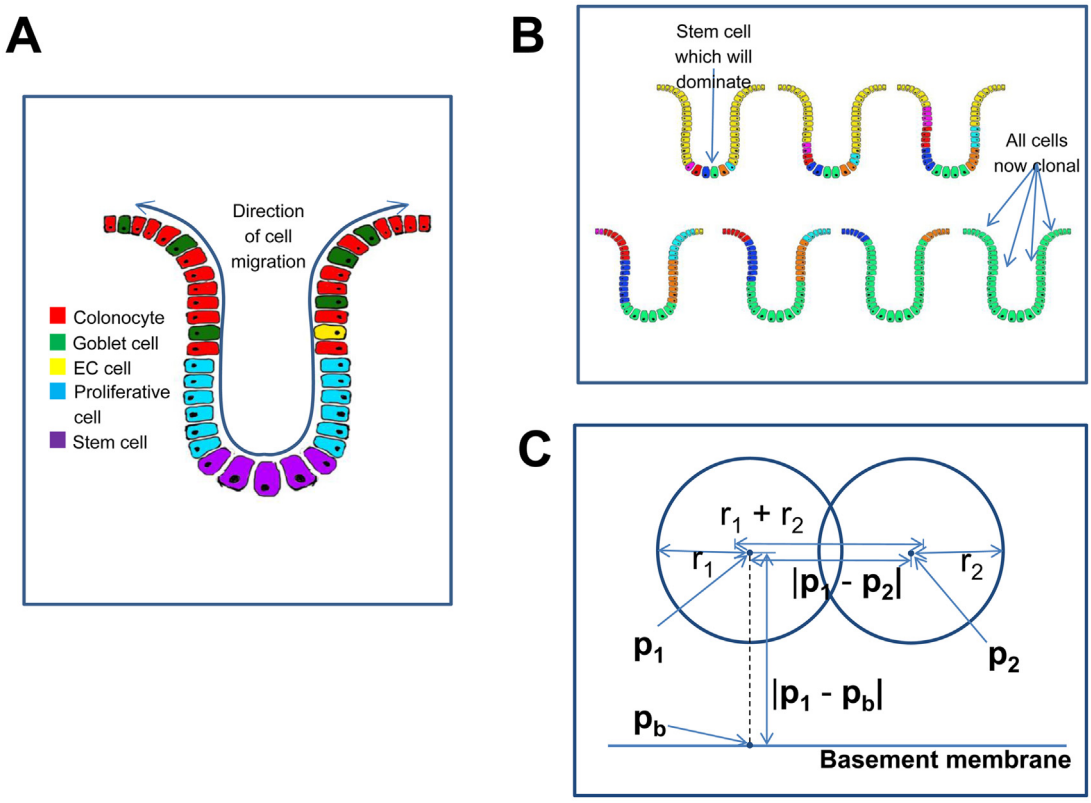

Fig. 1. The crypt. A The crypt is a structured cell factory with slow cycling stem cells at the bottom, rapidly cycling proliferative cells in the middle, and differentiated functional coloncytes at the top. Cells migrate from bottom to top. **B** Monoclonal conversion is a process whereby clonal expansion of a single stem cell eventually leads to all cells being clonal descendants of that original cell and hence carrying any mutation which existed in the original stem cell. **C** Diagram of two cells interacting with each other and the basement membrane.

of the Apc gene prevents the beta-catenin destruction complex from forming which allows beta-catenin to accumulate in the same manner as if the Wnt pathway were activated. This leads to cells proliferating in a similar manner to cells in a high WNT environment regardless of the actual level of WNT available [10].

β-catenin is also known to be vital for cell–cell adhesion [11] and this can also be regulated by Apc based destruction. Loss of Apc leads to more β-catenin being available to form cell adherens junctions and therefore stronger cell–cell adhesion. Adhesive interactions with the extra cellular matrix may affect the process of anoikis. An increase in adhesion with the extra cellular matrix may also lead to an increased amount of drag on passively migrating epithelial cells.

We hypothesise that these mechanical changes will result in mutated cells displaying different behaviour to wild-type cells, in particular at the crypt mouth.

1.2. Computational modelling

The dynamic nature of the processes within the crypt means that they are impossible to study through traditional experimental methods. Biopsies and animal models can only provide snapshots of the crypt at a single moment in time and extrapolating from one timepoint to another is challenging due to the emergent nature of certain processes. Due to these difficulties, the crypt is an attractive target for computational methods. A range of computational models have been applied to crypt dynamics, which vary in terms of their basic assumptions, underlying methodologies, and degree of spatial resolution.

Compartment models (Tomlinson et al. [12], Smallbone et al. [13]) consider the composite behaviour of different populations of cells within the crypt and implement rules governing the growth and interactions between these populations in the form of ordinary differential equations (ODEs). The crypt has also been modelled as a continuum [14] using partial differential equations to represent the spatial distribution of the different cell compartments. In this context, cells are still modelled as populations rather than discrete entities. The first models to consider cells as individual entities were lattice based models – an approach still in use due to its computational efficiency [4]. Here the crypt is modelled as a lattice, or grid, where each lattice point or node can be occupied by a cell. The limitation here is that cells can only move from space to space in discrete jumps meaning realistic intercellular interactions cannot be modelled. This limitation can be overcome by using a more complex modelling paradigm such as the Cellular Potts method, which was used to show that Ephrine signalling can cause cells to sort into spatially distinct regions within the crypt [15]. However these models have the disadvantage of being computationaly expensive.

Agent-based models (ABMs) represent cells as free agents moving in space [16]. Each cell acts as an independent agent with no globally overarching control. This approach is appealing for biological modelling as it captures the nature of biological cells as individual autonomous entities that can respond to signalling cues, and also allows the modeller to capture the important concept of intercellular heterogeneity [17].

In most existing models, cell death is not explicitly related to a biological mechanism, but attempts to capture phenomenologically the known behaviour that cells predominantly die at the top of the crypt. For instance, a deterministic cell death rule is activated as soon as a cell reaches the top of the crypt [16] or cells die stochastically with a probability that increases towards the crypt top [4].

Mirams et al. [18] developed an agent based model to study the effects of Apc gene mutation on the crypt. Increased proliferation, a larger proliferative compartment for Apc$^{-/-}$ (i.e. both copies of the Apc gene have been mutated) cells and a stronger basement membrane attachment for Apc $^{-/-}$ cells were modelled and placed in competition with wild type cells within a crypt. Survival advantages were found for all three effects of Apc loss. The geometry of the crypt mouth was not modelled and cell death was modelled by a rule which removed any cell that reached the top of the crypt, as such it was impossible to model the interaction between Apc loss and Anoikis.

Dunn et al. [19] used an agent based model to examine the role of the basement membrane in crypt formation and also included the concept of anoikis. The model predicted that whilst anoikis did occur at the crypt mouth, it also occurred throughout the crypt and was most prominent at the crypt base. As such, there was no significant cell migration in the simulated crypt and a phenomenological rule dictating cell death at the crypt mouth had to be introduced to give rise to the correct migration behaviour.

Previously we have developed an ABM to study homeostatic processes within the crypt [20]. This model extended earlier work by explicitly modelling the crypt mouth for the first time and including rules to simulate anoikis. Unlike the only previous study [19] to include anoikis this model was able to correctly predict the localisation of anoikis to the crypt mouth by incorporating a more accurate model of the cell geometry. Another prediction of this model was that anoikis regulates cellularity within the crypt and is a key homeostatic process. As suggested by biological experiment [21], anoikis rates emergently matched proliferation rates and constrained the crypt to a steady state under all test conditions. Changes in proliferation rates did lead to changes in the steady state equilibrium point for cellularity which displayed non-linearities and we hypothesise that these processes may be sensitive to the effects of Apc mutation. We were motivated to study the crypt mouth in order to fulfil our longer term aim of developing a multi-crypt model including a representation of the flat mucosa between adjacent crypts.

It has been shown that mutations in a crypt cell can become permanently fixed in the crypt through a process called monoclonal conversion (Fig. 1**B**). The influence of Apc loss on this process is not fully understood and the interaction of Apc loss, monoclonal conversion and anoikis has not previously been investigated.

We sought to extend our ABM [20] in order to explore the consequences of Apc loss on the crypt's homeostatic mechanisms. We added rules for mutated cells and code to track populations of such cells as described in Section 2.

2. Materials and methods

An agent based model was used to investigate the interaction of Apc mutation, monoclonal conversion, and anoikis. Unlike previous crypt models it explicitly includes a representation of anoikis and a realistic representation of the morphology of the crypt top. Details of this model are available in our previous paper [20] and a summary is presented below:

In the model each cell is represented by a software agent which behaves according to its own internal state and known biological signals, with no global control. Cells move in three dimensions due to a number of forces acting upon them. The main force is that of cell–cell repulsion which causes the majority of movement within the crypt. This is modelled as a pairwise damped spring system obeying Eq. (1).

$$\mathbf{F} = ((r_1 + r_2 - |\mathbf{p}_1 - \mathbf{p}_2|) * ((\mathbf{p}_1 - \mathbf{p}_2)/|\mathbf{p}_1 - \mathbf{p}_2|) * k) \text{iff} |\mathbf{p}_1 - \mathbf{p}_2| < r_1 + r_2 \quad (1)$$

Where k is a constant determining the strength of the force, $\mathbf{p}_1$ and $\mathbf{p}_2$ are the locations of the two cells, and r_1 and r_2 are the radii of the two cells (Fig. 1**C**). Neglecting inertial effects (i.e. assuming a dmaped spring model where momentum from the previous timestep can be ignored) the velocity of the cell is then determined solely from this force [16].

The agents progress through a simple cell cycle that incorporates quiescence, growth, and division depending on time and location within the crypt. This is based on the niche hypothesis [22] of cell function within the crypt and is driven by a simulated gradient of WNT3. The length of the growth phase (G1) for each cell is individually stochastically sampled from a normal distribution with mean and standard deviation taken from the literature [6], the timespan of the quiescent (G0) and division (M) phases are simple timespans which are identical across all cells and sourced in the same way as the value for growth phase.

An additional force represented using the damped spring model described by Eq. (2) and of the same form as Eq. (1) acts to keep cells in contact with the basement membrane. In the event that cells are forced away from the membrane, anoikis is induced when a threshold separation is reached.

$$\mathbf{F} = (\mathbf{p}_1 - \mathbf{p}_b) * k_b \quad (2)$$

Where k_b is the parameter controlling the strength of attachment to the basement membrane, $\mathbf{p}_1$ is the location of the cell, and $\mathbf{p}_b$ is the location of the closest point on the membrane to $\mathbf{p}_1$ (Fig. 1**C**).

The existing model was extended to allow mutated cells to be included, and particular properties (quiescent time, membrane attachment strength, and cell drag) varied depending on whether cell agents have those properties tagged as mutated or wldtype. Mutated properties are inherited by daughter cells following cell division.

The model results in a three-dimensional simulation of the crypt where cells originate in a small stem cell compartment at the bottom of the crypt and flow up to the flat mucosa, undergoing a period of rapid proliferation. Our previous paper showed the existing model is in good agreement with other models of the crypt and displays phenomena such as monoclonal conversion and passive migration of cells [16,20,22–25].

A number of in-silico experiments were undertaken using this model. In each case the simulation was run for a thousand timesteps, with each timestep corresponding to 30 s of biological time, to achieve a stable homeostatic condition before a single randomly selected cell near the crypt base was "mutated", as described in the previous paragraph. The size and spatial locations of the population of mutated cells was then tracked through the rest of the simulation. Total simulation time was equivalent to ~1 year of biological time. Each simulation was repeated ten times to account for stochasticity due to cell cycle times being sampled from a normal distribution to reflect biological reality.

Parameter values for the experiments were identical to those used in our previous paper [20], where a number of parameters were tested including mean cell cycle time and the attachment force parameter. In that study, the median values of a 30 h mean cell cycle time and a 0.001 (unitless) attachment force were used.

Here, we describe five virtual experiments assessing the impact of different aspects of Apc mutation on the crypt.

Experiment 1 studies the behaviour of a wild-type clonal population originating from a single cell with no mutation effects to provide a baseline for comparison.

Experiment 2 investigates the effects of increased adhesion of Apc mutated cells to the basement membrane. To do this the adhesion parameter of a single cell was increased ten-fold and this new value was inherited by any daughter cells upon division. The clonal population arising from this cell was then tracked throughout the simulation.

Experiment 3 examines the effects of increased cell drag from the basement membrane on Apc mutated cells. This was achieved by halving the velocity arising from the repulsive force between cells at each timestep for any cell in the clonal population of the original mutated cell, again this clonal population was tracked throughout the simulation.

Experiment 4 looked at the effect of reducing the quiescent time of stem cells in Apc mutation. In this experiment the initial mutant cell had its quiescent time reduced to 10%. Again the clonal population generated by this cell was tracked throughout the simulation.

Experiment 5 combined the three previously studied effects by modifying a single cell to have all three mutation effects and tracking its clonal offspring throughout the simulation.

3. Results

3.1. General properties and behaviours of a clonal population in the model crypt

The first experiment created a "neutral" mutation which could be tracked but did not confer any changes to the properties of the mutated cells. This was used as a baseline to determine the expected cell counts for a clonal population arising from a single cell.

An example of the crypt with this mutation is shown in Fig. 2**Ai**. Red cells are wild-type and black cells are mutated. Small groups of neutrally mutated cells emerge from the stem cell niche and enter the proliferating compartment where they expand into small streams of cells in the expected ribbon pattern seen in biological experiments [26]. This ribbon occurs as cells are being produced rapidly in an environment containing a directed flow, this is somewhat analogous to injecting smoke into a moving airflow. The clonal population dies out over time due to the phenomenon of monoclonal conversion which has been thoroughly examined in previous studies [18,24].

Fig. 2**Aii** shows the number of neutrally mutated stem cells in the crypt and in the flat mucosa with Fig. 2**Aiii** showing the percentages of crypt and flat mucosal cells which are neutrally mutated. From these data, it can be seen that a small clonal population arises in the crypt and persists for a period of time before dying out. It is also evident that the population in the flat mucosa lags that of the crypt population as expected from the fact that cells arise in the crypt and then migrate to the mucosa. Error bars give a baseline for the variance due to simulation stochasticity of a clonal population of wild type cells in the crypt allowing comparisons to be drawn with mutated cells in later simulations. Finally the neutral mutation did not approach crypt dominance in any of the simulations (Table 1), suggesting that this cell location cannot give rise to a dominant population without some change conferring an advantage in niche succession.

3.2. Individual and cumulative effects of apc-loss phenotype

The second simulation series created a mutation which increased the mutated cells' adhesion to the basement membrane of the crypt. Fig. 2**Bi** shows a snapshot of the simulation with this mutation. From this image (which is typical of the series) it can be seen that mutated cells are the majority of cells in the flat mucosa and also form small clusters whilst in the crypt.

Fig. 2**Bii** shows counts of mutated cells in the crypt and in the flat mucosa over time and Fig. 2**Biii** shows the percentage of crypt cells which are mutated in green and the percentage of mutated mucosal cells in blue. Both figures show that the flat mucosa supports a much larger population of mutated cells than in the case of neutral mutation which suggests that an increase in basement attachment confers a major advantage to cells in the flat mucosa.

Fig. 2**Bii** and **iii** also show that there was a small increase in the counts and percentages of mutated cells in the crypt compared to the neutral mutation, along with an increased variance. The raw data shows a single simulation run with approximately 50% mutated cells at the end and the mutated line being extinct in the other nine runs, additionally the mean time to mutant population extinction was longer in the other nine runs than in the simulations with a neutral mutation (Table 1).

A set of simulations were run where mutated cells were assigned a reduced cell–cell repulsion force to simulate the additional drag caused by increased membrane adhesion. A visualisation of a typical crypt from this run can be seen in Fig. 2**Ci.** This visualisation shows that cells with this mutation tend to form a small number of large clusters instead of many small groups, as was observed in the case of non-mutated cells.

Fig. 2**Cii** shows the counts of mutated cells in the crypt and flat mucosa, Fig. 2**Ciii** shows this data as percentages of cells mutated. These data show that crypt mutated cell counts are larger than for the neutral mutation, equating to a major survival advantage in the crypt. The graphs also show a very large standard deviation across these simulations. This can be explained by the fact that three of the ten crypt simulations resulted in predictions that the crypt would be 100% mutated by the end point whereas in the other seven runs the mutated population became extinct (Table 1). Additionally the mutated crypts had twice the cell count of the wild-type crypts.

The increases in mutated cell counts/percentages and variance can also be seen in the flat mucosa. These populations track the crypt population with a time lag as seen for the mutated populations in the neutral mutation experiments.

The fourth experiment investigated the effect of reducing the duration of the quiescent period in mutated stem cells, which is also believed to be an effect of Apc mutation [2]. Fig. 2**Di** is a snapshot taken from a crypt during this simulation. As can be seen a large continuous ribbon of mutated cells stretches from the niche to the crypt mouth, a phenomenon also observed in-vivo [26].

Fig. 2**Dii** and **Diii** show mutated stem counts and proportion of cells mutated for both crypt and flat mucosa. This shows that in all simulations the crypt became 100% mutated after approximately 50 days (Table 1). There was a larger variability than the neutral mutation during the mutant population expansion phase. These data clearly show that quiescence reduction confers a major advantage in the stem cell niche.

A large increase in the percentage of mutated cells within the flat mucosa is also apparent. This expansion within the flat mucosa followed expansion within the crypt in a similar manner to the neutral mutation. The mutated population did not occupy more than 70% of the flat mucosa despite the crypt supplying a constant stream of mutated cells into the mucosa.

The final set of simulations combined the three effects previously examined individually to represent the range of known effects of Apc loss. A visualisation of a typical crypt with this mutation can be seen in Fig. 2**Ei.** This shows all three effects in evidence: the niche has been colonised by mutant cells which form a very dense cluster and send a dense ribbon of mutated cells up the crypt while the flat mucosa has a large population of mutated cells. In addition the three effects are complementary.

These phenomenological observations are borne out by Fig. 2**Eii** and **Eiii** which show counts and percentage mutated respectively for both the crypt and the flat mucosa. These data show that the mutation causes dominance in the niche which leads to the crypt becoming entirely populated with mutated cells. This takeover of the crypt occurs faster than with just the quiescent mutation, being completed in approximately 30 days in this case (Table 1). The cell count data show that mutated crypts are much denser than wild

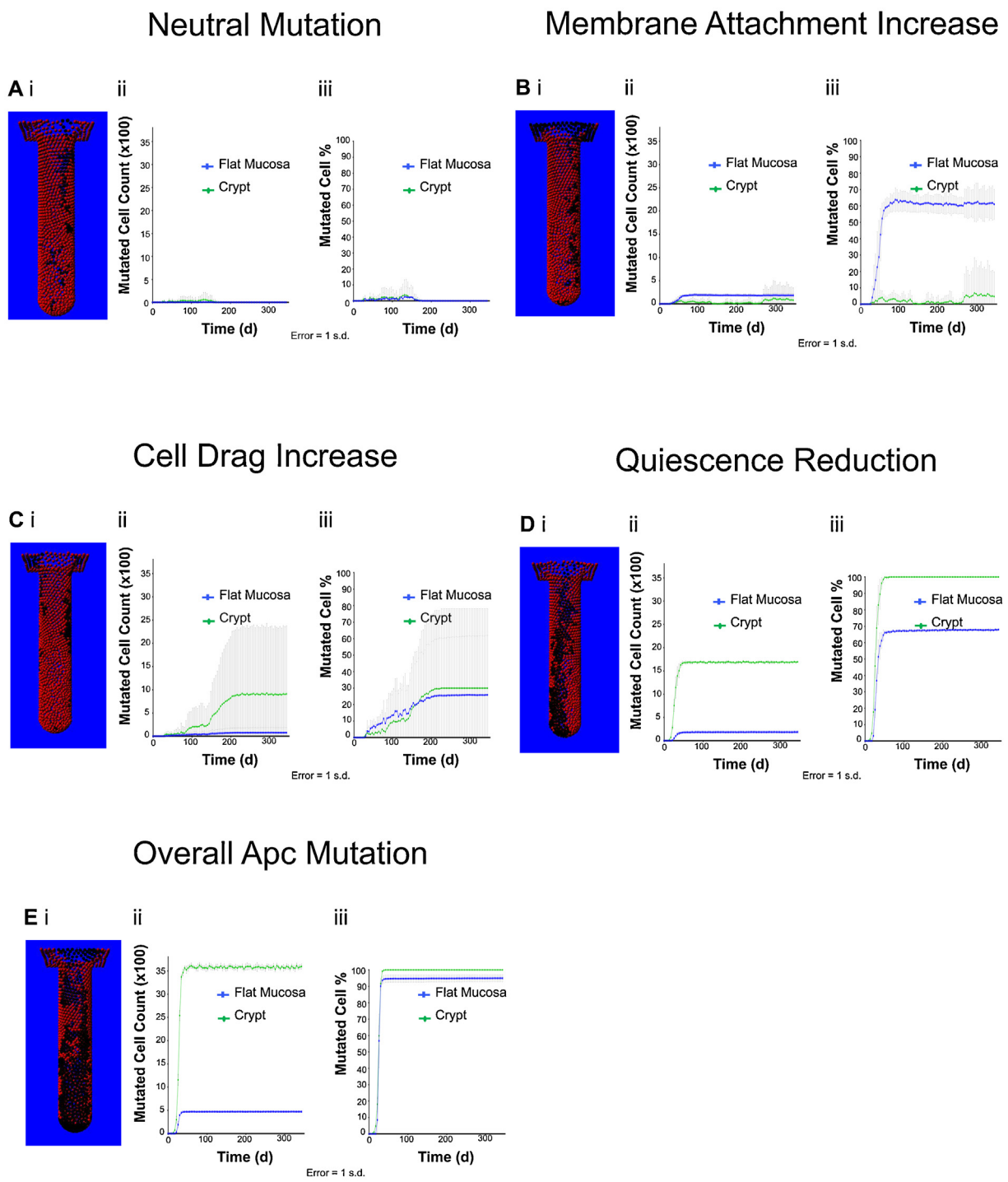

Fig. 2. Results. **A** Results of tracking a clonal population with no mechanic changes. **B** Results of increased cell-extracellular matrix adhesion. **C** Results of increased drag due to increased membrane adhesion. **D** Results of reducing stem cell quiescent time. **E** Results of overall Apc Mutation. In all figures: i) Visualistion from simulation with this mutation. ii) Absolute counts of mutated cells in crypt and flat mucosa over ten repeats. iii) Percentages of cells mutated in crypt and cells mutated in flat mucosa over ten repeats.

Table 1
Population extinctions across simulations.

Mutation Type	Crypts with mutant cells after 1 year	Mean time to mutant population extinction (d)	Mutant dominant crypts after 1 year	Mean time to mutant domination (d)
Neutral	0	68.5	0	N/A
Adhesion	1	87.3	0	N/A
Quiescence	10	N/A	10	48.8
Apc	10	N/A	10	31.8

type crypts associated with the neutral mutation, or arising from the simulations where the mutation affects quiescence alone.

The data also show that the flat mucosa becomes populated by approximately 95% mutated cells, which is a much higher percentage than for either the adhesion effect or quiescent effect alone. The time lag between crypt and flat mucosa infiltration was also reduced compared to previous simulations, with the exception of the adhesion-only mutation. Variability was low but consistent in the flat mucosa and very low in the crypt.

4. Discussion

Our results indicate that all three phenotypic alterations associated with Apc loss are selectively advantageous individually but with distinct effects. The combined Apc mutation results in a greater increase in mutated cell numbers than any of the individual mutations. A number of the results are non-intuitive and worth further examination:

- The adhesion change caused more mutated cells in the flat mucosa than in the crypt and appeared to give a small advantage in the stem cell niche
- The drag increase created very large standard deviation across the repeats and large increases in crypt cellularity
- Both quiescent time reduction and combined Apc mutation resulted in very large increases in mutated cell counts with very low standard deviations
- Apc mutation showed the separate events complementing each other

The adhesion change caused more mutated cells in the flat mucosa than in the crypt and appeared to give a small advantage in the niche – Fig. 2**B**.

There appeared to be a small advantage in the niche for cells with this phenotype, as in one of the ten simulations mutated cells were still alive at the end of the simulation compared to zero in ten for the neutral mutation. Additionally, in the nine simulations where the mutated population became extinct, survival was extended compared to the case for the neutral mutation simulations. The cause of this advantage is currently unclear, as niche processes are not affected by adhesion changes. A plausible hypothesis is that mutated cells in the flat mucosa cause additional downward pressure on the side of the crypt with the mutated stem cells which would act to prevent migration out of the niche, a similar mechanism to that found by Mirams et al. [18].

Adhesion favours mutated cells in the flat mucosa due to the role of anoikis, which is confined to the flat mucosa in the model in an emergent behaviour which has been explored previously [20]. A cell dies whenever it loses contact with the basement membrane. As such, cells which are more tightly bound to the basement membrane will be less likely to undergo anoikis.

Additionally the flat mucosa will consist of a mix of strongly-bound mutated cells and more weakly-bound wildtype cells. In this situation the mutated cells will tend to push the wildtype cells off the basement membrane and thus can survive for much longer in the flat mucosa than normal cells.

Whilst anoikis has recently been shown to be an active process, with cells signalling neighbouring cells to push them out [21], loss of contact with the basement membrane is still required and thus increased adhesion would slow this process in the manner captured by the rules of the model used in this study.

This advantage of mutated cells in the flat mucosa may act as a previously undiscovered process for mutations becoming fixed without directly dominating via monoclonal conversion. This is apparent from the fact that the mutated cells were swept out of the crypt in nine out of the ten repeat simulations and yet survived in large numbers in the flat mucosa in all ten simulations, often long after dying out from the crypt itself. This may allow mutated cells to spread through the flat mucosa and affect neighbouring crypts.

The drag increase resulted in large increases in crypt cellularity but with large variations across repeat simulations, Fig. 2**C**.

The very large standard deviation associated with the drag force effect has two key causes. The first is that cell populations with this mutation have an advantage in terms of monoclonal conversion. This is demonstrated in that three out of ten simulations have a mutated population that never dies out, as opposed to zero out of ten in the baseline case. This advantage is likely caused by a combination of cells with this mutation effect tending to form groups due to the increased drag compared to wild-type cells, increased compression due to drag forces allowing higher cell densities than wild-type cells, and increased drag forces making it harder for mutated cells to be swept out of the crypt than wild-type cells.

The second cause of the large standard deviation of this mutation effect is that the extra compression leads to the mutant dominant crypts having more cells than wildtype dominant crypts which further amplifies the difference between simulations where mutated cells dominate and simulations where the mutated population is swept out.

Both the change in quiescent time and the combined Apc mutation had very consistent effects Fig. 2**D**.

The small standard deviation in the cases of both quiescent time reduction and Apc mutation is due to the advantage that a shorter quiescent phase gives in the monoclonal conversion fight in both these cases. In both experiments the mutated populations quickly dominated the crypt in all ten simulations. This causes very little variability across the repeats.

The most striking effect of quiescent time reduction was the advantage it conferred to the mutated cells in the niche. A neutral mutation at this location was always swept out whereas a mutation resulting in a reduced quiescent phase never was. This effect causes mutated stem cells to divide fast enough to replace any cells which are swept out of the niche, while wildtype cells are not always able to replace swept out cells. This process inevitably leads to niche succession by the mutated stem cells.

Apc mutation showed the separate effects complementing each other Fig. 2**E**.

The combined Apc simulation showed that the separate effects reinforced each other. One outcome of these complementary effects is the large increase in cellularity seen within the crypt. This is due to the drag effect allowing more cells to fit in a single crypt combined with the mutant dominated niche providing a constant supply of mutated cells at a higher rate than the wildtype.

Another outcome is that the flat mucosa was ultimately 95% mutated. This is due to a combination of the additional adhesion conferring an advantage to the mutated cells in the flat mucosa and the niche succession providing a ready supply of fresh mutated cells from the crypt below. This combination of effects also accounts for the reduced lag between mutated populations in the crypt and those in the flat mucosa. The adhesion advantage causes the effects of mutated cells rising up from the crypt below the mucosa to manifest much more quickly.

This work could be extended in two main directions. Firstly it would be possible to model other mutations and perform a similar analysis for them. This could take the form of either two cells with different mutations arising spontaneously in the crypt or of a single cell undergoing two successive mutations. The second direction for future work will be to model a patch of multiple crypts connected by flat mucosa. This will allow predictions to be made about the effect of a mutated crypt on a wild-type neighbour crypt and is work that we are currently undertaking.

5. Conclusions

In conclusion, a model of the colonic crypt including novel features of anoikis and accurate geometry was used to investigate the effect of Apc loss on cells within the crypt. A number of non-intuitive results arose from the simulations carried out with our extended crypt model:

- The increase in cell-membrane adhesion seen in Apc mutation allows mutated cells to live indefinitely in the flat mucosa and may be a previously unknown method of mutation fixation
- Increases in cell drag forces due to strong contact with the basement membrane confers an advantage in the monoclonal method of mutation fixation and also results in grouping of mutated cells
- Reduction in the quiescent time of mutated stem cells confers a large advantage on the mutated cells in the monoclonal method of mutation fixation

These novel predictions may prove interesting candidates for future biological and computational investigation.

Acknowledgements

We would like to thank the University of Sheffield faculties of Engineering and Medicine for funding this project.

References

[1] A. Humphries, N.A. Wright, Colonic crypt organization and tumorigenesis, Nat. Rev. Cancer 8 (6) (2008) 415–424.
[2] H. Cheng, M. Bjerknes, J. Amar, Methods for the determination of epithelial-Cell kinetic-Parameters of human colonic epithelium isolated from surgical and biopsy specimens, Gastroenterology 86 (1) (1984) 78–85.
[3] A.-M. Baker, B. Cereser, S. Melton, A.G. Fletcher, M. Rodriguez-Justo, P.J. Tadrous, et al., Quantification of crypt and stem cell evolution in the normal and neoplastic human colon, Cell Rep. 8 (4) (2014) 940–947.
[4] R. Bravo, D.E. Axelrod, A calibrated agent-based computer model of stochastic cell dynamics in normal human colon crypts useful for in silico experiments, Theor. Biol. Med. Model. 10 (2013) 24.
[5] H. Cheng, C.P. Leblond, Origin, differentiation and renewal of 4 main epithelial-cell types in mouse small intestine, Am. J. Anat. 141 (4) (1974).
[6] C.S. Potten, Stem cells in gastrointestinal epithelium: numbers, characteristics and death, Philos. Trans. R. Soc. B-Biol. Sci. 353 (1370) (1998) 821–830.
[7] S.M. Frisch, H. Francis, Disruption of epithelial cell-matrix interactions induces apoptosis, J. Cell Biol. 124 (4) (1994) 619–626.
[8] M. Hausmann, K. Leucht, C. Ploner, S. Kiessling, A. Villunger, H. Becker, et al., BCL-2 modifying factor (BMF) is a central regulator of anoikis in human intestinal epithelial cells, J. Biol. Chem. 286 (30) (2011) 26533–26540.
[9] C.S. Potten, M. Kellett, S.A. Roberts, D.A. Rew, G.D. Wilson, Measurement of invivo proliferation in human colorectal mucosa using bromodeoxyuridine, Gut 33 (1) (1992) 71–78.
[10] O.J. Sansom, K.R. Reed, A.J. Hayes, H. Ireland, H. Brinkmann, I.P. Newton, et al., Loss of Apc in vivo immediately perturbs Wnt signaling, differentiation, and migration, Genes. Dev. 18 (12) (2004) 1385–1390.
[11] S. Yamada, S. Pokutta, F. Drees, W.I. Weis, W.J. Nelson, Deconstructing the cadherin-catenin-actin complex, Cell 123 (5) (2005) 889–901.
[12] I.P.M. Tomlinson, W.F. Bodmer, Failure of programmed cell-death and differentiation as causes of tumors – some simple mathematical-models, Proc. Natl. Acad. Sci. U. S. A. 92 (24) (1995) 11130–11134.
[13] K. Smallbone, B.M. Corfe, A mathematical model of the colon crypt capturing compositional dynamic interactions between cell types, Int. J. Exp. Pathol. 95 (1) (2014) 1–7.
[14] P.J. Murray, J.-W. Kang, G.R. Mirams, S.-Y. Shin, H.M. Byrne, P.K. Maini, et al., Modelling spatially regulated beta-catenin dynamics and invasion in intestinal crypts, Biophys. J. 99 (3) (2010) 716–725.
[15] S.Y. Wong, K.H. Chiam, C.T. Lim, P. Matsudaira, Computational model of cell positioning: directed and collective migration in the intestinal crypt epithelium, J. R. Soc. Interface 7 (2010) S351–S363.
[16] F.A. Meineke, C.S. Potten, M. Loeffler, Cell migration and organization in the intestinal crypt using a lattice-free model, Cell Prolif. 34 (4) (2001) 253–266.
[17] D.C. Walker, J. Southgate, The virtual cell-a candidate co-ordinator for 'middle-out' modelling of biological systems, Brief. Bioinform. 10 (4) (2009) 450–461.
[18] G.R. Mirams, A.G. Fletcher, P.K. Maini, H.M. Byrne, A theoretical investigation of the effect of proliferation and adhesion on monoclonal conversion in the colonic crypt, J. Theor. Biol. 312 (2012) 143–156.
[19] S.J. Dunn, P.L. Appleton, S.A. Nelson, I.S. Nathke, D.J. Gavaghan, J.M. Osborne, A two-dimensional model of the colonic crypt accounting for the role of the basement membrane and pericryptal fibroblast sheath, PLoS Comput. Biol. 8 (5) (2012) 20.
[20] T. Ingham-Dempster, D.C. Walker, B.M. Corfe, An Agent-based Model of Anoikis in the Colon Crypt Displays Novel Emergent Behaviour Consistent with Biological Observations, Royal Society Open Science: The Royal Society Publishing, 2017.
[21] G.T. Eisenhoffer, P.D. Loftus, M. Yoshigi, H. Otsuna, C.-B. Chien, P.A. Morcos, et al., Crowding induces live cell extrusion to maintain homeostatic cell numbers in epithelia, Nature 484 (7395) (2012), 546–U183.
[22] R.C. van der Wath, B.S. Gardiner, A.W. Burgess, D.W. Smith, Cell organisation in the colonic crypt: a theoretical comparison of the pedigree and niche concepts, PLoS One 8 (9) (2013).
[23] S.-J. Dunn, I.S. Naethke, J.M. Osborne, Computational models reveal a passive mechanism for cell migration in the crypt, PLoS One 8 (11) (2013).
[24] A.G. Fletcher, C.J.W. Breward, S.J. Chapman, Mathematical modeling of monoclonal conversion in the colonic crypt, J. Theor. Biol. 300 (2012) 118–133.
[25] C. Pin, A.J.M. Watson, S.R. Carding, Modelling the spatio-Temporal cell dynamics reveals novel insights on cell differentiation and proliferation in the small intestinal crypt, PLoS One 7 (5) (2012).
[26] T.G. Fellous, S.A.C. McDonald, J. Burkert, A. Humphries, S. Islam, N.M.W. De-Alwis, et al., A methodological approach to tracing cell lineage in human epithelial tissues, Stem Cells 27 (6) (2009) 1410–1420.

Tim Ingham-Dempster is a third year PhD researcher at the University of Sheffield's Insigneo Institute for In-Silico medicine. His research interests are centered around developing and using computational models of early stage colorectal cancers.

Dr Dawn Walker is an academic based in the Department of Computer Science, and Insigneo Institute of in silico Medicine at the University of Sheffield. Her primary research interest is the application of agent-based and multiscale modelling techniques to study cellular interactions in biological tissues.

Dr Bernard Corfe is an academic with research interests in lower-gut (colon) biology and disease. Particular focus includes the role of nutrients, especially fibre and vitamin D, in prevention of colorectal polyps and management of IBS. Work spans from the molecular scale, e.g. the role of short-chain fatty acids in molecular governance of protein function, through to patient scale, e.g. the prosecution of interventions to support human health. Dr Corfe collaborates with computational biologists to generate improved understanding and integration of findings.

Chapter 5: Multiple Scale Multi-crypt Modelling of APC$^-$ versus wild-type competition in the Human Colon Suggests Novel Processes of Field Cancerisation

This chapter is a manuscript which is intended for publication in the near future, it involves two studies, the first of which involved extending the model used in the previous chapter to simulate areas of tissue covering multiple crypts. The second study developed an entirely new model which was at the scale of crypts as agents.

The first study focused on the interaction between a mutated crypt and wild-type neighbour crypts. This is the first agent based model of the colonic crypt in the literature to simulate multiple crypts and as such produces novel predictions about the interaction between crypts. The model predicts that one hypothesised method of field spread does not occur and displayed a mechanism for field spread which has not previously been hypothesised. This model was then used to perform a sensitivity analysis to predict the outcome of varying the separate effects of APC loss on the interaction between crypts.

The second study contained the first model in the literature to simulate individual crypts as agents. This allowed simulations to be performed on a model of the whole colon for multiple decade timespans which appears to be a novel achievement. The ability to perform simulations of this size allowed the development of fields to be studied at scales that have been unavailable previously. The study used this ability in two experiments, the first tracked the expansion of a field over time and predicted results in agreement with in-vivo data. The second experiment studied different types of collision between fields, a phenomenon which has not previously been modelled.

I undertook the development of the models and designed and performed the studies using them, my supervisors provided guidance and suggestions throughout this process. I wrote the manuscript and my supervisors acted as editors.

Multiple Scale Multi-crypt Modelling of APC$^-$ versus wild-type competition in the Human Colon Suggests Novel Processes of Field Cancerisation

Tim Ingham-Dempster[12], Dawn C Walker[13], Ria Rosser[2] & Bernard Corfe[12]

Addresses / affiliations

1 INSIGNEO Institute, University of Sheffield, England

2 Molecular Gastroenterology Research Group, Department of Oncology and Metabolism, University of Sheffield, England

3 Department of Computer Science, University of Sheffield, England

Keywords

Colorectal cancer, field spread, carcinogenesis

Conflicts of interest

None

Word count:

8138

5.1: Abstract

Colorectal cancer (CRC) is a major cause of cancer mortality, both in Europe and world-wide. It is known that loss of function of the APC gene through mutation is one of the earliest steps in CRC initiation and that this is followed by the expansion of a field of mutated tissue. There is little information in the literature about the mechanisms and characteristics of this field spread.

The crypts of Lieberkühn are structures within the colon, it is known that APC mutation arising near the base of one of these crypts can become fixed and colonise the entire crypt. It has been hypothesised in the literature that cells from a mutated crypt will invade the neighbouring crypts surrounding it. An agent based model (ABM) is used to test this hypothesis, it predicts that neighbouring crypts will not be invaded but that the flat mucosa above them will be, which appears to be a novel prediction in the literature.

The literature states that fields develop over multiple decades and cover tens of thousands of crypts, scales which are computationally infeasible for models using cells as agents. To examine fields at these scales a computational model is developed which uses crypts as agents. This model simulates the entire colon for multiple decades and predicts fields developing to cover tens of thousands of crypts, in agreement with in-vivo data from the literature. Fields are predicted to be ~230 crypts in diameter, this would equate to 23mm in-vivo. This model is used to predict the relative probability of two hypothesised causes of fields colliding, the first (inter-field) being two separate fields growing into the same region of tissue, the second (intra-field) being the spontaneous mutation of a wild-type crypt beneath mutated flat mucosa. The model predicts that the probability of an inter-field collision is 3.5 – 8.0 higher than the probability of an intra-field collision over a twenty year timespan, the first time that these values have been predicted.

This study is the first to investigate field spread in-silico and make predictions for rates, sizes and characteristics of expanding fields. It is also the first to be able to simulate the whole colon for multi-decade timespans.

5.2: Introduction

The human colon consists of a monolayer epithelium punctuated by test-tube shaped invaginations known as the crypts of Lieberkuhn. These crypts supply the large number of cells required to maintain an epithelium in the hostile environment of the colon, necessitating a constant process of division and differentiation within the colon. Disruption of these processes is implicated in the formation of colorectal cancers (CRC) (Humphries and Wright, 2008).

Changes to the Adenomatus Polyposis Coli (APC) gene, and expression of its associated protein, are strongly linked to the initial stages of adenoma formation (Merritt et al., 1997). A number of changes to cell behaviour are associated with mutation of this gene including cells losing their rigidity (Sansom et al., 2004), a decrease in the quiescent time before cell cycle re-entry, and a resistance to anoikis (Sansom et al., 2004).

There is strong evidence that individual crypts are monoclonal in nature. This has been shown through studies on chimeric mice (Merritt et al., 1997) and in an XO/XY mosaic human (Novelli et al., 1996). The mechanism behind this monoclonal conversion (outcompetition and takeover of crypts by cells derived from a single stem progenitor) has been elucidated and examined via computational modelling techniques (Fletcher et al., 2012, Mirams et al., 2012). In contrast, in-vivo studies (Novelli et al., 1996, Merritt et al., 1997) indicated that adenomas are almost exclusively polyclonal in nature, which suggests that multiple crypts are involved in the formation of adenomas. These processes are extremely challenging to observe and so are poorly understood, as they occur over spatial and temporal scales which make them inaccessible to biological techniques. To date they have not been addressed by computational models, possibly as it is only recently that models of the crypt mouth have been able to accurately predict the spatial distribution of cell death events (Ingham-Dempster et al., 2017).

A number of studies (Bernstein et al., 2000, Yu et al., 2011), (Patel et al., 2015) have suggested that fields of tissue exist around adenomas which are macroscopically normal but carry mutations and have increased risk of further adenoma formation, this phenomenon is known as *field cancerisation*. Combined with the findings discussed above on adenoma polyclonality we posit that adenoma formation is linked to the interaction of multiple independent fields. This study aims to shed light on these processes.

There are two competing hypotheses in the literature as to the mechanism behind field spread. The top-down hypothesis (Shih et al., 2001) is that proliferative advantages caused by the pre-cancerous mutations present in a mutated crypt allow cells from that original crypt to invade neighbouring healthy crypts. Once this invasion has occurred the proliferative advantage of the mutated cells allows them to take over the neighbouring crypt by subverting the process of monoclonal conversion. When the immediate neighbours of the originally mutated crypt have been mutated the process repeats and the field spreads to the neighbours of the newly converted crypts.

The bottom up hypothesis (Preston et al., 2003) is centred around the process of crypt fission whereby one crypt divides into two. This process is known to occur in healthy tissue and is thought to be a normal part of the homeostasis of epithelial tissue. Fission is known to be accelerated by an order of magnitude in tissue of patients with a number of diseases related to CRC (Cheng et al., 1986) so it is hypothesised that crypts with pre-cancerous

mutations also have an elevated rate of crypt fission. This elevated rate of fission then causes mutated crypts to clone themselves at a higher rate than both the wild-type crypts surrounding them and the homeostatic replacement rate, leading to an expanding patch of mutated tissue. This is currently the most strongly supported of the two hypotheses with data from both computational and in-vivo studies (Kershaw et al., 2013, van der Wath et al., 2013).

Computer simulations are helping to address the challenge of obtaining biological data. In particular, agent based modelling (ABM) has been applied to elucidate the process behind crypt monoclonality (Fletcher et al., 2012), the effects of known pre-cancerous mutations on monoclonal conversion (Mirams et al., 2012), and cell migration in the crypt (Dunn et al., 2013) amongst others.

Agent based models (ABMs) capture the dynamic behaviour of complex systems by creating software agents, with each agent being an autonomous entity directly analogous to real world entities. Each software agent makes decisions based on its internal state and the local environment but is not governed by an overarching control mechanism. By combining many such agents with a suitable environment, complex behaviours arise which reflect the behaviour of the system being modelled. The agent based models of the colon crypt discussed above represent crypt cells as agents: an approach which is justified as biological cells act as fundamental units or entities which make decisions based on a combination of their internal state and local environment, with complex behaviours emerging via local coordination.

Our previous studies (Ingham-Dempster et al., 2018, Ingham-Dempster et al., 2017) considered the factors controlling homeostasis in a normal crypt and also the impact of known changes to crypt cell phenotype arising from pre-cancerous mutations. As described (Ingham-Dempster et al., 2018) in the previous study, this lower-scale model has been extended to represent some of the known effects of Apc loss on the virtual cells. Specifically, reduced cell stiffness and reduced stem cell quiescent time are modelled by modifying the parameters which control those attributes. Resistance to anoikis is modelled by increasing the strength of a cell's attachment to the basement membrane.

One of the predictions of the second study was that cells displaying behaviour typical for Apc mutation have a competitive advantage in the crypt mouth, and possibly in the flat mucosa, which allows them to rapidly dominate this region. As the crypt mouth is the junction between crypts we hypothesise that this behaviour may have bearing on the processes underlying field cancerisation.

The current study has three main aims:

> To examine the consequences of the behaviours seen in the previous study (Ingham-Dempster et al., 2018) where mutated cells exhibited a survival advantage over wild-type cells in the crypt mouth.
>
> To assess whether the predictions arising from both the previous and current studies are consistent with in-vivo findings.

To study the effect of behaviours identified at multi crypt level when modelled over a whole organ and a timescale of multiple decades using a larger scale agent-as-crypt model.

5.3: Methods

5.3.1: The Cell Level Model

An Agent-Based model (ABM), where one computational agent represents one biological cell (Ingham-Dempster et al., 2017), was used to investigate phenomena related to crypt homeostasis and pre-cancerous mutation in a number of simulation experiments.

For this study, an area of flat mucosa was added to the model connecting multiple crypts together and rules were created to allow cells to migrate between crypts based on proximity. The extent of the spread of mutated cells throughout a simulation was tracked and plotted. The existing model was extended from a single crypt into a model of a patch of colonic tissue covering multiple crypts, with each crypt connecting to the newly added flat mucosa. Patches of 5x5, 9x9, and 15x15 crypts were simulated, the 15x15 simulation involved the simulation of ~405,000 individual agents.

A variety of boundary conditions were tested to determine how large a simulation was necessary for the experiments to be undertaken without boundary effects influencing the predictions of the model. Additional validation of the predictions made by this model was performed by examining the literature for markers of APC mutation in colonic cells and reports of expression of these markers in-vivo.

5.3.2: The Crypt-Level model

An agent based model (henceforth referred to as the “crypt scale model”) was developed, which represents individual crypts as agents. This allows areas of millions of crypts to be simulated over multi-year timescales at the cost of granularity of results. The rules governing the behaviour of crypts are as follows:

Mutation - crypts can be defined as either *wild-type* or *mutated* (i.e. a cell within the crypt has at some point in the past mutated and come to colonise the crypt through monoclonal conversion (Fletcher et al., 2012)). When a crypt is designated as mutated, a variable representing the percentage of mutated cells within the flat mucosa above the crypt is incremented each timestep by either a fixed amount or an amount drawn from a normal distribution to represent mutated cells flowing into the flat mucosa from the mutated crypt below **(Box 1)**.

Mucosal field spread - if the flat mucosa contains more than 90% mutated cells, these cells will begin to overflow into the flat mucosa associated with neighbouring crypts. This is implemented via a rule which, for each pair of neighbouring crypts, increments the variable representing the percentage of mutated cells in the flat mucosa above the crypt with the lower mutation percentage and decrements the percentage of mutated cells in the flat mucosa above the crypt with the higher mutation percentage **(Box 2)**.

Growth - each wildtype crypt has a life cycle (Wasan et al., 1998) which consists of growing or shrinking at a constant rate until a target length is met. When this length is achieved the next target length is drawn from a normal distribution with mean equal to mean crypt length reported in the literature (Potten, 1998) and variance calculated to give a division rate matching that reported in in-vivo studies (Humphries and Wright, 2008) **(Fig 1Ai)**.

Fission - if a crypt is longer than a global length threshold, then the crypt divides into two crypts. This threshold and the normal distribution from which target lengths are drawn were

calibrated to create a fission rate which matches known biological data (Humphries and Wright, 2008).

Extinction - if a crypt shrinks below a certain length threshold the crypt will become extinct and be removed from the simulation. This rule is phenomenologically motivated in that whilst such extinctions have not been reported in the literature it is not obvious how they could be observed. An assumption is made that an adult biological system exists in a homeostatic state, and specifically that the rate of extinction (not directly observable) will be approximately equal to the rate of fission. These three rules are summarised in **Box 3.**

If a crypt is designated as mutated its lifecycle will change to one of constant, rather than stochastic growth (**Box 3 and Fig 5.1Aii)**. This produces a crypt division rate for mutated crypts which is approximately 20x higher than for wildtype crypts which matches known biological data (Humphries and Wright, 2008).

Movement - crypts can move over the 2 dimensional surface with inter-crypt forces resolved using a damped spring model to prevent crypts from overlapping. This model is similar to the one used to resolve cell-cell overlaps in the cell scale model and obeys **Eq1:**

$$\mathbf{v} = ((r_1 + r_2 - |\mathbf{p_1} - \mathbf{p_2}|) * ((\mathbf{p_1} - \mathbf{p_2}) / |\mathbf{p_1} - \mathbf{p_2}|) * k) \text{ if } |\mathbf{p_1} - \mathbf{p_2}| < r_1 + r_2 \quad (1)$$

Where v is the velocity of the crypt for this timestep, $\mathbf{p_1}$ and $\mathbf{p_2}$ are the positions of the two cells and r_1 and r_2 are their radii **(Fig 5.1B)**.

Boundaries - the colon is modelled as a rectangle representing an unwrapped cylinder, the y axis maps to the long axis of the cylinder and a wraparound boundary condition is applied along the longest boundaries to match the topology of a cylinder rather than a rectangle. If a crypt moves beyond the simulation boundary in the x dimension it is moved to the other side of the crypt. This forms a wraparound boundary to simulate the colon as an open ended cylinder. If a crypt moves beyond the simulation boundary in the y dimension a restoring force is applied proportional to the distance beyond the boundary that the crypt has moved. This creates a fixed boundary in the y dimension to represent the ends of the colon **(Fig 5.1C)**.

Crypts along one side of the simulation boundary in the x dimension can interact with crypts on the other side to complete the wraparound conditions. These interactions apply both to crypt overlap resolution forces and to the mucosal mutation spread rules.

Validation and calibration of this model were performed by simulating a small patch of tissue with both the cell scale model and the crypt scale model and comparing the results. To do this the crypt scale model was modified by disabling the rules for crypt fission and movement, which are not present in the cell scale model. A 6x6 array of crypts was created and simulated for one year of biological time. This was repeated with different values of the mutated cell production parameter. The cell scale model was then used to run an equivalent 6x6 crypt simulation and the results of both sets of simulations were plotted and compared.

5.4: Results

5.4.1: Modelling Apc loss in a multi-crypt environment predicts invasion of the flat mucosa by precancerous cells

APC loss cells have previously been predicted to have a competitive advantage in the crypt mouth where crypts join (Ingham-Dempster et al., 2017). To investigate the potential of Apc^- cells to invade neighbouring crypts in a top-down manner due to this advantage an array of 5x5 crypts was initialised and run for 8 hours of biological time to reach an equilibrium state. At this point, one cell in the centre crypt of the array was designated as mutated and both wild-type and mutated cells were tracked for a further year of biological time. Wildtype cells were coloured red and mutated cells green so that the behaviour of the two populations could be visualised separately. A representative visualisation of the simulation is provided in **Fig 5.2** showing mucosal field spread in a typical simulation.

The main observation from this simulation experiment was that cells carrying a mutation causing APC loss would spread through the flat mucosa of neighbouring crypts but would not invade these crypts.

5.4.2: Different mutation effects induce field cancerisation at different rates

Apc mutation is associated with altered parameters for quiescence, apoptosis and attachment (Humphries and Wright, 2008, Sansom et al., 2004). In the initial simulations, a standard set of perturbations was associated with Apc mutation. In order to evaluate the contribution of each pleiotropy to the expansion of Apc loss fields, a multiple parameter sensitivity analysis was undertaken. Three features of field expansion were measured: the time taken from initial mutation to the onset of field expansion, the rate of expansion, and the overall size of field achieved.

The runs simulated approximately one year of biological time and maximum mutated cell migration distance was output, in addition a condition was added to track the originating crypt of a mutated cell population and any cell achieving a depth of 25% or greater in a crypt from which it did not originate would be considered to have invaded that crypt. These invasion events were logged and recorded along with the migration data to determine if any biologically realistic set of parameters would lead to crypt invasion.

The means of the spread rate of each simulation were plotted against time, a typical example being shown in **Fig 5.3A**, and three features were identified. The first is that as expected, there is a lag between the mutation event and the onset of field spread, the second is that the fields eventually reach a maximum size and stop spreading, and the third is the rate at which the fields reach this maximum size.

These three features were then extracted from the data for each combination of parameter values and plotted to determine the contribution of each mutation effect to each feature. In all of the plots each value of the quiescent time modification parameter was plotted as an individual plane of results, with the attachment force parameter plotted on the x-axis, the cell stiffness plotted on the y-axis and the feature being measured plotted on the z-axis.

Quiescent time had the largest effect on lag phase time, with lower quiescent times causing lower lag times **(Fig 5.3B)**. Reducing cell stiffness also affected lag time, with stiffer cells having shorter lags, this effect was emphasised for lower quiescent times. Attachment force and cell stiffness both affect total field spread **(Fig 5.3C)**, increasing stiffness reduces the

overall size of the field whereas increasing attachment force increases the final field size. Rate of spread can be separated by quiescent time change, but the effects appear to be inconsistent **(Fig 5.3D)**. Attachment force and cell stiffness appear to have interrelated effects on spread rate, with maximal rates of spread occurring at high attachment force when there is low stiffness and low attachment force when there is high stiffness. Parameter sets where both attachment force and cell stiffness are low correspond to minimal spread rate, as do cases where both mutation effects are high.

Top-down invasion of neighbouring crypts (as opposed to their flat mucosa) was not seen for any combination of values tested in the parameter sweep, but was infrequently observed for biologically implausible parameter values, (see online supplement for further data).

5.4.3: Validating and Calibrating the Mucosal Invasion Mechanism in the Crypt Scale Model

In order to examine the potential expansion of mutated cells beyond a 25 crypt area, an ABM at crypt scale was developed. The model was initially validated at small scale against the lower scale predictions.

It was necessary to validate the mucosal invasion mechanism in the crypt scale model and to calibrate the mutated cell production parameter. To do this the crypt scale model was modified to better represent the cell scale model, specifically the crypt cycle and movement process was disabled as the processes are not present in the cell scale model.

An array of six by six crypts (the crypt scale model has a technical limitation which requires the dimensions to be divisible by two) was created in both the cell scale model and the crypt scale model. After reaching equilibrium the crypt at the (2,2) position (using 0-indexing) was designated as mutated and the spread of mutated cells was tracked. In the crypt scale model a crypt's flat mucosa was considered to have been colonised when its mutated cells percentage reached 50%. The distance from the crypt with the original mutation to each crypt with invaded flat mucosa was calculated and the maximum such distance was output at every timestep as a measure of the spread of mutated cells in this model.

Five crypt scale simulations were run with different values for the number of mutated cells produced by the mutated crypt each timestep, these values were 10, 20, 30, 40, and 50 cells per timestep. Plots of spread against time were produced for each value and these were compared with a plot from the cell scale model to determine the similarity of predictions from the two models. Crypt scale simulations were run for approximately one year of biological time as with the cell scale simulations, however this required only five hundred timesteps as opposed to one million for the cell scale simulations due to the longer timestep of the crypt scale model.

Predictions of spread distance against time were examined for the crypt level model and compared to those of the cell level model, a visualisation of this experiment is shown in **Fig 5.4A** and shows the mutated central crypt with a surrounding region of invaded flat mucosa, which is consistent with the predictions of the cell scale model.

The effect of varying the number of mutated cells generated per timestep (i.e. the cell production parameter) was investigated. In **Fig 5.4B** the field spread vs time generated using several values of this parameter are plotted, along with the similar results from a typical simulation generated using the cell level model. This graph shows that spread rate

for the crypt scale model has the same characteristic period of rapid expansion which falls off over time as the cell scale model. Additionally, spread rate is predicted to vary based on the value of the cell generation parameter in the crypt scale model and good agreement with the predictions of the cell level model can be achieved by choosing a value of 30 cells per timestep.

5.4.4: The crypt level model predicts a field of mutated crypts surrounded by a larger field of mutated mucosa

Fields of mutated tissue are known to surround lesions but the growth rate and extent of such fields is not well understood as these processes are inaccessible to traditional biological techniques and occur over multi-decade time spans. The cell level experiments identified one process of field development through competitive advantage of mutated cells and another field growth process has been hypothesised based on the observed increase in crypt division rate for mutated crypts.

To examine these processes, the spread of mutated cells and crypts over biologically relevant timescales was examined using the crypt scale model. The model was initialised with an array of two hundred crypts in each dimension, giving a total of forty thousand crypts, or approximately 1% of a human colon (Humphries and Wright, 2008).

The simulation was run for ten thousand timesteps to represent the dynamic state of the tissue in an individual of twenty years of age, at which point a single crypt near the centre of the simulation was mutated. The simulation was then run for a further two decades of biological time and the spread of both mucosal invasion and mutated crypts was measured. These data were output every ten timesteps and then plotted against time to characterise the predicted spread. Five repeat simulations were run to account for stochasticity in the crypt cycle.

This experiment predicted a growing field of mutated tissue consisting of two concentric sub-fields. The outer field consisted of wild-type crypts with mutated flat mucosa while the inner field consisted of fully mutated crypts. This inner field consisted of clonal offspring of the original mutated crypt produced by crypt fission and was able to displace the wild-type crypts which previously existed in this location to the edges of this field of mutated crypts **(Fig 5.4C)**.

The expansion of both inner and outer fields accelerates over time in an exponential manner. The outer field of wild-type crypts with mutated mucosa initially grows faster than the inner field of mutated crypts and creates a fringe around the fully mutated field. Growth of both fields accelerates over time, with the outer field accelerating more slowly than the inner leading to a thinning of this outer field over time. **(Fig 5.4D)**. The mean size of a field at the end of the simulations was 230 crypts in diameter which corresponds to approximately 23mm and comprises ~41,000 crypts in total.

5.4.5: Whole organ simulation predicts independent collisions are more likely than collisions arising from a wild-type crypt with invaded flat mucosa

The expansion of mutant cells through flat mucosa and estimations of the size of fields led us to explore two alternate hypotheses about how polyclonal adenoma might arise: (i) inter-field collision where expanding fields might come into contact at their periphery (the current prevailing model); (ii) intra-field collison, here a new mutation may arise and fix beneath an

existing field. These possibilities were tested using the crypt scale model: a total of 4 million crypts, representing the scale of the entire human colon, were initialised as in 5.3.3 but rather than setting a pre-determined initial single mutation, mutation events were randomly generated in multiple crypts with a small probability. This simulated mutation arising in a stochastic fashion throughout the colon. Values tested for the probability of a mutation arising in a single crypt on any given timestep were 0.001, 0.005, 0.01, 0.05, and 0.1, chosen to span as large a range of the parameter space as possible with the resources of this study.

At each timestep, every crypt was checked for one of two conditions, either a mutated crypt coming into contact with a clonal population from another mutated crypt, or a crypt undergoing mutation arising from its own proliferating cell population after its flat mucosa had already been invaded. Upon either condition being reached, the simulation terminated and the condition which occurred was recorded along with the length of time since the initial mutation event. The simulation was run one hundred times for each choice of mutation probability and the number of times each condition occurred was recorded to compare the relative likelihood of each event.

Fig 5.4E shows the number of collision events of each type within the whole organ crypt scale model for each mutation threshold parameter tested. For each threshold, the number of simulations which ended when two established fields collided through growth was larger than either the number of simulations where a wild-type crypt with invaded flat mucosa spontaneously mutate or the simulation ran to completion without a collision. For these final two outcomes the number of simulations where a mutation arose below invaded flat mucosa was larger than the number of simulations which ran to completion for all mutation probabilities tested except for the mutation probability of 0.01.

Fig 5.4F shows the average time taken until a collision for each of the threshold values tested. For both inter-field and intra-field collisions the mean time to collision was around ten years, except for the case where mutation probability was 0.05 in which case the mean time to collision was approximately 15 years for intra-field collision. In all cases the time to collision had a very large variance.

5.5: Discussion

The first part of this study investigated the behaviour of APC loss in cells in a multi-crypt environment to examine the hypothesis that the competitive advantage conferred by APC loss at the crypt mouth would lead to invasion of neighbouring crypts. Such invasion has been hypothesised in the literature, with arguments being made both for (Shih et al., 2001) and against (Preston et al., 2003) this mechanism, however the in-vivo evidence is ambiguous and no modelling studies have been published which address this issue.

The first experiment with the cell scale model (5.4.1), which simulated wild-type and APC mutated cells in a patch of 5x5 crypts, showed that there was no top-down invasion of crypts but that mutated cells did invade the flat mucosa above and surrounding neighbouring crypts. The model predicts such a distribution which suggests that this mechanism may reflect an in-vivo process. It is recommended that follow-up work is done to determine if this is the case and to what extent these cells could participate in carcinogenic processes.

Cell Experiment 2 (5.4.2) sought to quantify the relationship between the three effects of APC loss represented in the model, and the characteristic properties of field spread. This large sensitivity analysis showed a number of relationships between effects and characteristics which can be explained by the mechanisms at play in the crypt. For instance lag time between mutation initiation and the start of field spread was affected by stem cell quiescent time, with a shorter quiescent time leading to a shorter lag. This relationship is due to this parameter affecting the time until monoclonal conversion occurs (Ingham-Dempster et al., 2018); a shorter quiescent period gives a competitive advantage in the stem cell niche which reduces the time taken for monoclonal conversion and hence the time until mutated cells emerge from the crypt onto the flat mucosa. In addition, stiffer cells have shorter lag times, as stiff cells are driven up the side of the crypt more quickly by the mitotic pressure which drives passive migration in the crypt. As the cells move up the crypt walls more quickly it takes less time before they emerge from the crypt mouth.

Spread extent was asymptotically limited due to the quadratic relationship between the diameter of a field and the number of cells required to fill it. This asymptotic limit occurred in both the cell scale and crypt scale model, though in the larger crypt scale experiments it was counteracted by the increasing number of mutated crypts. The location of this asymptote had no discernible relationship with stem cell quiescent time. This is because quiescent time has very little effect on overall cell production rates, due to the majority of cell production arising from the division of transit amplifying cells which, unlike stem cells, do not have a quiescent phase. Increased attachment force led to increased spread because, as previously demonstrated (Ingham-Dempster et al., 2018), high attachment force provides a competitive advantage that allows mutated cells to invade the flat mucosa. Reducing the cell stiffness also caused an increase in spread rate. This is due to the forces which cause anoikis being moderated by the lower stiffness of the mutated cells, leading to reduced anoikis in the latter, providing a competitive advantage in the crypt mouth and flat mucosa.

Rate of spread also did not appear to be affected by quiescent time, again because stem cell quiescent time has negligible effect on cell production rates in the crypt. Low cell stiffness combined with high attachment force gave rise to the largest maximum for spread rate, driven by the same mechanisms. There was a second, lower, local maximum in spread rate which corresponded to low attachment force and high cell stiffness. The mechanism which causes this is unknown but may be related to lower overall spread being obtained, as the

relationship between the size of a field and the number of cells contained within is quadratic, so the initial expansion is rapid and falls off with distance.

For no parameter combination explored in Cell Experiment 2 was top down crypt invasion observed, which suggests that such events are difficult or impossible to achieve in a purely mechanical fashion. It was, however, discovered that increasing cell stiffness occasionally gave rise to crypt invasion (see supplementary information). Increased cell stiffness is unlikely to happen in-vivo as cancerous cells are consistently observed to be less stiff than wildtype ones (Sansom et al., 2004). However there is a signalling mechanism which could potentially create a similar effect: it is known that EphB signalling mediates cell-cell adhesion forces in order to create a sorting mechanism within the crypt (Holmberg et al., 2006) and a disruption of this mechanism could create an advantage for mutated cells very similar to the one seen by increasing cell stiffness beyond normal levels. These two cell experiments predicted that mutated cells from one crypt can spread through the flat mucosa above other crypts but are unable to invade them.

The flat mucosal invasion mechanism predicted by the cell scale model appears to be novel in the literature, as a previously unknown process by which mutated cells can spread through the colon this may have consequences for the prevention of metachronous adenomas.

A promising avenue for future work is investigating the invasion events seen using biologically infeasible parameters in the sensitivity analysis. This prediction suggests that a disruption of the Ephrin B signalling pathway could lead to invasion of neighbouring crypts. Extending the cell scale model to include the EphB pathway would be a straightforward task and this model could then be used to explore strong an invasive advantage would have to be conferred by EphB disruption in order to overcome the resistance to invasion caused by cell migration occurring in the wild-type crypts.

The second part of the study used a model at a larger scale to examine the behaviour of fields over a whole organ for multiple decades of time. The field spread mechanisms studied were the mucosal invasion mechanism predicted by the first part of the study and a mechanism based on increased rates of fission within mutated crypts reported in the literature (Humphries and Wright, 2008).

The first crypt scale experiment (5.4.4) predicted a two phase field growing from a single mutated crypt. The first phase was a fringe of invaded flat mucosa which initially grows more quickly than the second phase, a core of fully mutated crypts resulting from fission. The invaded mucosa eventually created a fringe approximately ten crypts wide before contracting to a narrow zone around the fully mutated region. This later contraction is most likely a geometrical effect, arising from the fact that, as the field expands the area required to expand the mucosal field grows as the square of the radius of the field but the number of mutated cells being created to invade that area only grows linearly with the radius of the fully mutated field. This acts as a brake on the expansion of the mucosal field.

This experiment appears to be the first example of a simulation of a growing field at these time and length scales. The total number of mutated crypts was approximately 41,000, which is in good agreement with the sizes of fields reported in-vivo in the literature (Humphries and Wright, 2008). It is worth noting that this size of field would then comprise

the majority of crypts within the simulation and so there is a possibility of boundary effects being a factor in these results. Further work can be done both in-vivo and in-silico to refine and validate the in-silico model to produce more detailed and accurate field spread predictions which could potentially have clinical or prognostic uses.

The second crypt scale experiment (5.4.5) predicted that collisions are much more likely between two independently originating fields than from a mutation spontaneously occurring beneath an area of invaded flat mucosa. Collisions of both types were more likely than the experiment reaching the end of the simulated twenty year period with no collision. This conclusion held even when exploring a two order of magnitude variation of the mutation probability threshold.

This study is also the first to predict field spread rates and structure, with predicted fields growing to sizes which agree with in-vivo data, with emergent fields consisting of invaded flat mucosa preceding a region of fully mutated crypts. The model also predicted that collisions were more likely to occur between two spreading fields than by a spontaneous mutation below an area of flat mucosa, this suggests that future efforts to study field collision should be directed towards the collision of independent fields.

The crypt scale model could be modified to include more realistic causes of carcinogenesis, for example a small area could be given a higher probability of mutation occurring to represent an area of tissue with chromosomal instability, or an area of increased mutation probability which moves along the colon could be created to represent carcinogens absorbed through a patient's diet.

Additionally, as the crypt scale model can simulate the entire organ over a two-decade time span in only 12 hours of computational time there is great scope for doing extensive studies such as simulating populations and cohorts to examine statistical outcomes of changes between groups, for example under different treatment regimes.

5.6: Conclusions

This study has used two agent based models to investigate the spread of pre-cancerous fields in the colonic epithelium. The key findings are:

- The cell level model predicts that mutated cells will spread through the flat mucosa above wildtype crypts but that invasion of neighbouring crypts will not occur. In-vivo biopsy data suggests that this is indeed the case.
- The crypt level model produces predictions that agree with those of the cell level model but is efficient enough to be run at whole organ scale for multiple decades of biological time.
- Running the crypt level model at this scale predicts growing lesions surrounded by fringes of flat mucosa with collisions mainly occurring between growing independent fields.

Our crypt level agent-based model is the first example of such a representation of this organ and will provide a platform to explore carcinogensis and other pathologies in the colon on clinically relevant time and length scales.

5.7: References

BERNSTEIN, C., BERNSTEIN, H., PAYNE, C. M. & GAREWAL, H. 2000. Field defects in progression to adenocarcinoma of the colon and esophagus. *EJB Electronic Journal of Biotechnology,* 3**,** 1-22.

CHENG, H., BJERKNES, M., AMAR, J. & GARDINER, G. 1986. CRYPT PRODUCTION IN NORMAL AND DISEASED HUMAN COLONIC EPITHELIUM. *Anatomical Record,* 216**,** 44-48.

DUNN, S.-J., NAETHKE, I. S. & OSBORNE, J. M. 2013. Computational Models Reveal a Passive Mechanism for Cell Migration in the Crypt. *Plos One,* 8.

FLETCHER, A. G., BREWARD, C. J. W. & CHAPMAN, S. J. 2012. Mathematical modeling of monoclonal conversion in the colonic crypt. *Journal of Theoretical Biology,* 300**,** 118-133.

HOLMBERG, J., GENANDER, M., HALFORD, M. M., ANNEREN, C., SONDELL, M., CHUMLEY, M. J., SILVANY, R. E., HENKEMEYER, M. & FRISEN, J. 2006. EphB receptors coordinate migrationand proliferation in the intestinal stem cell niche. *Cell,* 125**,** 1151-1163.

HUMPHRIES, A. & WRIGHT, N. A. 2008. Colonic crypt organization and tumorigenesis. *Nature Reviews Cancer,* 8**,** 415-424.

INGHAM-DEMPSTER, T., CORFE, B. & WALKER, D. 2018. A cellular based model of the colon crypt suggests novel effects for Apc phenotype in colorectal carcinogenesis. *Journal of Computational Science,* 24**,** 125-131.

INGHAM-DEMPSTER, T., WALKER, D. C. & CORFE, B. M. 2017. An agent-based model of anoikis in the colon crypt displays novel emergent behaviour consistent with biological observations. Royal Society Open Science: The Royal Society Publishing.

KERSHAW, S. K., BYRNE, H. M., GAVAGHAN, D. J. & OSBORNE, J. M. 2013. Colorectal cancer through simulation and experiment. *Iet Systems Biology,* 7**,** 57-73.

MERRITT, A. J., GOULD, K. A. & DOVE, W. F. 1997. Polyclonal structure of intestinal adenomas in Apc-(Min)/+ mice with concomitant loss of Apc(+) from all tumor lineages. *Proceedings of the National Academy of Sciences of the United States of America,* 94**,** 13927-13931.

MIRAMS, G. R., FLETCHER, A. G., MAINI, P. K. & BYRNE, H. M. 2012. A theoretical investigation of the effect of proliferation and adhesion on monoclonal conversion in the colonic crypt. *Journal of Theoretical Biology,* 312**,** 143-156.

NOVELLI, M. R., WILLIAMSON, J. A., TOMLINSON, I. P. M., ELIA, G., HODGSON, S. V., TALBOT, I. C., BODMER, W. F. & WRIGHT, N. A. 1996. Polyclonal origin of colonic adenomas in an XO/XY patient with FAP. *Science,* 272**,** 1187-1190.

PATEL, A., TRIPATHI, G., GOPALAKRISHNAN, K., WILLIAMS, N. & ARASARADNAM, R. P. 2015. Field cancerisation in colorectal cancer: A new frontier or pastures past? *World Journal of Gastroenterology,* 21**,** 3763-3772.

POTTEN, C. S. 1998. Stem cells in gastrointestinal epithelium: numbers, characteristics and death. *Philosophical Transactions of the Royal Society B-Biological Sciences,* 353**,** 821-830.

PRESTON, S. L., WONG, W. M., CHAN, A. O. O., POULSOM, R., JEFFERY, R., GOODLAD, R. A., MANDIR, N., ELIA, G., NOVELLI, M., BODMER, W. F., TOMLINSON, I. P. & WRIGHT, N. A. 2003. Bottom-up histogenesis of colorectal adenomas: Origin in the monocryptal adenoma and initial expansion by crypt fission. *Cancer Research,* 63**,** 3819-3825.

SANSOM, O. J., REED, K. R., HAYES, A. J., IRELAND, H., BRINKMANN, H., NEWTON, I. P., BATLLE, E., SIMON-ASSMANN, P., CLEVERS, H., NATHKE, I. S., CLARKE, A. R. & WINTON, D. J. 2004. Loss of Apc in vivo immediately perturbs Wnt signaling, differentiation, and migration. *Genes & Development,* 18**,** 1385-1390.

SHIH, I.-M., WANG, T.-L., TRAVERSO, G., ROMANS, K., HAMILTON, S. R., BEN-SASSON, S., KINZLER, K. W. & VOGELSTEIN, B. 2001. Top-down morphogenesis of colorectal tumors. *Proceedings of the National Academy of Sciences of the United States of America,* 98**,** 2640-2645.

VAN DER WATH, R. C., GARDINER, B. S., BURGESS, A. W. & SMITH, D. W. 2013. Cell Organisation in the Colonic Crypt: A Theoretical Comparison of the Pedigree and Niche Concepts. *Plos One,* 8.

WASAN, H. S., PARK, H. S., LIU, K. C., MANDIR, N. K., WINNETT, A., SASIENI, P., BODMER, W. F., GOODLAD, R. A. & WRIGHT, N. A. 1998. APC in the regulation of intestinal crypt fission. *Journal of Pathology,* 185**,** 246-255.

YU, D. C. W., BURY, J. P., TIERNAN, J., WABY, J. S., STATON, C. A. & CORFE, B. M. 2011. Short-chain fatty acid level and field cancerization show opposing associations with enteroendocrine cell number and neuropilin expression in patients with colorectal adenoma. *Molecular Cancer,* 10.

Software accessibility:

The cell scale model is available at https://github.com/TimInghamDempster/Cell-Centre-Crypt-Cpp

The crypt scale mode is available at https://github.com/TimInghamDempster/Crypt-Model

Pseudocode:

Box 1:

```
For each crypt
        If(Crypt Is Mutated)
                Mucosal Mutation Amount += Mutated Cell Production Rate
```

Flat mucosal invasion of a mutated crypt

Box 2:

```
For each crypt
        For each NeighbourCrypt
                If(Mucosal Mutation of Either Crypt > 90%)
                        Number of Cells Migrating = Difference in Mucosal
                        Migration * Flow Constant
                        Largest Mucosal Invasion -= Number of Cells Migrating
                        Smallest Mucosal Invasion += Number of Cells Migrating
```

Invasion of neighbouring mucosa from a mutated crypt

Box 3:

```
For each crypt
        If(Crypt Isn't Mutated)
                If(Length < target)
                        Length += growthRate
                Else
                        Length -= growthRate
                If(Length > divisionThreshold)
                        Divide
                If(Length < 0)
                        Remove from Simulation

        Else If(Crypt Is Mutated)
                Length += growthRate
                If(Length > divisionThreshold)
                        Divide
```

The crypt cycle governing the growth, division, and death of crypt agents in the simulation

Figures:

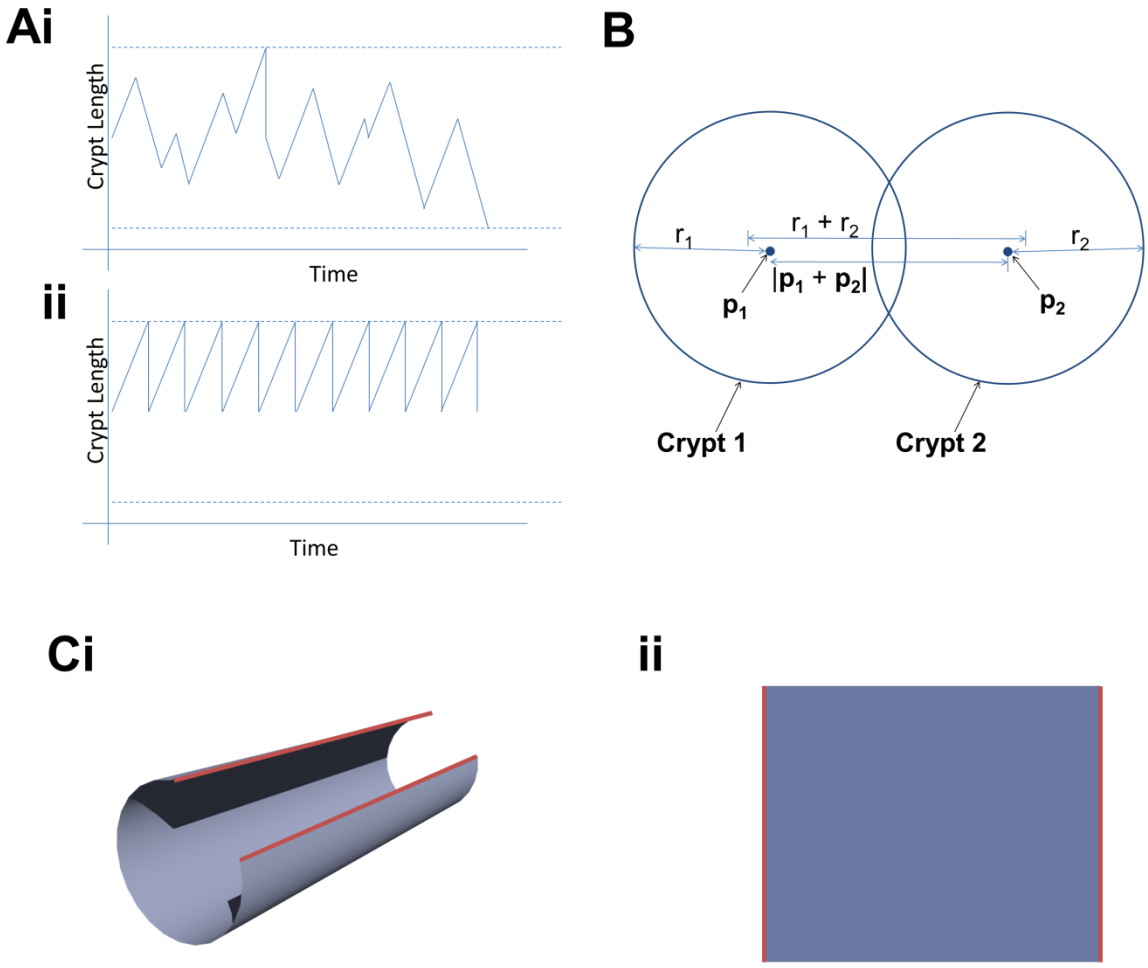

Figure 5.1: Diagrams of the Models Ai: The crypt cycle of wild-type crypts in the crypt scale model. In this example the crypt would fission once and die at the end of the example timespan, **ii:** The crypt cycle of a mutated crypt, in this example the crypt would fission ten times and never die. **B:** Overlap resolution in the crypt scale model showing the various parameters referenced in **Eq1**. **C** a cylindrical surface **(i)** such as the colonic epithelium can be unwrapped and represented as a rectangle **(ii)** as long as any objects crossing the boundary which maps to the seam of the cylinder (red lines) are moved to the opposite side of the rectangle

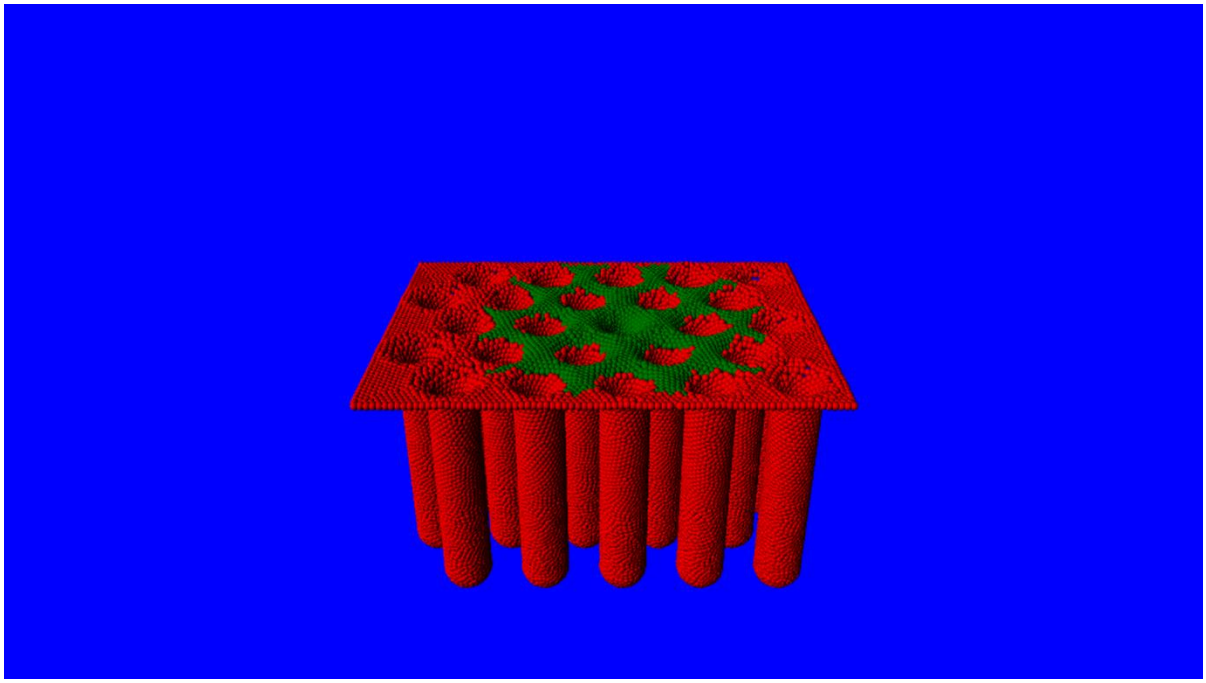

Figure 5.2: Flat Mucosal Invasion Visualisation of the cell scale model showing mutated cells (green) from the central crypt invading the flat mucosa above neighbouring crypts (red), note that no mutated cells are present within the neighbour crypts themselves.

Each layer plots the results for one value of quiescent parameter as follows:

Q = 0.10

Q = 0.25

Q = 0.50

Q = 0.75

Q = 1.00

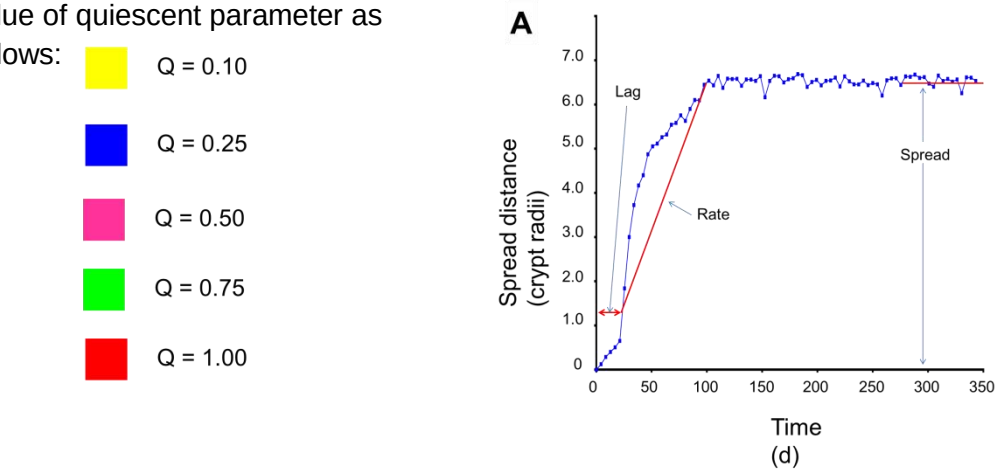

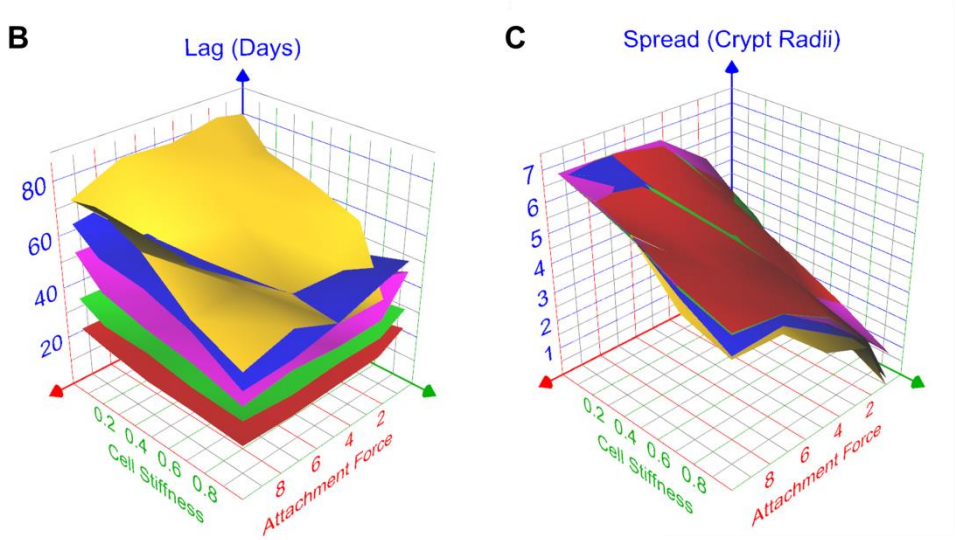

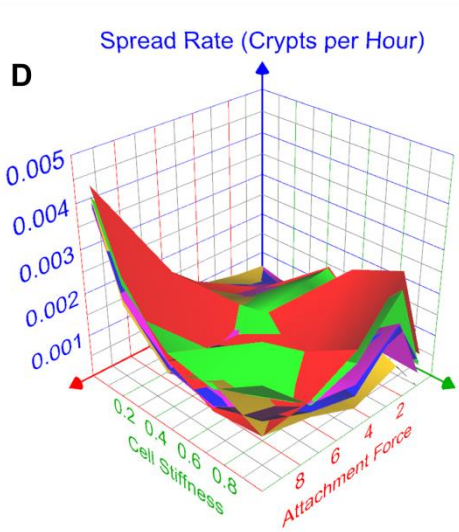

Figure 5.3: Effects of APC Loss on Field Spread A: A plot of spread distance against time for a typical simulation showing the three characteristic features measured in the parameter sweep experiment, specifically lag, spread rate, and overall spread distance. **B:** Three dimensional plot showing the effect of quiescent time reduction, attachment force increase and cell stiffness reduction on the lag time before field spread onset. **C:** Three dimensional plot of overall spread resistance plotted by the three mutation effects. **D:** Plot of the effect of quiescent time reduction, attachment force increase, and cell stiffness on the rate of field spread. Values tested for stem cell quiescent time were 10%, 25%, 50%, 75% and 100% of wild-type quiescent time. Cell stiffnesses examined were 10%, 25%, 75% and 100% of wild-type stiffness. Anoikis resistance was modelled by multiplying the mutated cell's membrane attachment strength by 1, 2.5, 5, 7.5, and 10 compared to wild-type.

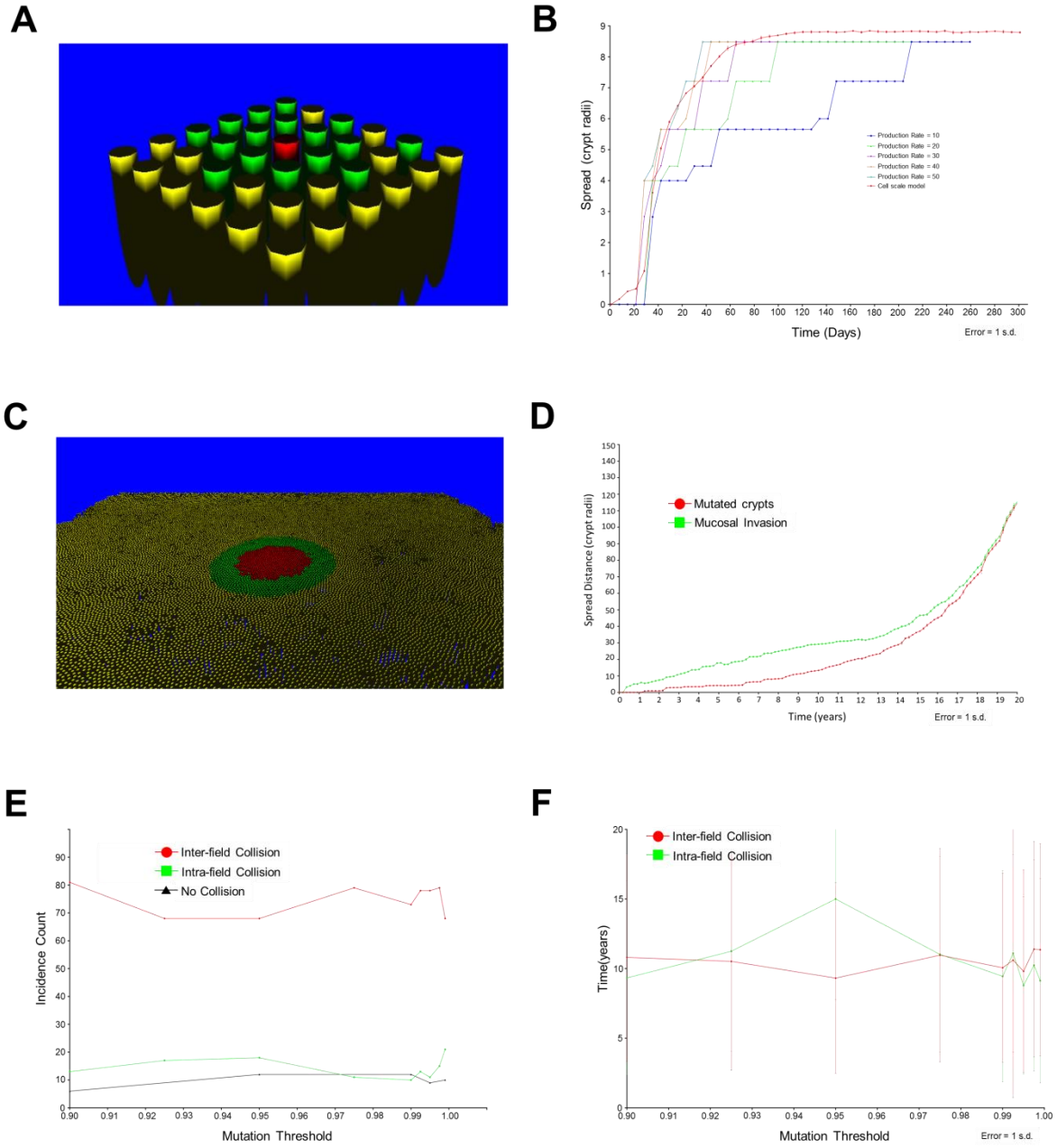

Figure 5.4: Field Spread in the Crypt Scale Model A: Visualisation of the crypt scale model used to validate the mucosal invasion rule. **B:** Plot of spread over time for multiple choices of cell production parameter in the crypt scale model and from a 6x6 simulation using the cell scale model. **C:** Visualisation of the full sized crypt scale model sometime after a single mutation event showing the growing fields of mutated crypts (red) and invaded mucosa (green). **D:** A plot of spread distance against time for the experiment visualised in **C**, showing that both fields grow exponentially, with the mucosal field (green) initially growing faster than the fully mutated field (red) which later catches up. **E:** Plot of the number of independent collisions (red), mutations below an invaded mucosal field (green), and simulations with no collisions (black), against the mutation threshold parameter. **F:** Plot of time taken for collision to occur against the mutation threshold parameter for collisions of independent fields (red) and mutations arising beneath invaded flat mucosa (green).

5.8: Online Supplement

5.8.1 Determining the Size of Simulation Required to Measure Field Spread

Due to the high computational cost of a large cell scale model it was necessary to determine the minimum necessary simulation size so that the large sensitivity analysis could be performed as efficiently as possible. To do this the simulation from Cell Experiment 1 was repeated with different sizes of simulation and the spread of mutated cells were output every 200 timesteps (approximately every 1.6hrs of biological time). These data were then plotted to determine the effect of simulation size on mutated cell spread.

The investigation proceeded as for Cell Experiment 1 but was conducted with three different sizes of crypt array: 5x5, 9x9 and 15x15. Additionally, a fourth set of simulations was conducted on a 5x5 array but with boundary conditions changed to kill cells rather than reflect them back into the simulation. This represents the most permissive possible simulation but may, but may potentially have produced unrealistic results due to the lack of boundary resistance. The 15x15 simulation was only run for six months of biological time, as opposed to one year for the other simulations due to the high computational cost of such a large simulation. Each simulation was repeated five times to account for stochasticity.

The results of these simulations are displayed in **Supplementary Fig 1** and show that simulation size had little overall effect on spread, with the difference between the largest and smallest simulations being less than one crypt radius. This is less than 1% of the size of a field predicted by the crypt level experiment, and less than one millionth of the size of the whole colon.

Based on these results the 5x5 simulation with boundaries that kill cells that cross it was chosen for the sensitivity analysis (Cell Experiment 2). This was because it was the least computationally intensive of the sizes tested and compared to the other 5x5 simulation, produced results closer to the largest simulation tested.

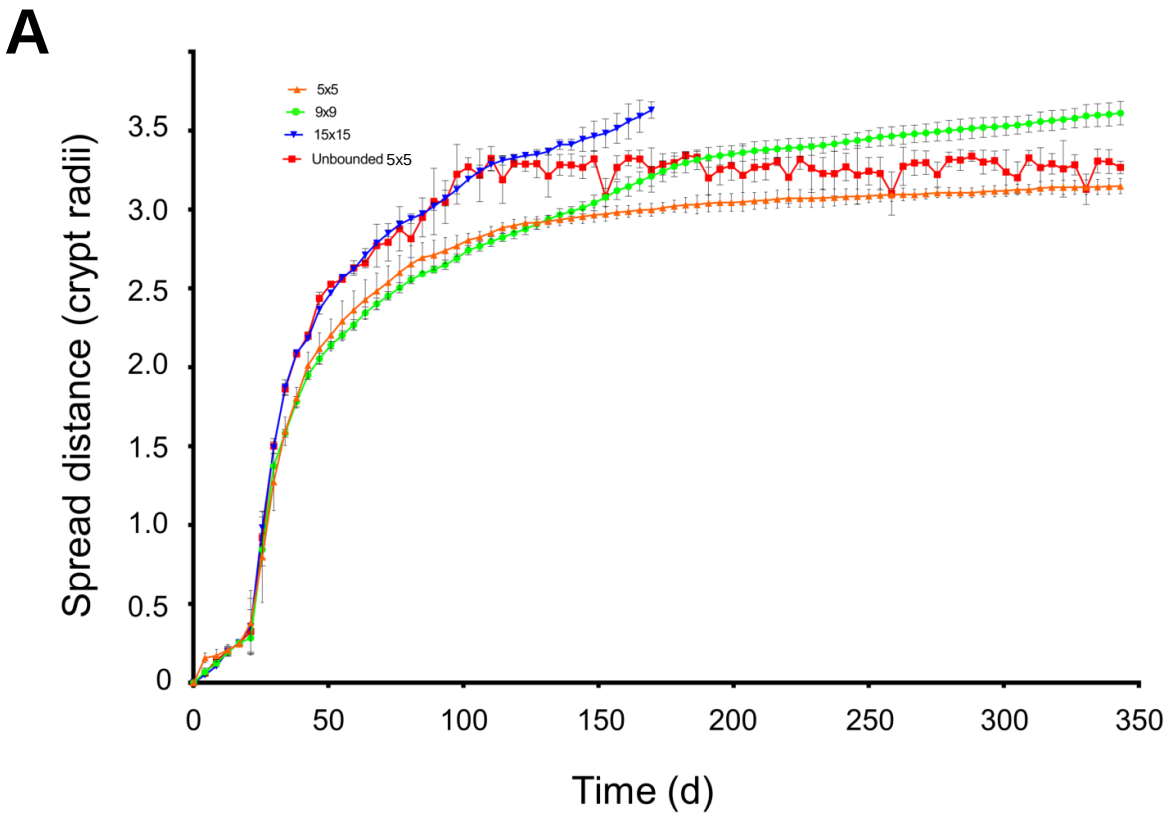

Figure 5.5: Supplementary Figure Comparison of spread against time in days for different simulation sizes and boundary conditions.

Chapter 6: Overall Conclusions

Over the course of this project a clear narrative has emerged which describes how the state of the art has been pushed forward by this work in the field of colorectal cancer modelling.

6.1: The work conducted

6.1.1: Chapters 2 & 3

Chapters 2 (Ingham-Dempster et al., 2017), & 3 describe the cell scale model that was developed for the study. This model initially recreated previous work in the field of crypt modelling (Meineke et al., 2001) and consisted of an agent based model of the colonic crypt using cells as the agents within the model. This model was able to recapitulate the predictions of existing crypt models such as monoclonal conversion (Fletcher et al., 2012) and passive migration (Dunn et al., 2013) of cells from the stem cell compartment at the crypt base up the crypt walls to the crypt mouth.

From this base the model was extended to include the crypt mouth which is unusual in the field. There have been models which have attempted to produce crypt geometry emergently (Dunn et al., 2012) which have had an area of crypt similar to a mouth. These models were too compromised by the emergent nature of the geometry to be useful predictive tools, which they were not intended to be. The majority of models, however, model the crypt mouth as a rule which removes any cell which crosses an arbitrary vertical threshold in the crypt. The model in this study is the first one to explicitly model the geometry of the crypt mouth.

The model in this study also added a rule for anoikis. Although this has been included in a previous model (Dunn et al., 2012), it was compromised by the emergent nature of the crypt geometry in that case. This rule was necessary as the inclusion of the crypt mouth meant that the standard method of simply killing any cell that passed a certain threshold was not possible.

The anoikis rule chosen was biologically inspired: when a cell moves away from the basement membrane of the crypt it will attempt to move back towards the membrane like a biological cell which is anchored to the membrane, if the cell is more than a certain threshold distance away from the membrane then it will die as would a biological cell. It has been suggested by an in-vivo study (Eisenhoffer et al., 2012) that anoikis is an active signalling process rather than the passive mechanical process as assumed in the model, however that study also suggested that the conditions which trigger the active anoikis process are the same conditions which cause anoikis to occur mechanically in the model. This means that the model gives a justified, albeit slightly abstracted, representation of anoikis.

As well as recapitulating the predictions of existing models (Meineke et al., 2001, Mirams et al., 2012, Fletcher et al., 2012), the model created for this study was able to predict a novel feedback mechanism for regulation of crypt cellularity. There is little mention in the literature of the means by which a crypt maintains a stable cell count and there has been no investigative effort on this front. Because this model did not arbitrarily kill cells which reached the crypt mouth it was possible to investigate the dysregulation of cell homeostasis by modifying the cycle time of proliferating cells and studying the effect this had on crypt cellularity. The outcome of this experiment was the discovery of a mechanism whereby

increased rates of proliferation caused increased rates of anoikis. This is because increasing the production of cells above the rate of cell death causes an increase in the forces which trigger anoikis, since these triggers are shared with the signalling mechanism that is thought to trigger anoikis in-vivo (Eisenhoffer et al., 2012) it is expected that this regulatory feedback loop will be present in-vivo and is not just an artefact of the model.

6.1.2: Chapter 4

The third paper (Ingham-Dempster et al., 2018), reproduced in chapter 4, took the model from chapters 2 & 3 and extended it to include mutated cells. The chosen mutation was loss of the APC gene which is strongly implicated in the formation of colorectal cancers (Merritt et al., 1997). This mutation was represented by modifying the properties of mutated cells in three ways: they have a lower quiescent time when acting as stem cells, they have lower overall stiffness, and they are partially resistant to anoikis. When a cell is given one or more of these properties they will be inherited by any descendants of that cell. The model was also modified to allow clonal populations of mutated cells to be tracked through the simulation.

The core of the third paper was the running of five experiments with this modified model. The first experiment tracked a wild-type clonal population through the simulation to provide a baseline, the next three each tracked a clonal population with one of the mutation effects discussed previously, and the final experiment tracked a clonal population displaying all three mutation effects.

A study has previously been performed examining the effect of APC mutation on the process of monoclonal conversion in the crypt (Mirams et al., 2012), and the current work predicted similar advantages to those predicted previously, with the only major difference being that the current study predicted a stronger advantage for mutated cells than the previous one. This is probably because the current model uses a more accurately shaped crypt niche than the previous one which would tend to amplify the effects in the niche.

The behaviour of mutated cells in the crypt mouth was an area of particular focus as this has never been simulated before. The expected behaviour was for the mutated cells to survive longer than the wild-type cells due to their anoikis resisting properties but to otherwise behave in a similar manner to the wild-type cells. The observed behaviour was very different however: the resistance to anoikis meant that mutant cells had a significant survival advantage in the crypt mouth. They quickly populated the crypt mouth which increased the rate of anoikis in the wild-type cells. Over a short period of time all wild-type cells in the crypt mouth underwent anoikis leaving only mutated cells in the crypt mouth, even before the process of monoclonal conversion of the crypt by mutated cells was complete.

The crypt mouth and associated flat mucosa forms the joint between two crypts so it was hypothesised that this process of flat mucosal colonisation could be a mechanism of field spread by allowing mutated cells which had colonised the mucosa of their origin crypt to invade the mucosa of neighbouring crypts. Once the neighbouring flat mucosa was invaded the mutated cells might then invade the crypts beneath said flat mucosa. The remainder of the project focused on the consequences of this flat mucosal colonisation as a possible mechanism of field spread.

6.1.3: Chapter 5

Chapter 5 expanded on the findings of the third paper (Ingham-Dempster et al., 2018) in three ways. The first was to investigate the consequences of mutated cells colonising the crypt mouth by extending the model to include multiple crypts and the flat mucosa which connects them. A number of simulation experiments where then carried out using this multi-crypt model with the aim of testing the hypothesis that the mutated cells would invade neighbouring crypts, as proposed in the top-down hypothesis of field cancerisation (Shih et al., 2001).

The simulations consistently predicted that mutated cells would not invade neighbouring crypts but would invade the flat mucosa above the wild-type crypts. A large number of parameters for different strengths of mutation effect were tested and all predicted the same mucosal invasion with no instances of crypt invasion. Crypt invasion was seen very rarely when some non-biological parameter values were tested. These conditions could not arise in biological tissue due to purely mechanical effects, but similar conditions could occur due to disruption of EphB signalling (Genander et al., 2009) which is a potential avenue for future research. The idea of mutated cells spreading through the colon by invading only the flat mucosa has not previously been suggested in the literature and appears to be a novel concept.

The third and final part of chapter 5 examined the consequences of the predictions from the first part over much larger scales of space and time. To do this a new model was developed which represented crypts, rather than individual cells, as agents which allowed a region of tissue to be simulated using many fewer agents and also allowed each update of the simulation to represent a longer period of biological time without introducing instabilities into the model. This model was able to simulate four million crypts, which is the approximate number in the human large intestine (Humphries and Wright, 2008), over a span of twenty years which is in the order of the mean time between crypt fissions (Wasan et al., 1998). This is the first simulation to model whole crypts as agents, the first time that a model of the colon has been run over these time-spans, and also the first time that the human colon has been modelled as a whole organ.

This crypt as agent model required a representation of the crypt lifecycle which was developed from a combination of data from the literature and predictions from the cell as agent model. Crypts are able to move in a passive manner to maintain optimal packing within the tissue, this is extrapolated from the fact that crypts fission regularly (Humphries and Wright, 2008) and some re-arrangement would be necessary to maintain the tissue. Crypts have a lifecycle which involves growing until an upper threshold is reached at which point fission occurs, or shrinking until a lower threshold is reached at which point the crypt is considered extinct. The process of shrinking and extinction is extrapolated from the fact that without such a mechanism the regular fission events which are known to occur would lead to an age related increase in crypt density which has not been reported in the literature.

The predictions from the cell scale model about flat mucosal invasion were incorporated into the crypt as agent model by creating a mucosal compartment above each crypt which was populated with wild-type cells. A mutated crypt would begin to populate its mucosal compartment with mutated cells and once this process reached a certain stage the mutated cells would begin to colonise the mucosal compartments of neighbouring crypts.

Simulations of this process were run and compared to the predictions of the cell scale model to validate this representation of mucosal invasion.

The new model allowed experiments to be performed over the whole organ which is much more representative of the scales involved in field cancerisation than the patch of twenty five crypts which was practicable with the cell scale model. One experiment studied the extent of field spread over a two decade period and predicted mutated fields covering tens of thousands of crypts. Investigating phenomena over these scales is impossible in a cell scale model, whether that model is the one described earlier or any of the models described in the literature.

The crypt scale model was then used to perform an experiment examining which of two conditions is most likely to be responsible for the collision of mutated fields. The first hypothesis is that two independent fields arise and grow towards each other until they collide, the second is that a wild-type crypt mutates beneath the area of invaded flat mucosa surrounding a mutated crypt. The experiment mutated random crypts within the simulation at a predefined rate and various choices of this rate were tested to determine if there was a link between the rate and the type of field collision which occurred. The model predicted that the collision of independent fields is far more likely than mutations arising below invaded flat mucosa for any value of the rate parameter.

6.2: How the project has advanced the state of the art

6.2.1: Biology

Rules governing anoikis have only been included in one model (Dunn et al., 2012) and that model was not able to re-capitulate the known distribution of anoikis events within the crypt. That model was also one of crypt formation so this project contains the first model in the literature to include a detailed anoikis process in a model of a crypt in a homeostatic condition. This is an important step forward as anoikis is one half of the system responsible for maintaining homeostasis within the crypt.

The question of how crypts regulate cellularity has not been well addressed in the literature, with most descriptions of the crypt focussing on either cell production or cell death but none examining a homoeostatic link between the two. Modelling has not been able to address this issue as no model before the one developed for this project includes both a mechanism for anoikis and a representation of the crypt in a homeostatic steady state, however the model developed for this project included both.

By perturbing the parameters controlling cell production in the model it was possible to predict the resulting change in crypt cellularity and hence identify any mechanism which would affect cellularity in addition to the increase in the number of cells being produced. It was found that increasing the rate of cell production above the rate of cell death increased the overall cellularity of the crypt, but that this was not an indefinite process and a new steady state cellularity level was reached.

The inability to cause a runaway increase in cellularity implied a regulatory mechanism was present in the model, and possibly in-vivo. The interactions giving rise to this mechanism were identified: if cell production is higher than cell death then cellularity increases as expected. Since the amount of space in a crypt does not increase more cells in the same space causes increased compression. The forces responsible for triggering anoikis in the

model are compression forces and so these forces increase along with cellularity, this increase in compression forces causes the anoikis rate to rise until it balances the increased cell production rate. An equivalent process occurs to lower the anoikis rate if it is higher than the rate of cell production.

The study which elucidated some of the mechanisms underlying anoikis in-vivo (Eisenhoffer et al., 2012) showed that compression forces are a trigger for anoikis therefore it is likely that the homeostatic mechanism discovered in the model also exists in-vivo. This is an important finding for any examination of crypt cellularity and regulation.

Another novel prediction of the model developed for this project was that mutated cells will invade the flat mucosa of surrounding tissue. This is due to anoikis resistance giving these cells a competitive advantage in this region of the crypt. This mechanism of field spread does not appear to have been hypothesised previously as no mention of it can be found in the literature. A member of the research group separate to this project has sought evidence on the presence of this phenomenon in-vivo and has found evidence in biopsy samples of mutated cells in the flat mucosa but not the crypts distant from a lesion. These findings match the mucosal invasion predicted by the model. This process, if confirmed to occur in-vivo, would have implications for the risk of adenoma recurrence after a lesion has been removed if the area of invaded mucosa is not also removed.

The crypt as agent model predicted that collisions are more likely to occur between two independently growing fields than as a mutation arising spontaneously below an existing field of invaded flat mucosa. This helps to unravel the polyclonal nature of adenomas (Merritt et al., 1997) and can be extended to examine other aspects of polyclonality.

6.2.2: Modelling

By including the crypt mouth in the model it was possible to model multiple crypts in a neighbourhood comprising a small patch of tissue. This model is the first in the literature to do so and enabled phenomena involving the interaction of multiple crypts to be modelled for the first time. It was possible to simulate patches of up to 125 crypts in this model whereas previous published models have only simulated a single crypt. This is possible due to the highly optimised nature of the model developed for this project which allowed a very large number of cells to be simulated with the computational resources available. This is significant because many of the processes associated with colon carcinogenesis are known to involve multiple crypts (Merritt et al., 1997).

Finally in terms of modelling, this project developed an agent based model of the colon where each agent represents an individual crypt. This model was able to simulate the entire colon over multiple decade time spans, compared to traditional models of the crypt which have covered at most around a hundred crypts (0.003% of the gut) for six months. This efficiency allows much larger scale processes such as field cancerisation to be studied. It was possible for a spreading field to be tracked over biologically relevant scales (i.e. millions of crypts over multiple decades of time) for the first time using this model and for colliding fields to be simulated and studied which is unique in the literature.

6.2.3: Future work

Several promising avenues for future research have been identified as part of this project. The first is to integrate the signalling based anoikis process which was published after the cell scale model was developed. This would be a simple addition to the existing model, requiring the addition of just two new rules, one which would detect the conditions to trigger anoikis and one which would apply a force to any cell in contact with another cell expressing the anoikis signal. The purpose of this project would be to examine the effects of signalling based anoikis on the predictions made in this project. Specifically, it would examine whether anoikis based cellularity regulation and mucosal invasion still occur when anoikis is modelled as an active process, and may allow drug interventions targeted at this mechanism to be tested in-silico before costly in-vivo development is done.

Another signalling based project would be to include a representation of EphB based signalling which is known to co-ordinate cell clustering in the crypt (Holmberg et al., 2006). This would also be a small modification to the existing model. The rules governing cell migration can trivially be extended to include cell-cell adhesion forces and EphB acts by modulating these forces. The purpose of this project would be to investigate the possibility of top-down crypt invasion due to perturbed EphB signalling, expanding on the outlier results where invasion was predicted in this project. As with the invasion experiments in this project the simulation would be run on a patch containing multiple crypts.

Finally, there are a large number of possibilities for the crypt as agent model. Amongst the most promising is the idea of using the model to study effects at a population level. To do this the mechanisms underlying the process in question would be added to the model and then a large number of simulations would be run. This would allow statistical analysis of the results for a given population which could be compared to data from biological populations in order to test whether a given hypothesis agrees with in-vivo data or not. If the model could be validated then these studies could be used to predict the reaction of specific populations to a given intervention.

The main challenge with all future projects is the validation of the model against in-vivo data as this data is limited and hard to obtain under controlled conditions. The currently advancing area of crypt organoids has the potential to provide much of the required data once the technique matures (Grabinger et al., 2014). An iterative project wherein in-vivo organoid data is incorporated into models which are then used to direct further organoid experiments is itself an attractive future project.

6.3: Conclusion

In conclusion, this project has for the first time developed a model of the crypt which includes the crypt mouth and can recapitulate the distribution of anoikis events seen in-vivo. This model predicted a mechanism of regulatory feedback which is responsible for the homeostasis of cellularity within the crypt and was not previously considered in the literature. The model also predicted a previously unknown method of field cancerisation whereby mutated cells spread through the flat mucosa of the gut. Initial in-vivo studies of keratin levels support this prediction.

The project also developed a model where each agent represented a whole crypt, which to the best of our knowledge is entirely novel. With this model it was possible to simulate the whole organ for multiple decades of biological time, there is currently no other model

capable of modelling the colon on this scale and so it was possible to investigate phenomena which occur over much larger scales than were accessible with previous models, such as field cancerisation.

6.4: References

DUNN, S.-J., NAETHKE, I. S. & OSBORNE, J. M. 2013. Computational Models Reveal a Passive Mechanism for Cell Migration in the Crypt. *Plos One,* 8.

DUNN, S. J., APPLETON, P. L., NELSON, S. A., NATHKE, I. S., GAVAGHAN, D. J. & OSBORNE, J. M. 2012. A Two-Dimensional Model of the Colonic Crypt Accounting for the Role of the Basement Membrane and Pericryptal Fibroblast Sheath. *Plos Computational Biology,* 8**,** 20.

EISENHOFFER, G. T., LOFTUS, P. D., YOSHIGI, M., OTSUNA, H., CHIEN, C.-B., MORCOS, P. A. & ROSENBLATT, J. 2012. Crowding induces live cell extrusion to maintain homeostatic cell numbers in epithelia. *Nature,* 484**,** 546-U183.

FLETCHER, A. G., BREWARD, C. J. W. & CHAPMAN, S. J. 2012. Mathematical modeling of monoclonal conversion in the colonic crypt. *Journal of Theoretical Biology,* 300**,** 118-133.

GENANDER, M., HALFORD, M. M., XU, N.-J., ERIKSSON, M., YU, Z., QIU, Z., MARTLING, A., GREICIUS, G., THAKAR, S., CATCHPOLE, T., CHUMLEY, M. J., ZDUNEK, S., WANG, C., HOLM, T., GOFF, S. P., PETTERSSON, S., PESTELL, R. G., HENKEMEYER, M. & FRISEN, J. 2009. Dissociation of EphB2 Signaling Pathways Mediating Progenitor Cell Proliferation and Tumor Suppression. *Cell,* 139**,** 679-692.

GRABINGER, T., LUKS, L., KOSTADINOVA, F., ZIMBERLIN, C., MEDEMA, J. P., LEIST, M. & BRUNNER, T. 2014. Ex vivo culture of intestinal crypt organoids as a model system for assessing cell death induction in intestinal epithelial cells and enteropathy. *Cell Death & Disease,* 5.

HAMMOUDI, A., SONG, F., REED, K. R., JENKINS, R. E., MENIEL, V. S., WATSON, A. J. M., PRITCHARD, D. M., CLARKE, A. R. & JENKINS, J. R. 2013. Proteomic profiling of a mouse model of acute intestinal Apc deletion leads to identification of potential novel biomarkers of human colorectal cancer (CRC). *Biochemical and Biophysical Research Communications,* 440**,** 364-370.

HOLMBERG, J., GENANDER, M., HALFORD, M. M., ANNEREN, C., SONDELL, M., CHUMLEY, M. J., SILVANY, R. E., HENKEMEYER, M. & FRISEN, J. 2006. EphB receptors coordinate migrationand proliferation in the intestinal stem cell niche. *Cell,* 125**,** 1151-1163.

HUMPHRIES, A. & WRIGHT, N. A. 2008. Colonic crypt organization and tumorigenesis. *Nature Reviews Cancer,* 8**,** 415-424.

INGHAM-DEMPSTER, T., CORFE, B. & WALKER, D. 2018. A cellular based model of the colon crypt suggests novel effects for Apc phenotype in colorectal carcinogenesis. *Journal of Computational Science,* 24**,** 125-131.

INGHAM-DEMPSTER, T., WALKER, D. C. & CORFE, B. M. 2017. An agent-based model of anoikis in the colon crypt displays novel emergent behaviour consistent with biological observations. Royal Society Open Science: The Royal Society Publishing.

MEINEKE, F. A., POTTEN, C. S. & LOEFFLER, M. 2001. Cell migration and organization in the intestinal crypt using a lattice-free model. *Cell Proliferation,* 34**,** 253-266.

MERRITT, A. J., GOULD, K. A. & DOVE, W. F. 1997. Polyclonal structure of intestinal adenomas in Apc-(Min)/+ mice with concomitant loss of Apc(+) from all tumor lineages. *Proceedings of the National Academy of Sciences of the United States of America,* 94**,** 13927-13931.

MIRAMS, G. R., FLETCHER, A. G., MAINI, P. K. & BYRNE, H. M. 2012. A theoretical investigation of the effect of proliferation and adhesion on monoclonal conversion in the colonic crypt. *Journal of Theoretical Biology,* 312**,** 143-156.

SHIH, I.-M., WANG, T.-L., TRAVERSO, G., ROMANS, K., HAMILTON, S. R., BEN-SASSON, S., KINZLER, K. W. & VOGELSTEIN, B. 2001. Top-down morphogenesis of colorectal tumors. *Proceedings of the National Academy of Sciences of the United States of America,* 98**,** 2640-2645.

WASAN, H. S., PARK, H. S., LIU, K. C., MANDIR, N. K., WINNETT, A., SASIENI, P., BODMER, W. F., GOODLAD, R. A. & WRIGHT, N. A. 1998. APC in the regulation of intestinal crypt fission. *Journal of Pathology,* 185**,** 246-255.